U.S. DEPARTMENT OF COMMERCE
National Technical Information Service

PB-294 997

Polymeric Interfaces for Stack Monitoring

North Carolina State Univ at Raleigh

Prepared for

Environmental Sciences Research Lab, Research Triangle Park, NC

Nov 78

TECHNICAL REPORT DATA
(Please read Instructions on the reverse before completing)

1. REPORT NO. EPA-600/2-78-214	2.	3. RECIPIENT'S ACCESSION NO. PB294997
4. TITLE AND SUBTITLE POLYMERIC INTERFACES FOR STACK MONITORING		5. REPORT DATE November 1978
		6. PERFORMING ORGANIZATION CODE
7. AUTHOR(S) Richard M. Felder and James K. Ferrel		8. PERFORMING ORGANIZATION REPORT NO.
9. PERFORMING ORGANIZATION NAME AND ADDRESS Department of Chemical Engineering North Carolina State University Raleigh, North Carolina 27607		10. PROGRAM ELEMENT NO. 1AD712
		11. CONTRACT/GRANT NO. 801578
12. SPONSORING AGENCY NAME AND ADDRESS U.S. Environmental Protection Agency-RTP, NC Office of Research and Development Environmental Research Center Research Triangle Park, N.C. 27711		13. TYPE OF REPORT AND PERIOD COVERED Final 1/73 - 6/76
		14. SPONSORING AGENCY CODE EPA/600/09

15. SUPPLEMENTARY NOTES

→SO2

16. ABSTRACT

Research has been performed on the use of polymeric interfaces for in-situ continuous stack monitoring of gaseous pollutants. Permeabilities of candidate interface materials to SO_2 were measured at temperatures from ambient to 200°C, and the results were used to design interfaces for field tests. A portable field monitoring system was constructed and used to carry out SO_2 monitoring runs in two SO_3 absorption tower stacks, and in oil-fired and coal-fired power plant boiler stacks. The results were in excellent agreement with data obtained by standard wet chemical methods. The SO_2 concentrations in the sample gases varied linearly with the concentrations in the stack; water vapor, acid mist, and particulates in the stack gases had no effect on the interface performance; and fluctuations in the stack SO_2 concentration were mirrored rapidly and accurately in the measured responses. The results suggest the potential value of in-situ polymeric interfaces for continuous monitoring in stack environments too dirty or corrosive for conventional devices to be used.

17. KEY WORDS AND DOCUMENT ANALYSIS

a. DESCRIPTORS	b. IDENTIFIERS/OPEN ENDED TERMS	c. COSATI Field/Group
* Air pollution Sulfur dioxide * Interfaces * Polymers Monitors	In-situ stack monitoring	13B 07B 07D

18. DISTRIBUTION STATEMENT RELEASE TO PUBLIC	19. SECURITY CLASS (This Report) UNCLASSIFIED	21. NO. OF PAGES 186
	20. SECURITY CLASS (This page) UNCLASSIFIED	22. PRICE CA09/MF A01

EPA Form 2220-1 (Rev. 4-77) PREVIOUS EDITION IS OBSOLETE

United States
Environmental Protection
Agency

Environmental Sciences
Research Laboratory
Research Triangle Park NC 27711

EPA-600/2-78-214
November 1978

Research and Development

PB 294997

EPA

Polymeric Interfaces for Stack Monitoring

REPRODUCED BY
NATIONAL TECHNICAL
INFORMATION SERVICE
U.S. DEPARTMENT OF COMMERCE

RESEARCH REPORTING SERIES

Research reports of the Office of Research and Development, U S. Environmental Protection Agency, have been grouped into nine series. These nine broad categories were established to facilitate further development and application of environmental technology. Elimination of traditional grouping was consciously planned to foster technology transfer and a maximum interface in related fields. The nine series are:

1. Environmental Health Effects Research
2. Environmental Protection Technology
3. Ecological Research
4. Environmental Monitoring
5. Socioeconomic Environmental Studies
6. Scientific and Technical Assessment Reports (STAR)
7. Interagency Energy-Environment Research and Development
8. "Special" Reports
9. Miscellaneous Reports

This report has been assigned to the ENVIRONMENTAL PROTECTION TECHNOLOGY series. This series describes research performed to develop and demonstrate instrumentation, equipment, and methodology to repair or prevent environmental degradation from point and non-point sources of pollution. This work provides the new or improved technology required for the control and treatment of pollution sources to meet environmental quality standards.

This document is available to the public through the National Technical Information Service, Springfield, Virginia 22161.

EPA-600/2-78-214
November 1978

POLYMERIC INTERFACES FOR STACK MONITORING

by

Richard M. Felder and James K. Ferrell
Department of Chemical Engineering
North Carolina State University
Raleigh, North Carolina 27607

Grant No. R-801578

Project Officer
James B. Homolya

Emissions Measurement and Characterization Division
Environmental Sciences Research Laboratory
Research Triangle Park, N. C. 27711

ENVIRONMENTAL SCIENCES RESEARCH LABORATORY
OFFICE OF RESEARCH AND DEVELOPMENT
U.S. ENVIRONMENTAL PROTECTION AGENCY
RESEARCH TRIANGLE PARK, NC 27711

DISCLAIMER

This report has been reviewed by the Environmental Sciences Research Laboratory, U. S. Environmental Protection Agency, and approved for publication. Aprroval does not signify that the contents necessarily reflect the views and policies of the U. S. Environmental Protection Agency, nor does mention of trade names or commercial products constitute endorsement or recommendation for use.

PERFACE

Traditional methods of monitoring gaseous pollutant concentrations in process and power plant stacks involve grab sampling and wet chemical analysis. In recent years, the need to assemble large quantities of monitoring data to demonstrate compliance with federal emission standards has led to the development of automatable techniques for continuous sampling and analysis. A drawback associated with these techniques is the need to remove particulate matter, water, and other condensable vapors from the samples; a related problem is the difficulty of assuring that the conditioned sample is truly representative of the stack gas, since the conditioning steps could very likely alter the concentration of the pollutant in the sample gas.

In 1973 a three-year developmental study was undertaken by the North Carolina State University Department of Chemical Engineering on the use of polymeric interfaces for continuous monitoring. Candidate interface materials for SO_2 monitoring were screened, gas transport properties needed to design interfaces for specific applications were measured, and field tests were performed in several stack environments. This report outlines the experimental and calculational procedures followed in this study, and summarizes the results and conclusions.

ABSTRACT

This research program was undertaken with several objectives in mind.

1. To screen candidate polymeric materials for use as in-situ stack monitoring interfaces, and to define and measure the gas transport properties of these materials needed to design interfaces for specific applications.
2. To design and field test interfaces in a variety of stack environments, and to demonstrate their ability to yield accurate monitoring data over extended periods of time.
3. To demonstrate the effects (or lack of effects) of such parameters as stack temperature , liquid and solid particulate loading, and stack gas humidity on the performance characteristics of polymeric interfaces.

A laboratory system was constructed which permitted the simulation of any desired stack gas environment at temperatures from ambient to 200°C. Polymer membranes or hollow tubes were inserted in the system, and their SO_2 permeabilities and diffusivities were measured. The results were used to design interfaces for field tests; they were also interesting in and of themselves, since almost no SO_2 transport properties had previously been reported at temperatures above about 35°C.

A portable field monitoring system based on the permeable interface concept was designed and constructed, and was used to carry out SO_2 monitoring runs in two SO_3 absorption tower stacks, and in oil-fired and coal-fired power plant stacks. The Teflon interfaces used in these tests performed extremely well, yielding continuous data in excellent agreement with data obtained by grab sampling and wet chemical analysis using Federal Register Method 6. The interfaces provided sample gases with SO_2 concentrations that varied linearly with the SO_2 concentrations in the stacks; the presence of water vapor, acid mist, and solid particulate matter in the stack gases had no effect on the performance of the interfaces, and fluctuations in the stack concentrations were mirrored accurately in the measured responses. The field test results suggest the potential value of the in-situ polymeric interface approach for monitoring in stack environments too dirty or corrosive for conventional continuous monitors.

In the course of the research, a new method for measuring diffusivities of gases in polymers was developed and applied to the determination of SO_2 diffusivities, and the effects of plasticizers on the permeabilities of polyvinylidene fluoride membranes to SO_2 were determined.

This report is submitted in fulfillment of Grant No. 801578 by North Carolina State University under the sponsorship of the U. S. Environmental Protection Agency. The report covers the period January 1, 1973 to May 31, 1976.

CONTENTS

Preface--iii
Abstract---iv
Figures--vi
Tables---viii
Acknowledgements---ix

1. Introduction-- 1
2. Conclusions--- 2
3. Recommendations--- 4
4. Permeation of Sulfur Dioxide through Polymers--------------- 5
    4.1 Theory and preliminary experiments---------------------- 5
    4.2 Compilation of permeability data------------------------ 8
    4.3 Humidity effects-- 8
    4.4 Plasticizer effects------------------------------------- 10
5. Permeation of Nitrogen Oxides and Water through Polymers---- 17
    5.1 Permeation of nitrogen oxides--------------------------- 17
    5.2 Permeation of water------------------------------------- 19
        5.2.1 Literature Survey--------------------------------- 19
        5.2.2 Permeability measurements------------------------- 19
6. Field Tests of Stack Monitoring Interfaces------------------ 20
    6.1 Stack monitoring system--------------------------------- 20
    6.2 Summary of results-------------------------------------- 23
        6.2.1 SO_3 absorption tower stack: single contact process-- 23
        6.2.2 SO_3 absorption tower stack: double contact process-- 23
        6.2.3 Oil-fired power plant boiler stack---------------- 25
        6.2.4 Coal-fired power plant boiler stack--------------- 25
    6.3 Conclusions--- 28
7. Measurement of Gas Diffusivities in Polymers---------------- 29
    7.1 Procedure for diffusivity measurements------------------ 29
    7.2 Diffusivities of sulfur dioxide------------------------- 30

References--- 31

Appendices

A. Permeation of Sulfur Dioxide through Polymers--------------- 32
B. Effect of Moisture on the Performance of Permeation Sampling Devices-- 66
C. Permeation Data for NO_x and H_2O---------------------------- 84
D. Polymeric Interfaces for Continuous SO_2 Monitoring in Process and Power Plant Stacks------------------------------------ 105
E. A Method for the Dynamic Measurement of Diffusivities of Gases in Polymers--- 129
F. A Method of Moments for Measuring Diffusivities of Gases in Polymers-- 147

FIGURES

Number Page

1. Schematic of laboratory apparatus---------------------------------- 6
2. Flux vs. Δp isotherms for SO_2 in an FEP Teflon membrane---------- 7
3. Arrhenius plot of SO_2 permeabilities for an FEP Teflon membrane-- 9
4. Membrane permeation chamber-- 11
5. Effect of sulfolane on permeability of Kynar films--------------- 13
6. Effect of sulfolene on permeability of Kynar films--------------- 14
7. Effect of total pressure on SO_2 permeability of plasticized and unplasticized Kynar films-- 15
8. Schematic of stack monitoring system----------------------------- 21
9. Monitoring data: Single contact process stack-------------------- 24
10. Monitoring data: Double contact process stack-------------------- 26
11. Monitoring data: Oil-fired boiler stack-------------------------- 27

TABLES

Number Page

1. Permeabilities of plasticized and unplasticized films---------- 12
2. Field test parameters-- 22

ACKNOWLEDGMENTS

The experimental work carried out in the course of this project was initiated by Mr. Charles Rodes and was carried on by Dr. Roger Spence and Mssrs. James Spivey, Lanny Treece, and Chen-Chi Ma. The contributions of the two grant monitors during the course of the project--Mr. Rodes and Mr. James Homolya--are gratefully acknowledged.

SECTION 1

INTRODUCTION

Most of the work described in the abstract of this report has been pulbished in a series of journal articles which are included as appendices. The main body of the report provides a detailed summary of the published work and an exposition of results which have not yet been published.

The organization of the report is as follows. Sections 2 and 3 summarize conclusions and recommendations. Section 4 surveys measurements of SO_2 permeability, and section 5 reviews permeation of oxides of nitrogen and of water through polymers. Section 6 summarizes the results of SO_2 monitoring field tests. Section 7 ourlines the derivation of a technique developed in this study for the measurement of gas diffusivities, and summarizes the SO_2 diffusivities measured using this technique.

SECTION 2

CONCLUSIONS

Portable systems based on in-situ polymer interfaces can be used to monitor stack gas SO_2 concentrations ranging from tens to thousands of parts per million. The technique yields reproducible results, and provides continuous analyses that agree well with readings obtained by grab sampling and standard wet chemical analysis.

The presence of water vapor in a stack gas does not effect the rate of permeation of SO_2 through the interface, so that the analyzer reading need not be corrected for the stack gas humidity. Moreover, Teflon is sufficiently impermeable to water to preclude the possibility of condensation in the sample line or the analyzer. There is consequently no need for heated sample lines, cold traps, or drying columns in the sampling train.

The presence of liquid or solid particulate matter including acid mist in the stack gas has no measurable effect on the performance of the interface; using a Teflon interface, therefore, eliminates the need for frequent filter changes, making long-term unattended continuous monitoring in exceptionally dirty and corrosive environments a good possibility.

Responses obtained using polymer interfaces follow changes in the stack gas SO_2 concentration accurately and rapidly, suggesting the potential applicability of such devices as feedback control loop components.

The only observed drawback to the use of polymeric interfaces is that the sensitivity of the interface permeability to the stack gas temperature makes continuous correction for temperature fluctuation necessary. However, the nature of the temperature dependence is well established, and automatic temperature correction can easily be achieved using modern microprocessor technology.

A gas transport model based on Henry's law for solution and Fick's law for diffusion correlates permeation data well for pollutant concentration levels characteristic of those found in stacks, making calibration of interfaces a straightforward task.

Sulfolane, sulfolene, and N, N, N', N', tetra-phenyl-p-phenyldiamine (TPD) were used to plasticize polyvinylidene fluoride (Kynar) membranes, and the permeabilities of the plasticized membranes to SO_2 were measured over a range of temperatures. No significant permanent increase in SO_2 permeability was found which could be attributed to the addition of sulfolane or TPD; when increases were observed, they were either temporary or the results of overplasticization. Permeability increases of up to 80% were obtained when sulfolene was used as a plasticizer.

A method of moments for determining the diffusivity of a gas in a polymer has been formulated and its validity has been verified experimentally. Diffusivities are important quantities in the context of this research, since they determine the time response of permeable interfaces; moreover, the diffusivity is the primary variable governing the performance of plastic grab sample containers, and of permeation tubes for analyzer calibrations, so that the technique developed could have benefits to environmental technology well beyond the scope of this study.

SECTION 3

RECOMMENDATIONS

The results of the field tests performed to date suggest the potential usefulness of polymeric interfaces for continuous stack monitoring for SO_2. Future efforts should be directed toward exploring the range of conditions in which devices of this sort can function, with particular emphasis on traditionally difficult-to-monitor environments such as those found in ore smelting processes, pulp mills, and flue gas scrubbers.

The technique should be extended to other pollutants, such as NO_x, CO, H_2S, and various hydrocarbons. The use of interfaces for selective monitoring of specific pollutants in mixtures should be studied; included in this investigation would be the use of plasticizers or other additives to enhance the permeabilities of polymers to selected mixture components.

SECTION 4

PERMEATION OF SULFUR DIOXIDE THROUGH POLYMERS

4.1 THEORY AND PRELIMINARY EXPERIMENTS

The relationship between the concentration of a pollutant in a stack gas and the rate of penetration of the pollutant into a polymeric interface is governed by the permeability of the polymer to the pollutant. (Crank and Park, 1968) By definition, the permeability P is the ratio $J/(\Delta p/h)$, where J is the flux of the penetrating gas through a flat membrane of thickness h, and Δp is the partial pressure difference across the membrane. The permeability depends on temperature according to the Arrhenius law

$$P = P_o \exp(-E_p/RT) \qquad (4.1)$$

where

P = permeability, cm^3(STP)/s.cm.cm Hg
P_o = preexponential factor, units of P
E_p = activation energy for permeation, cal/g-mole
R = gas constant, 1.987 cal/g-mole·°K
T = temperature, °K

The solution of the steady state diffusion equation yields the relationship between the permeation rate ϕ[cm^3(STP)/s] and the partial pressure driving force Δp. For a flat membrane of cross sectional area A (cm^2) and permeability P[(cm^3/STP)/s·cm·cmHg]

$$\phi = PA\Delta p \qquad (4.2)$$

and for a hollow cylindrical tube of inner radius a and outer radius b,

$$\phi = \frac{2\pi P\Delta p}{\ln(b/a)} \qquad (4.3)$$

In a preliminary series of experiments, SO_2 permeabilities were measured for several polymers at temperatures between 120°C and 230°C, using an apparatus shown schematically in Figure 1. Span gas mixtures of SO_2 and air with SO_2 concentrations between 100 and 10,000 ppm were passed on one side of a flat polymer membrane or on the outside of a hollow tube in a thermostatically-controlled oven. SO_2 permeated through the polymer into a carrier gas stream of dry air. The carrier gas and the SO_2 that permeated into it passed to a flame photometric detector, and the SO_2 concentration was recorded. The SO_2 permeation rate was calculated as the product of the carrier gas flow rate and the SO_2 concentration.

Experiments of this type were carried out at a fixed temperature for several span gas SO_2 concentrations, and plots of ϕ vs. the appropriate function of Δp (see Eqs. 4.2 and 4.3) were used to determine the permeabilities. Representative plots are shown in Figure 2.

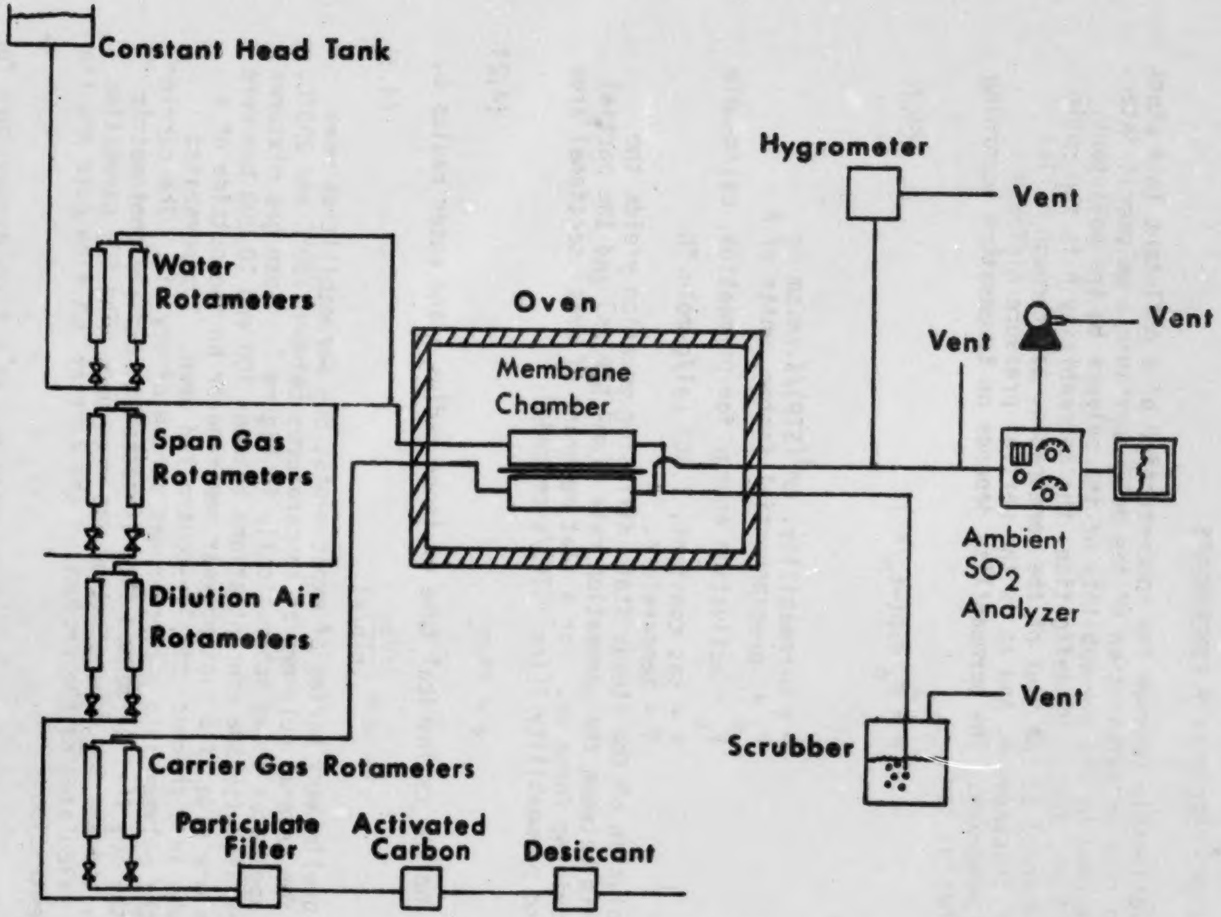
Constant Head Tank
Water Rotameters
Span Gas Rotameters
Dilution Air Rotameters
Carrier Gas Rotameters
Particulate Filter
Activated Carbon
Desiccant
Oven
Membrane Chamber
Hygrometer
Vent
Vent
Vent
Ambient SO_2 Analyzer
Scrubber
Vent

Figure 1. Schematic of laboratory apparatus

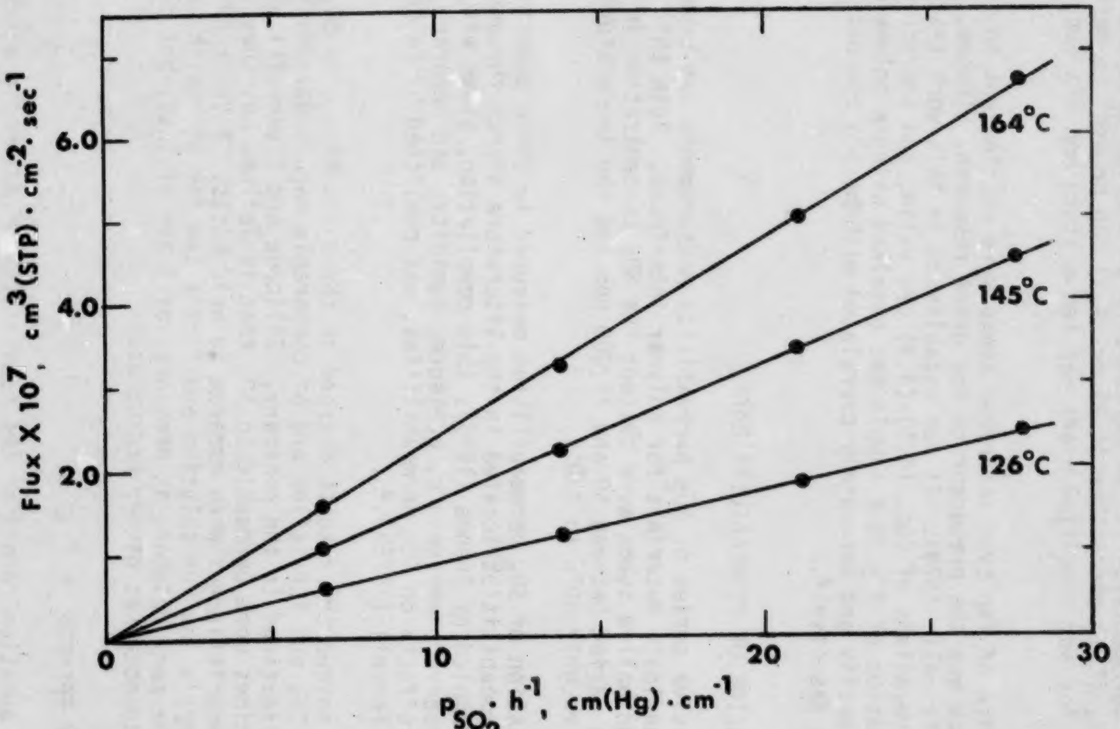

Figure 2. Flux is Δp isotherms for SO_2 in an FEP Teflon membrane.

Permeabilities determined in this manner were plotted against reciprocal temperature, and the slopes were used to determine the activation energy for permeation. A representative Arrhenius plot of this type is shown in Figure 3.

Once the permeability vs. temperature functionality is known for a polymer, Eq. (4.1) and either (4.2) or (4.3) can be used to design an interface for any specified stack gas temperature and SO_2 concentration range.

Experiments of the type described above were carried out in the research which was the precursor to the grant research. (Rodes, Felder, and Ferrell, 1973). It was established in this work that the theoretical relations of Eqs. (4.1)-(4.3) are valid, and therefore that the concentration of SO_2 in a sample gas obtained using a polymer interface can be easily and accurately correlated with the SO_2 concentration in the stack gas itself.

4.2 COMPILATION OF PERMEABILITY DATA

An extensive series of SO_2 permeability measurements was undertaken to screen candidate materials for polymer interfaces. Both thin membranes and hollow tubes were tested; the SO_2 concentration in the span gas was varied between 50 and 15,000 ppm and the temperature was varied from roughly 30°C to 230°C.

A compilation of SO_2 permeabilities measured in these experiments and other permeabilities located in the literature search through April 1974 was assembled by Spence (1975); this compilation, along with a survey of observed temperature, pressure, humidity, and membrane plasticizer effects on SO_2 permeabilities, was published by Felder, Spence, and Ferrell (1975a).*

Several noteworthy results emerged in these studies. The SO_2 permeabilities of TFE and FEP Teflon are of comparable magnitude, contradicting published assertions to the contrary. Silicone and fluorosilicone rubbers are 10-100 times more permeable to SO_2 than is Teflon, but they are also subject to embrittlement when exposed to acid mists. A transport model based on Henry's law for solution and Fick's law for diffusion correlates data well for many polymers at pressures of 1 atm or less, but deviations are likely to occur at higher pressures.

4.3 HUMIDITY EFFECTS

A major question regarding the feasibility of polymeric stack sampling interfaces was the potential effect of the stack gas humidity on their performance. Two possible deleterious effects were envisioned: first, water might permeate through the membrane, condense, and absorb SO_2 from the sample gas, leading to an erroneous analyzer reading; second, the presence of the water could alter the permeability of the interface to SO_2 (possibly by swelling the polymer), again causing an erroneous reading.

---

*Attached as Appendix A

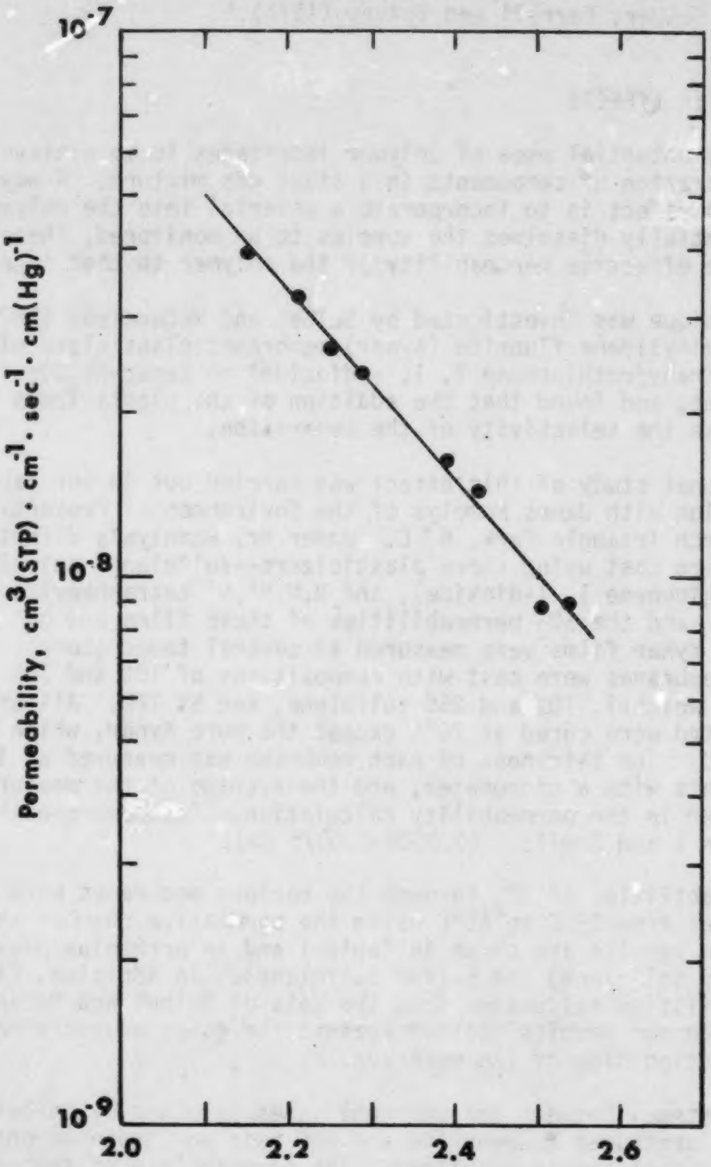

Figure 3. Arrhenius plot of SO_2 permeabilities for an FEP Teflon membrane.

The problem was studied by measuring SO_2 permeabilities using span gases containing up to 20% water by volume. In all cases studied, neither of the anticipated effects was observed; the water permeation rate was sufficiently low to preclude condensation in the sample gas line, and the effective SO_2 permeabilities of the tubes (TFE Teflon, FEP Teflon, and a fluorosilicone rubber) were unaffected by the presence of the water. This work is described in detail by Spivey (1974), and is summarized by Felder, Ferrell and Spivey (1974).*

4.4 PLASTICIZER EFFECTS

One of the potential uses of polymer interfaces is to achieve a selective separation of components in a stack gas mixture. A way of enhancing this effect is to incorporate a material into the polymer which preferentially dissolves the species to be monitored, thereby increasing the effective permeability of the polymer to that species.

This technique was investigated by Seibel and McCandless (1974), who used polyvinylidene fluoride (Kynar) membranes plasticized with sulfolane (tetrahydrothiophene 1, 1, - dioxide) to separate SO_2 from SO_2-N_2 mixtures, and found that the addition of the plasticizers did indeed increase the selectivity of the separation.

An additional study of this effect was carried out in our laboratory in collaboration with James Homolya of the Environmental Protection Agency, Research Triangle Park, N. C. Under Mr. Homolya's direction, Kynar films were cast using three plasticizers--sulfolane, sulfolene (2-5 dihydrothiophene 1, 1-dioxide), and N,N,N',N' tetraphenyl-p-phenyldiamine (TPD)--and the SO_2 permeabilities of these films and of unplasticized Kynar films were measured at several temperatures. The plasticized membranes were cast with compositions of 10% and 25% sulfolane (by weight), 10% and 25% sulfolene, and 5% TPD. All of the membranes tested were cured at 75°C except the pure Kynar, which was cured at 105°C. The thickness of each membrane was measured at 10 different points with a micrometer, and the average of the measured values was used in the permeability calculation. The membrane thicknesses varied between 1 and 3 mils (0.0025-0.0075 cm).

The permeabilities of SO_2 through the various membranes were determined at temperatures from 25°C to 65°C using the permeation chamber shown in Figure 4. The results are shown in Table 1 and in Arrhenius plots in Figures 5 (for sulfolane) and 6 (for sulfolene). In addition, Figure 7 shows permeabilities calculated from the data of Seibel and McCandless (1974) and from our results plotted against the gauge pressure on the high concentration side of the membrane.

The consistency between the permeabilities obtained by Seibel and McCandless at pressures between 100 and 500 psig and those we obtained at atmospheric pressure is excellent. The permeability of the unplasticized film apparently remains independent of the chamber gas pressure up to approximately 400 psig, while that of plasticized film begins to increase at a much lower pressure. The increases in P due to the

---

* Attached as Appendix B

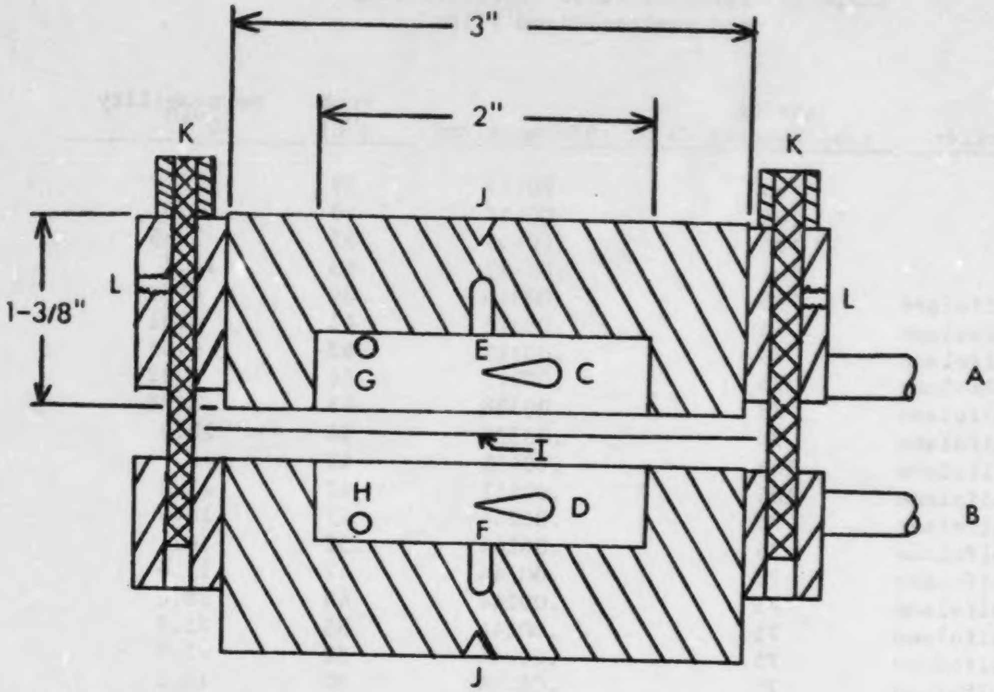

A - Carrier gas inlet

B - Span gas inlet

C - Carrier gas inlet port (two tangential ports located diagonally)

D - Span gas inlet port (two tangential ports located diagonally)

E - Carrier gas outlet port (exits from center then bends 90° to come out front of chamber)

F - Span gas outlet port (exits from center then bends 90° to come out front of chamber)

G - Thermocouple tap

H - Pressure tap

I - Membrane

J - Notch for C-clamp

K - Guide posts

L - Set screw

Figure 4. Membrane permeation chamber

Table 1. Permeabilities of plasticized and unplasticized films

plasticizer	curing temperature(°C)	thickness(cm)	temp. (°C)	permeability 10^{-10}
none	105	.00417	39	3.20
none	105	.00417	45	4.62
none	105	.00417	55	7.56
none	105	.00417	65	12.2
10% sulfolane	75	.00315	39	4.84
10% sulfolane	75	.00315	43	4.31
10% sulfolane	75	.00315	53	9.05
10% sulfolane	75	.00315	56	8.32
10% sulfolane	75	.00338	43	5.28
10% sulfolane	75	.00338	56	10.0
10% sulfolane	105	.00411	48	5.74
10% sulfolane	105	.00411	62	12.2
25% sulfolane	75	.00244	27	14.6
25% sulfolane	75	.00244	32	14.1
25% sulfolane	75	.00244	42	15.6
25% sulfolane	75	.00244	48	18.0
25% sulfolane	75	.00244	55	21.9
25% sulfolane	75	.00244	58	21.5
25% sulfolane	75	.00284	30	13.2
25% sulfolane	75	.00284	59	21.4
5% TPD	75	.00696	32	2840
10% sulfolene	75	.00335	43	4.22
10% sulfolene	75	.00335	50	6.09
10% sulfolene	75	.00335	54	7.77
10% sulfolene	105	.00315	40	4.53
10% sulfolene	105	.00315	52	10.2
10% sulfolene	105	.00315	63	17.3
25% sulfolene	75	.00424	43	5.27
25% sulfolene	75	.00424	48	6.79
25% sulfolene	75	.00424	54	8.61

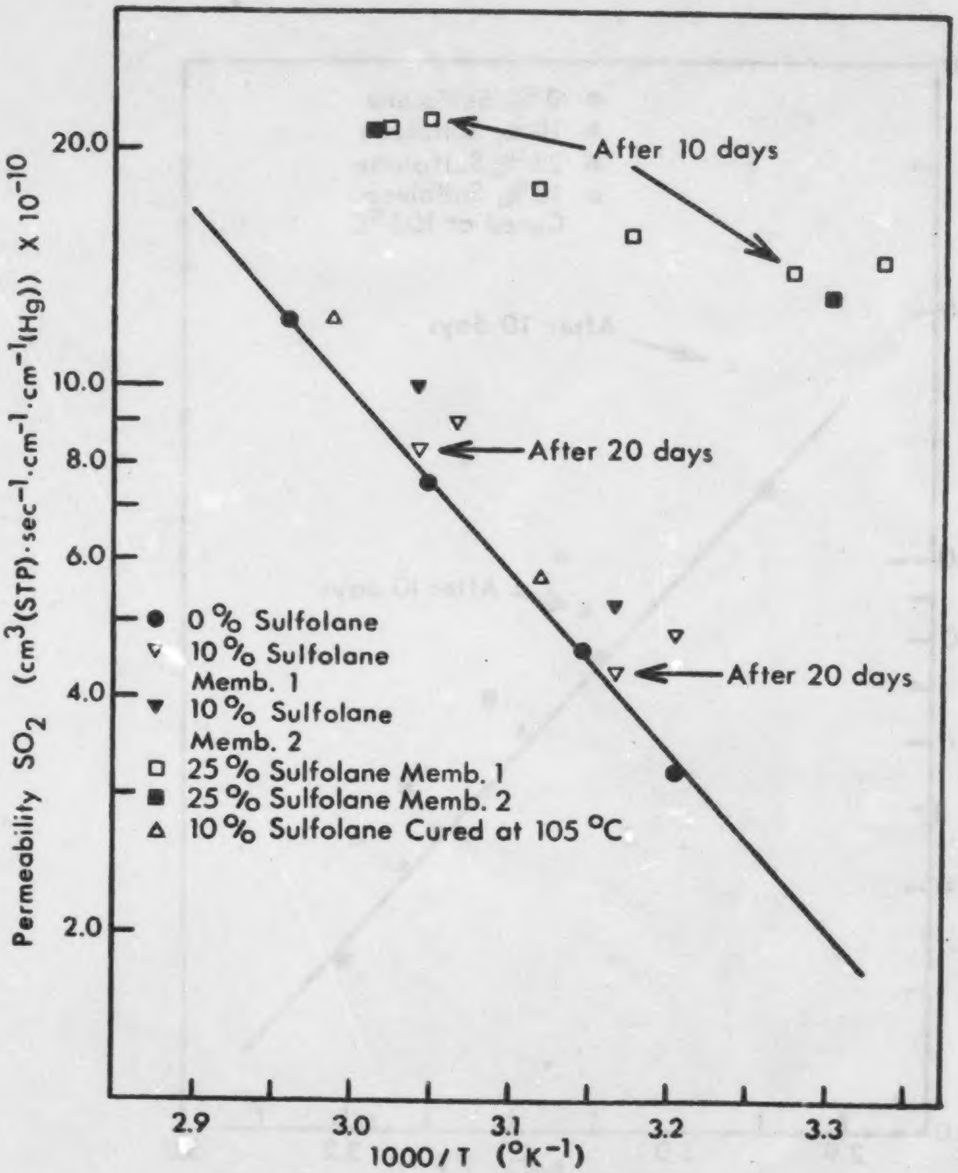

Figure 5. Effect of sulfolane on permeability of Kynar films

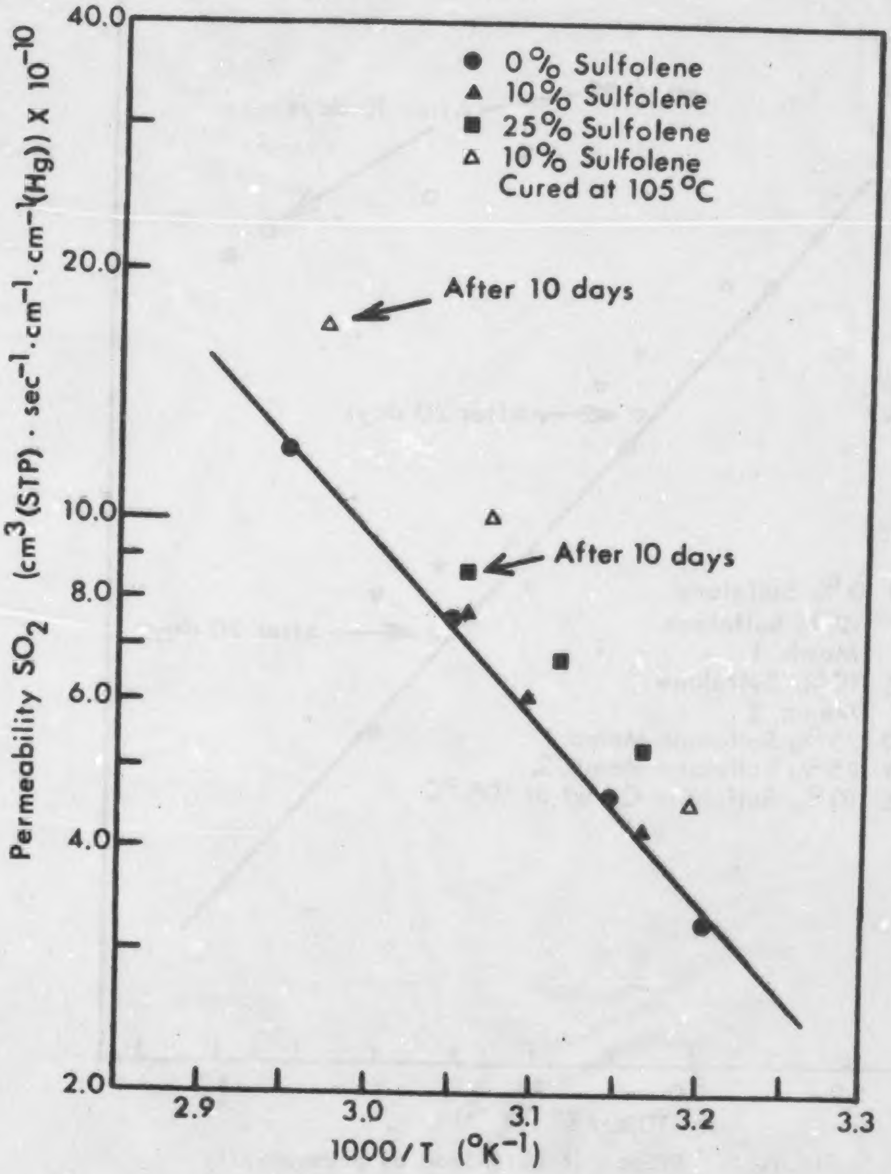

Figure 6. Effect of sulfolene on permeability of Kynar films

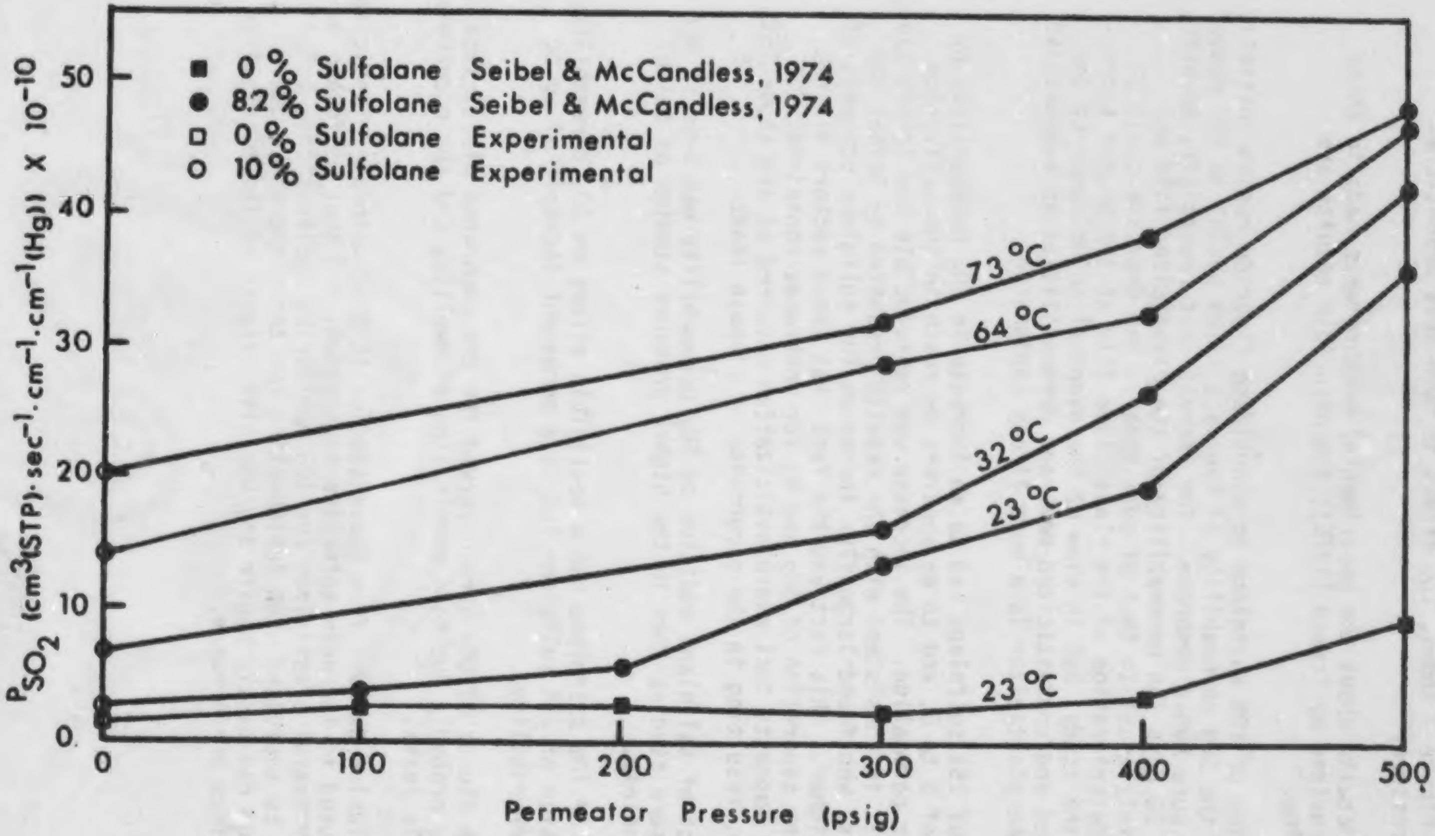

Figure 7. Effect of total pressure on SO_2 permeability of plasticized and unplasticized Kynar films

addition of the sulfolane observed by Seibel and McCandless were consequently due in large part to the pressure range in which they were operating; as Figure 7 shows, the effect is much less dramatic at atmospheric pressure.

Complete details about the experimental measurements made in these studies are provided by Treece (1975); the principle results are summarized below.

1. The addition of 10% sulfolane to vinylidene fluoride resins initially increased the SO_2 permeability of the cast films by 25% to 50% above that of a pure Kynar membrane. The increase was reversible, however, and after 20 days the permeability of the plasticized film was approximately equal to that of pure Kynar. The decrease could be due to a deterioration of the plasticized film at the higher temperature of the study, but in view of the eventual coincidence of the plasticized and unplasticized membrane permeabilities an evaporative loss of the plasticizer is a more likely explanation.

2. Addition of 25% sulfolane led to an increase in SO_2 permeability by a factor of 3 to 8, and to an apparent decrease in the activation energy for permeation. The increase was reproducible and irreversible. This result is consistent with the results presented by Seibel and McCandless, who found large flux increases for sulfolane contents of 15% and higher. This fact and the fact that these authors did not observe any separation of SO_2 and N_2 for membranes containing 20% sulfolane suggests that overplasticization occurred at and above 15% sulfolane, resulting in the occurrence of pinhole leaks.

3. The effect of sulfolane addition on SO_2 permeability was less in our low pressure studies than in the higher pressure studies of Seibel and McCandless.

4. Addition of 10% sulfolene had a negligible effect on SO_2 permeability, and addition of 25% sulfolene led to a permanent increase of up to 80% in permeability.

5. Very high fluxes of SO_2 were observed for the membranes plasticized with TPD, probably due to a combination of swelling and the occurrence of pinhole leaks.

The conclusion derived from these studies is that membrane plasticization can be used to increase selective separation, and that sulfolene is a potentially useful plasticizer for SO_2 monitoring applications, but caution must be exercised when implementing the technique since overplasticization can easily negate any positive effects of the plasticizer on the interface performance.

SECTION 5

PERMEATION OF NITROGEN OXIDES AND WATER THROUGH POLYMERS

The extent to which water is screened out of a sample gas by a polymer interface is governed by the permeability of the polymer to water. A limited literature search on water permeabilities was carried out, and permeabilities were measured in our laboratory for interface materials used in the SO_2 measurements described in the previous section. In addition, a literature search on NO_x permeation was carried out in anticipation of the use of polymer interfaces for monitoring this pollutant.

The results of the literature searches are reported in detail in Appendix C. The following sections summarize the principle findings, and report on the results of the water permeability measurements carried out in our laboratory.

5.1 PERMEATION OF NITROGEN OXIDES

Almost all reported permeation data are for the NO_2 - N_2O_4 system, whose equilibrium under ideal conditions is given by

$$\frac{(p_{NO_2})^2}{p_{N_2O_4}} = 7.1\times10^9 \exp(-14{,}600/RT) \qquad (5.1)$$

(Getman and Daniels, 1946). A degree of uncertainty is associated with almost all permeation data for this system, reflecting an uncertainty about which species was in fact permeating.

Pasternak et.al. (1970) showed that a nominal permeability

$$P_n = \frac{p_{NO_2}\, P_{NO_2} + 2\, p_{N_2O_4}\, P_{N_2O_4}}{p_{tot}} \qquad (5.2)$$

may be determined from permeation rate data, but that there is no way to determine P_{NO_2} or $P_{N_2O_4}$ from data taken at a temperature where both substances are present. The authors overcame this difficulty by carrying out runs using TFE membranes at temperatures above 100°C, where the gas could be assumed to be pure NO_2. An Arrhenius function fit to the P_{NO_2} data was extrapolated to lower temperatures, $P_{N_2O_4}$ was determined as a function of temperature from the measured values of P_{NOx} and the extrapolated values of P_{NO_2} using Eq. (5.2), and an Arrhenius function was then fit to the N_2O_4 permeabilities. The results are shown in Table 1 of Appendix C along with other published Arrhenius parameters for NO_2-N_2O_4 permeation through TFE and FEP.

Permeability data are given in Appendix C for NO_2, N_2O and NO in dimethyl silicone membranes at 25°C. The reported NO permeability of dimethyl silicone is seen to be an order of magnitude less than the NO_2 permeability.

The remaining NO_x permeabilities given in Table C2 were obtained at temperatures in the range 20 - 40°C with a vapor-liquid equilibrium mixture of NO_2 - N_2O_4 on one side of the membrane. The flux of NO_x through a membrane can be calculated from the effective permeability in the table from the following relations.

1. Flat membranes of thickness h (cm)

$$F_m \, (cm^3 \; NO_2(STP)/cm^2 \cdot s) = P_e \, h(p_{NO_2} + p_{N_2O_4}) \tag{5.3}$$

2. Hollow tubes: inner radius = r_1 (cm), outer radius = r_2 (cm)

$$F_t \, (cm^3 \; NO_2(STP)/cm.s) = 2 \, \pi P_e(p_{NO_2} + p_{N_2O_4})/\ln \, (r_2/r_1) \tag{5.4}$$

5.2 PERMEATION OF WATER

5.2.1 Literature Survey

A large body of data exists for the permeation of water through polymers. Water permeabilities, diffusivities and solubilities for a number of materials are listed in Table C.3, Appendix C, and activation energies for permeation and diffusion are given in Table C.4, Appendix C.

5.2.2 Permeability Measurements

Water permeabilities were measured in tubes of TFE Teflon, FEP Teflon, and fluorosilicone rubber. The experimental apparatus was that shown in Figure 1, with the addition that metered water was vaporized with electrical heating tape, and fed into a tee in the span gas line. The concentration of water in the sample gas was measured with a Panametrics Model 2000 continuous flow hygrometer. Additional details are given by Felder, Ferrell, and Spivey (1974).*

The results of these studies, which are given in Appendix C, parallel those for SO_2. Water permeabilities in TFE and FEP Teflons are comparable, both being an order of magnitude less than that in the fluorosilicone rubber. In all cases, the results show that using any of the tested materials as a polymer interface would provide a sample gas with a dew point well below ambient temperatures, so that condensation in the line to the analyzer could not possibly occur. For example, if a fluorosilicone rubber tude were used to monitor a stack gas at 177°C with a dew point of 61°C, the dew point of a carrier gas flowing at 655 cm^3 (STP)/min would be -29.5°C, and would be even lower if a Teflon tube were used.

---

*Attached as Appendix B.

SECTION 6

FIELD TESTS OF STACK MONITORING INTERFACES

A program of stack monitoring field tests was carried out in parallel with the laboratory permeability measurements. In most of these tests, Teflon tubes or membranes were used as interfaces in 1-day or 2-day SO_2 monitoring runs. The principal results of these tests are summarized in this section.

6.1 STACK MONITORING SYSTEM

A portable interface system was designed and constructed for continuous stack monitoring tests. A diagram of the interface configuration in the stack is given in Figure 8.

The system included a central control panel with mounted pressure gauges, flow meters, and gas cleaning and drying columns, a U-shaped stainless steel probe with the permeable interface mounted as a segment of one of the arms, an ambient SO_2 or NO_x analyzer and recorder, a thermocouple, potentiometer and recorder, an air compressor, and the calibration gas sources required for the analyzer and the interface. A hollow sheath mounted on the probe could be slipped over the interface, and a span gas could then be passed over the outside of the interface for calibration purposes. The sheath could then be withdrawn, exposing the interface to the stack gases. The carrier gas flowing through the inside of the tube picked up the pollutant which permeated in from the stack, and passed out of the probe to the analyzer.

Raw data had to be corrected for variations in the stack temperature. The thermocouple mounted on the probe provided a continuous reading of temperature in the stack, which with the activation energy for permeation known from the laboratory measurements permitted the corrections to be made.

Summarizing the monitoring procedure, a polymer tube was mounted in the probe and positioned in the stack with the sheath in the calibration position. The components of the testing system were connected and checked for leaks. Following calibration of the analyzer, the interface was exposed to a span gas containing a known concentration of SO_2, the carrier gas flow rate was adjusted to its desired value, the flow was directed to the analyzer, and the steady-state analyzer reading was noted. A plot of span gas concentration versus analyzer reading obtained in this manner was used as a calibration curve for the subsequent stack monitoring. The sheath was then withdrawn, exposing the polymer tube to the stack, and the analyzer signal was recorded continuously. The recorded signal was later corrected for variations in the stack temperature, and the results were used to calculate the stack gas pollutant concentration from the calibration curve.

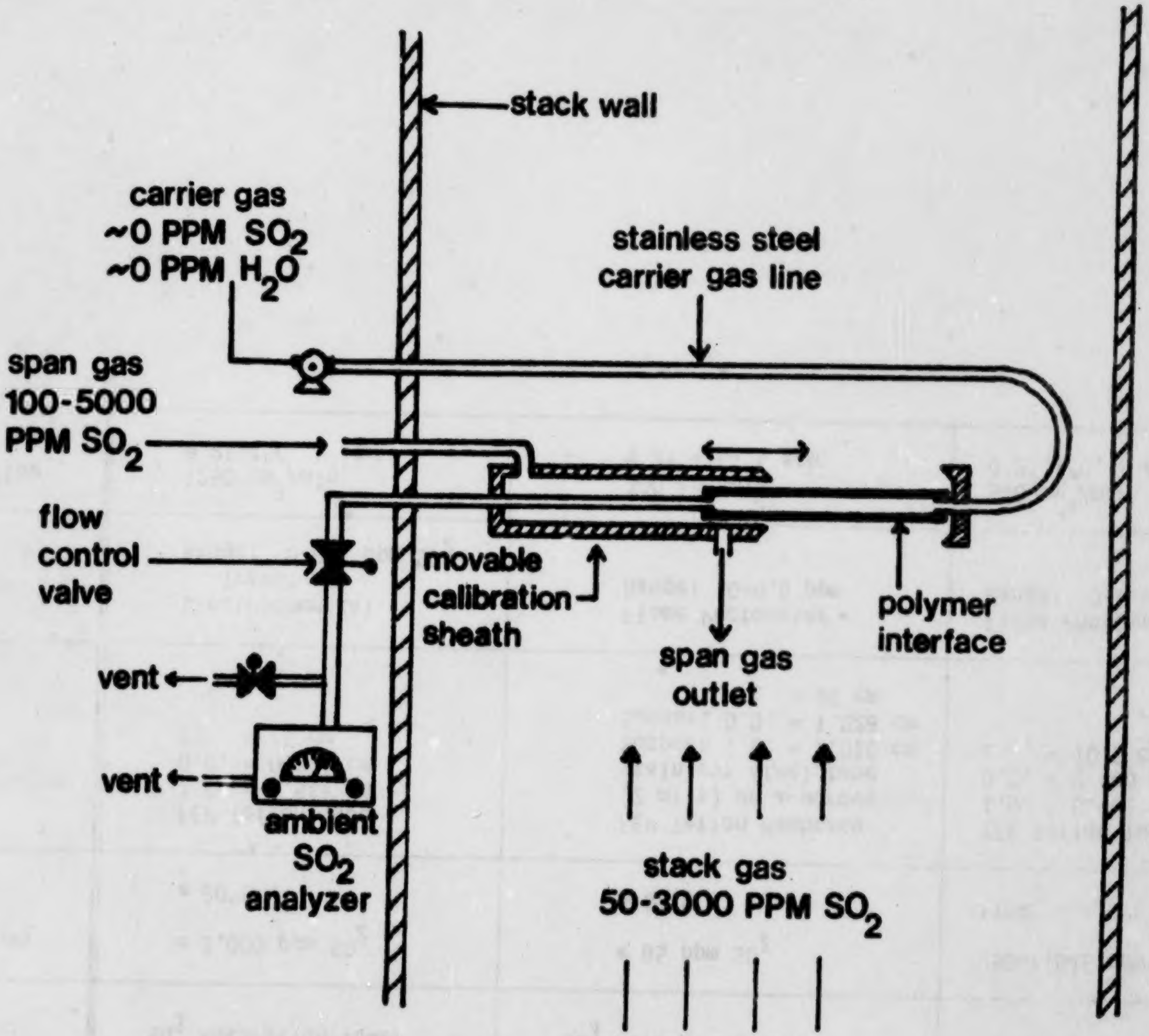
stack wall
carrier gas
~0 PPM SO_2
~0 PPM H_2O
stainless steel
carrier gas line
span gas
100-5000
PPM SO_2
flow
control
valve
movable
calibration
sheath
polymer
interface
span gas
outlet
vent
vent
ambient
SO_2
analyzer
stack gas
50-3000 PPM SO_2

Figure 8. Permeable Stack Sampling Interface

Table 2. Field Test Parameters

Stack Location	Single-Contact Process SO_3 Absorption Tower	Double-Contact Process SO_3 Absorption Tower	Oil-Fired Power Plant Boiler
Stack Conditions	$\approx$ 2,000 ppm SO_2 $\approx$ 80°C	$\approx$ 85 ppm SO_2 $\approx$ 67°C	250-1,045 ppm SO_2 170°C - 213°C
Interface	FEP Teflon Tube I.D. = 0.544 cm O.D. = 0.604 cm L = 75 cm	FEP Teflon Membrane (2 mils) on a porous stainless steel tube Support I.D. = 1.016 cm Support O.D. = 1.026 cm L = 44 cm	TFE Teflon Tube I.D. = 0.403 cm O.D. = 0.480 cm L = 70.5 cm
Analyzer	Electrochemical Transducer Range: 0-0.1 ppm SO_2	Flame Photometer Range: 0-0.5 ppm	Flame Photometer Range: 0-0.5 ppm
Carrier Gas Flow Rate	1250 cm^3/min @ 21.4°C, 1 atm	300 cm^3/min @ 21.4°C, 1 atm	500 cm^3/min @ 21.4°C, 1 atm

SO_2 monitoring runs were performed in two SO_3 absorption tower stacks, an oil-fired boiler stack, and a coal-fired boiler stack. The experimental parameters of all but the last of these tests are summarized in Table 2; the test in the coal-fired boiler was preliminary in nature and only qualitiative behavior was observed. Details of these tests and plots of the data are given by Treece, Felder, and Ferrell (1976)*; the principal results are summarized below.

6.2 SUMMARY OF RESULTS

6.2.1 SO_3 Absorption Tower Stack: Single Contact Process

A 1-day run was carried out using an FEP Teflon sampling tube. The stack gas contained approximately 2,000 ppm SO_2 and the stack temperature was roughly 80°C. The results are shown in Figure 9. There were no significant operating problems, and excellent agreement was obtained between the continuous monitoring results and those obtained by intermittent sampling and analysis using Federal Register Method 6.

A heavy acid mist was present in the stack, and considerable dropwise condensation on the tube took place. The SO_2 permeability of the condensate-coated tube was experimentally indistinguishable from that of the clean tube material, indicating that the condensate had no effect on the tube performance.

In another experiment, the SO_2 permeability of a TFE Teflon tube was measured, the tube was inserted in the absorption tower stack for one year, and the permeability was then remeasured. A permeability decrease of about 15% was found. This change would appear as a span drift, and would easily be accounted for by periodic recalibration of the device. This result suggests the potential usefulness of Teflon interfaces for long-term continuous unattended monitoring in corrosive atmospheres.

On the other hand, a fluorosilicone rubber tube placed in the stack showed obvious signs of deterioration after 12 hours, suggesting that this material is unsuitable for use in an acid mist environment.

6.2.2 SO_3 Absorption Tower Stack: Double Contact Process

A 2-day monitoring run was carried out in the SO_3 absorption tower stack of a double contact process sulfuric acid plant. The average concentration of SO_2 in the stack gas was 85 ppm, and the stack gas temperature was 67°C. To obtain a permeation rate sufficiently high for the carrier gas SO_2 concentration to be within the operating range of the analyzer (0.02-0.5 ppm), a tube with a very thin wall had to be constructed; this was done by wrapping and heat-sealing a 2-mil (0.005 cm) FEP Teflon membrane about a porous stainless steel support. The continuous readings obtained using this device were compared with readings obtained with an on-stream stack gas analyzer operated by plant employees.

---

*Attached as Appendix D.

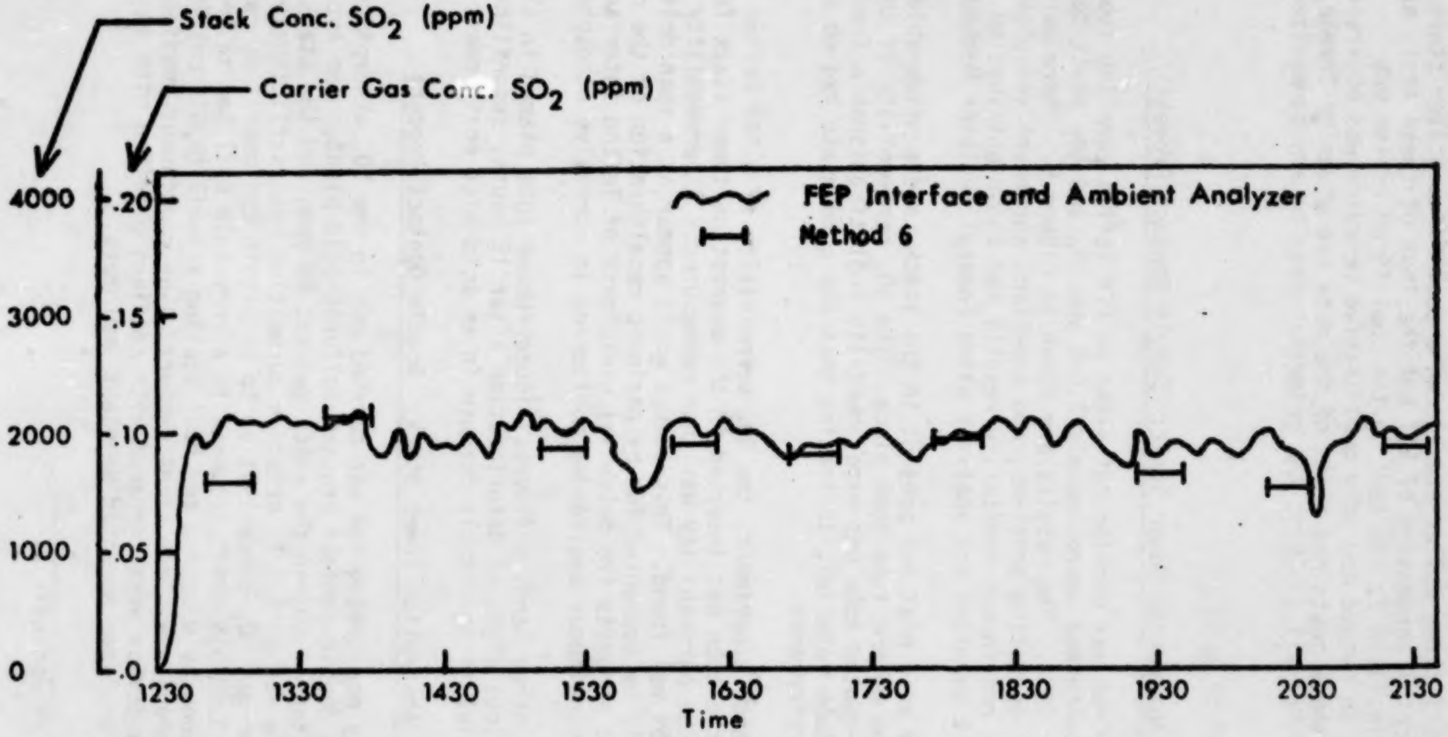

Figure 9. Monitoring data: Single contact process stack.

The results of these tests are shown in Figure 10. The data obtained using the permeable interface exhibited less fluctuation and greater day-to-day reliability than the results of on-stream measurements. Moreover, the use of the plant instrument since the test has had to be curtailed due to the effects of corrosion, a problem less likely to occur if the in-situ interface were used on a continuing basis.

These results and those obtained in the single contact process stack indicate that polymeric interfaces can be used to monitor stacks containing SO_2 at concentrations which vary over a wide range. The concentration in the first stack, ≈2,000 ppm, is typical of uncontrolled emissions from many process and power plant stacks, while that in the second stack, ≈85 ppm, is characteristic of a controlled emission. A system composed of two probes and a single analyzer might therefore be used to measure the effectiveness of an SO_2 removal process by monitoring both the inlet and outlet SO_2 concentrations.

6.2.3 Oil-Fired Power Plant Boiler Stack

Monitoring runs were carried out in an oil-fired power plant boiler at North Carolina State University. A No. 6 fuel oil containing 1.9% sulfur was burned, and the SO_2 content of the stack gas varied between 250 and 1,045 ppm as the load on the boiler was changed. The stack temperature fluctuated between 170 and 213°C.

Monitoring data obtained in a 2½-hour interval are shown in Figure 11. The feed rate of oil to the furnace, which correlates with the SO_2 concentration in the stack, is also shown as a function of time in Figure 11.

The results of these tests again showed excellent agreement between measurements obtained with the permeable interface and others obtained by direct sampling and analysis using Federal Register Method 6. Moreover, the ability of the sampling interface to follow changes in the SO_2 concentration in the stack is illustrated by the results: as the plots of Figure 11 indicate, changes in the boiler loading were followed extremely rapidly by proportional changes in the analyzer signal.

A gross measurement of the particulate concentration in the stack using Federal Register Method 5 yielded a loading of 0.21g/m^3. Inspection of the sampling tube at the conclusion of the tests revealed a slight powdery deposit on the tube surface, but recalibration measurements indicated that this layer had no effect on the SO_2 permeability of the tube.

6.2.4 Coal-Fired Power Plant Boiler Stack

A 1-day monitoring run was carried out in the stack of a coal-fired power plant boiler, under extremely heavy particulate loading conditions.

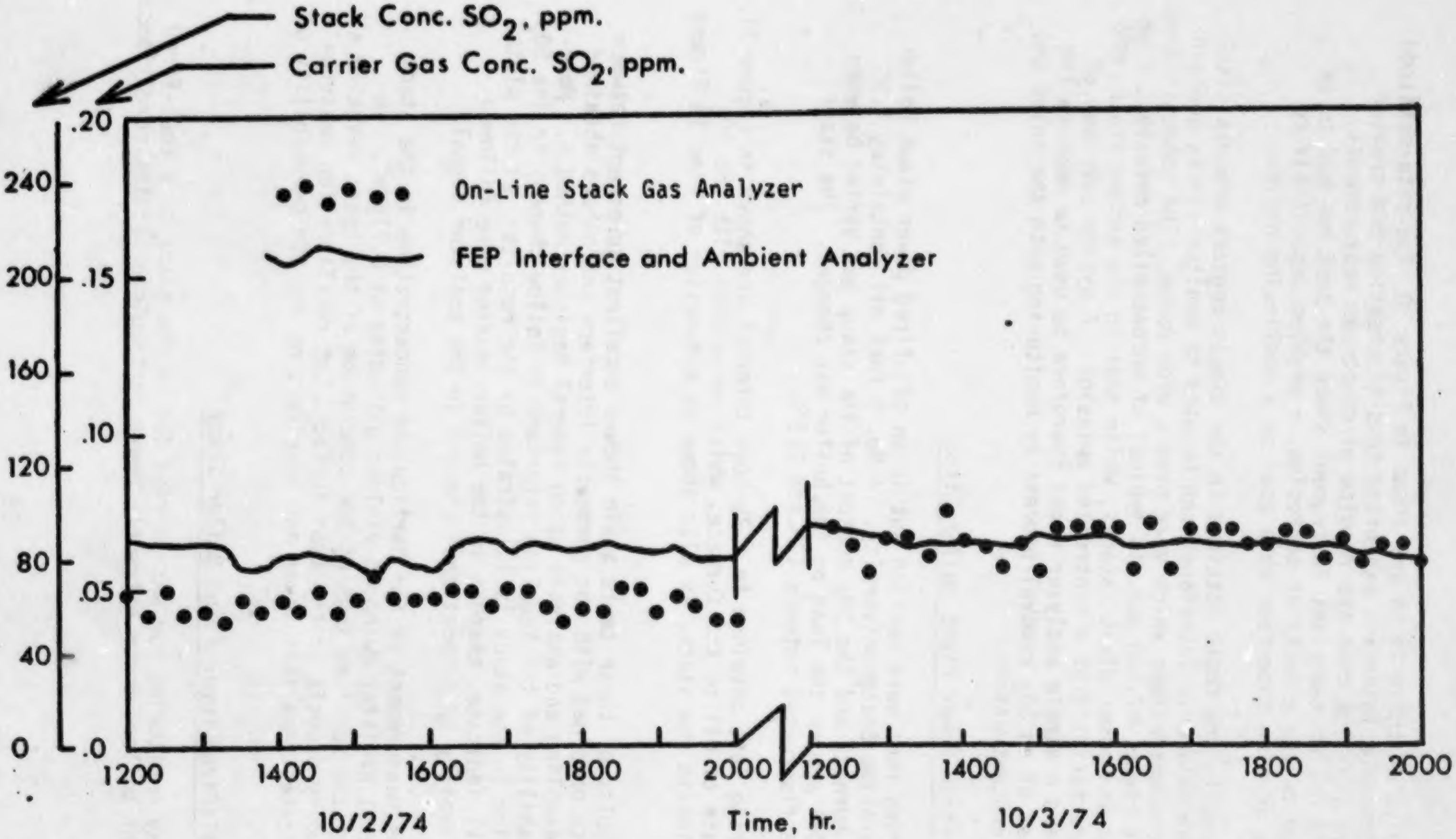

Figure 10. Monitoring data: Double contact process stack.

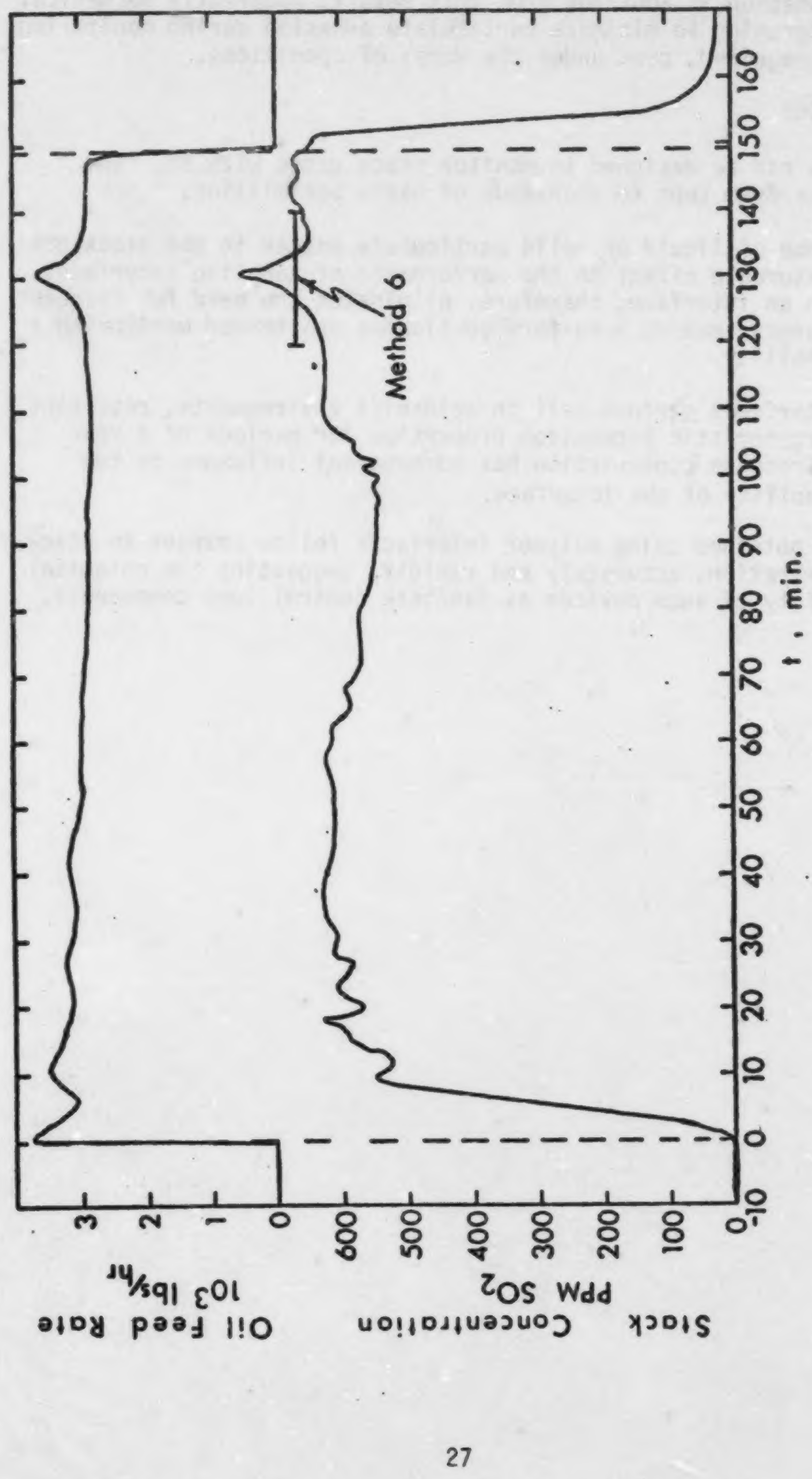

Figure 11. Monitoring data: Boiler stack, 1-day run.

At the end of this monitoring run, the probe was withdrawn and inspected. The stainless steel portions of the probe were literally invisible, caked with a layer of soot, while the Teflon interface was almost completely clean. The ability of Teflon interfaces to resist particulate adhesion is apparent from this result; apparently mechanical vibrating or scraping to minimize particulate adhesion during monitoring should not be required, even under the worst of conditions.

6.3 CONCLUSIONS

1. Interfaces can be designed to monitor stack gases with SO_2 concentrations from tens to thousands of parts per million.

2 The presence of liquid or solid particulate matter in the stack gas has no measurable effect on the performance of sampling interfaces. Using such an interface, therefore, eliminates the need for frequent filter changes, making long-term continuous unattended monitoring a good possibility.

3. Teflon interfaces perform well in acid mist environments, retaining their characteristic permeation properties for periods of a year and up. Dropwise condensation has no apparent influence on the SO_2 permeability of the interface.

4. Responses obtained using polymer interfaces follow changes in stack gas concentrations accurately and rapidly, suggesting the potential applicability of such devices as feedback control loop components.

SECTION 7

MEASUREMENT OF GAS DIFFUSIVITIES IN POLYMERS

The rate of permeation of a gas into a polymer interface is determined by the permeability of the interface material to the gas. The permeability is the product of the solubility and the diffusivity of the gas in the polymer, but these terms individually have no effect on the steady-state response of the device. The transient response of an interface to changes in stack conditions is another matter, however; the dissolution of the gas in the polymer can be considered instantaneous, so that the diffusivity alone is the prime factor in determining the time required for the interface to respond to changes in its environment.

Initial tests of interface response times to changes in span gas SO_2 concentrations were purely empirical. (Rodes et al, 1973) To better understand the nature of the responses, it was decided to measure diffusivities of SO_2 in the materials used as interfaces. A technique was developed whereby these measurements could be made in the continuous-flow apparatus which had been used for the permeability studies; although this was initially done for convenience, the method proved to possess considerable advantages over the techniques which have been traditionally used for diffusivity measurements.

7.1 PROCEDURE FOR DIFFUSIVITY MEASUREMENTS

A polymer tube or membrane is mounted in the chamber used for permeability measurements, and the chamber is placed in the thermostatically-controlled oven. The schematic diagram of Figure 1 depicts the system.

The flow rate of the span gas with a known penetrant concentration commences at a time t=0, and the response R(t) of the analyzer to the carrier gas penetrant concentration is recorded. The run is terminated when R(t) has leveled off to a value of R_s and remained there for at least 15 minutes. The following quantities are then calculated:

$$M_0' = \int_0^\infty \left[1 - \frac{R(t)}{R_s}\right] dt \qquad (7\text{-}1)$$

$$\tau_a = \int_0^\infty \left[1 - \frac{R_a(t)}{R_{as}}\right] dt \qquad (7\text{-}2)$$

where $R_a(t)$ is the response of the SO_2 analyzer to a step change in SO_2 concentration at its inlet, and R_{as} is the asymptotic(steady-state) value of this response. Both M_0' and τ_a are determined by numerical integration of measured response data.

$$\tau_1 = \frac{\text{Volume of span gas line preceding chamber}}{\text{Volumetric flow rate of span gas}} \qquad (7\text{-}3)$$

$$\tau_2 = \frac{\text{Volume of span gas chamber}}{\text{Volumetric flow rate}} \qquad (7\text{-}4)$$

$$\tau_3 = \frac{\text{Volume of carrier gas line following chamber}}{\text{Volumetric flow rate of carrier gas}} \qquad (7\text{-}5)$$

$$M_0 = M_0' - (\tau_a + \tau_1 + \tau_2 + \tau_3) \qquad (7\text{-}6)$$

The diffusivity can be calculated from M_o and geometrical parameters of the interface. For a flat membrane of thickness h,

$$D = h^2/6M_0 \qquad (7\text{-}7)$$

and for a hollow cylindrical tube of inner radius a and outer radius b

$$D = [a^2 - b^2 + (a^2+b^2)\ \ln (b/a)]/4M_0\ \ell n(b/a) \qquad (7\text{-}8)$$

The derivation of Eqs. (7-7) and (7-8) is given by Felder, Spence, and Ferrell (1975b),[*] and Eqs. (7-1) - (7-6) for calculating M_o from measured response data are derived by Felder, Ma, and Ferrell (1976).[+]

Once the diffusivity D has been determined for a polymer in the manner indicated, and the permeability P has been measured as outlined in Section 4, the solubility of the gas in the polymer may be calculated as S = P/D.

7.2 DIFFUSIVITIES OF SO_2

Diffusivities of SO_2 have been measured at temperatures from 21°C to 227°C in Teflon and fluorosilicone rubber tubes. The results are given by Felder, Spence and Ferrell (1975b)[*] and Felder, Ma, and Ferrell (1976).[+]

The Arrhenius plots of the measured diffusivities shown in the figures of Appendices E and F are linear, although variations are observed between different tubes of the same material. Several span gas SO_2 concentrations were used; the near coincidence of the diffusivities measured for the different concentrations at a fixed temperature suggests the constancy of D at the SO_2 partial pressures of 10 mm Hg and less normally encountered in stack gases. As a test of the validity of the diffusivity estimation technique, the theoretical expression for the transient response was evaluated using diffusivities estimated at three different temperatures. The close correspondence between the theoretical curves and the measured responses at each temperature shown in Figure 3 of Appendix F validates both the diffusivity estimation technique and the diffusion model upon which the technique is based.

---

[*] Attached as Appendix E.

[+] Attached as Appendix F.

REFERENCES

Crank, J. and G. S. Park, in Diffusion in Polymers (J. Crank and G. S. Park, eds.). Academic Press, New York (1968), p. 1.

Felder, R. M., J. K. Ferrell, and J. J. Spivey. Effects of Moisture on the Performance of Permeation Sampling Devices. Anal. Instrumentation, 12, 35 (1974).

Felder, R. M., C-C Ma and J. K. Ferrell. A Method of Moments for Measuring Diffusivities of Gases in Polymers. A.I.Ch.E. Journal, 22, 724 (1976).

Felder, R. M., R. D. Spence and J. K. Ferrell, (a) Permeation of Sulfur Dioxide through Polymers. J. Chem. Eng. Data, 20, 235 (1975); (b) A Method for the Dynamic Measurement of Diffusivities of Gases in Polymers. J. Appl. Poly. Sci, 19, 3193 (1975).

Rodes, C. E., R. M. Felder, and J. K. Ferrell. Permeation of Sulfur Dioxide through Polymeric Stack Sampling Interfaces. Environ. Sci. Technol., 7, 545 (1973).

Seibel, D. R. and F. P. McCandless. Separation of Sulfur Dioxide and Nitrogen by Permeation through a Sulfolane Plasticized Vinylidene Fluoride Film. Ind. Eng. Chem. Proc. Des. Dev., 13, 76 (1974).

Spence, R. D. Development of a Polymeric Interface as an SO_2 Stack Monitor. Ph.D. Thesis, North Carolina State University, Raleigh, N. C. (1975).

Spivey, J. J. Effects of Water Vapor on the Performance of Polymeric Stack Sampling Interfaces. M.S. Thesis, North Carolina State University, Raleigh, N. C. (1974).

Treece, L. C. Development and Testing of Polymeric Materials for Use as a Stack Sampling Interface. M.S. Thesis, North Carolina State University, Raleigh, N. C. (1975).

Treece, L. C., R. M. Felder and J. K. Ferrell. Polymeric Interfaces for Continuous SO_2 Monitoring in Process and Power Plant Stacks. Env. Sci. Technol. 10, 457(1976).

APPENDIX A

PERMEATION OF SULFUR DIOXIDE THROUGH POLYMERS*

R. M. Felder, R. D. Spence and J. K. Ferrell
Department of Chemical Engineering
North Carolina State University
Raleigh, North Carolina 27607

ABSTRACT

Permeabilities, diffusivities, solubilities and activation energies for permeation and diffusion are reported for the permeation of SO_2 through various polymers. Effects of gas pressure and humidity and membrane plasticization on SO_2 permeabilities are summarized.

---

*Published as J. Chem. Eng. Data 20, 235 (1975). Reprinted by permission of the American Chemical Society.

INTRODUCTION

The permeability of a polymer to a gas or vapor is the ratio $J/(\Delta p/h)$, where J is the flux of the gas through a flat membrane of thickness h, and Δp is the partial pressure difference across the membrane. If the equilibrium sorption of the gas in the polymer varies linearly with the partial pressure in the gas phase and diffusion of the gas through the polymer is Fickian with a constant diffusivity, then

$$P = DS \qquad (1)$$

where

P = permeability, $cm^3(STP)/s \cdot cm \cdot cm\ Hg$

D = diffusivity, cm^2/s

S = solubility, $cm^3(STP)/cm^3$

The temperature dependence of gas permeabilities frequently follows an Arrhenius relationship

$$P = P_o \exp(-E_p/RT) \qquad (2)$$

where E_p is the activation energy for permeation. Techniques for the measurement of P, D and S are reviewed by Crank and Park (6), and factors which affect the values of these parameters are discussed by Stannett (34).

SO_2 permeabilities of a number of materials have been measured at temperatures from 25°C to 232°C, and activation energies for permeation have been calculated. This paper reports the results of these experiments. In the course of this study, a literature search on the permeation of SO_2 through polymers was carried out, covering references through April 1974.

Relatively few reported permeabilities were found, but a number of papers presented permeation rate data from which permeabilities could be calculated. These calculations have been performed, and the results are also reported in this paper.

EXPERIMENTAL

Span gas mixtures of SO_2 in air with SO_2 concentrations in the range 1,000-10,000 ppm were passed on one side of a flat polymer membrane or on the outside of a hollow tube in a thermostatically-controlled oven. SO_2 permeated through the polymer into a carrier gas stream of pure air, which passed to an SO_2 analyzer. The SO_2 permeation rate was calculated as the product of the carrier gas flow rate and the SO_2 concentration in this gas at steady-state; the permeability of the polymer to SO_2 was then calculated from the permeation rate, the SO_2 partial pressures in the span gas and the carrier gas, and the dimensions of the membrane or tube.

The experimental and calculational procedures for determining permeabilities and the permeation chamber used for hollow tubes are described in detail by Rodes, Felder and Ferrell (23). A two-piece hollow stainless steel cylinder with OD = 7.62 cm, ID = 5.08 cm, and outside height = 7.0 cm was used as a permeation chamber for flat membranes. The membranes were clamped between the two halves of the chamber, and the span gas and carrier gas were fed into the chamber on opposite sides of the membrane. The entrance and exit ports were situated such that the gases entered tangentially and swept across the entire membrane surface before exiting.

Span gas SO_2 concentrations were determined by passing a measured volume of the gas through a 3% H_2O_2 solution to absorb the SO_2, and then titrating with a 0.01N barium perchlorate solution in the presence of Thorin indicator (9). Carrier gas SO_2 concentrations were measured with a Meloy Laboratories Model SA-160 total sulfur analyzer or an Envirometrics Model NS-300M SO_2 analyzer.

PERMEABILITIES, DIFFUSIVITIES AND SOLUBILITIES

Materials for which SO_2 permeabilities, diffusivities and/or solubilities have been found include TFE Teflon, FEP Teflon, several silicone and fluorosilicone rubbers, polyvinyl fluoride (Tedlar), polyvinylidene fluoride (Kynar), polycarbonate (Lexan), polyethylene, polypropylene, polyvinyl chloride, copolymers of polyvinyl chloride and polyvinylide chloride, several natural rubbers, polyisobutene, polymethyl methacrylate, polyethylterephthalate (Mylar), several cellulosic films, and a chlorinated polyether (Penton), and a polyethylene glycol liquid membrane. While most of the data are for temperatures in the range 15-30°C, permeabilities have been measured over temperature ranges broad enough to permit the determination of activation energies for TFE and FEP Teflon, a fluorosilicone and a silicone rubber, polyethylene, polyvinyl fluoride, and polyvinylidene fluoride. Measured and estimated permeabilities, diffusivities and solubilities are summarized in Table 1, and Arrhenius law parameters are listed in Table 2.

The permeabilities of TFE and FEP Teflon are similar, despite the probable differences in the degree of crystallinity of these two substances. This result supports a claim by Stern et. al. (35) that the two substances have similar permeabilities, but conflicts with assertions by Saltzman (24,25) that TFE may be as much as 10 times more permeable than FEP at the same temperature.

Extended use at temperatures close to 200°C did not affect either TFE or FEP, either in physical appearance or in permeability to SO_2. The fluorosilicone rubber (Dow-Corning: SILASTIC LS-63U®) maintained a constant permeability with extended usage, although it underwent a discoloration and deteriorated when subjected to an acid mist environment. The silicone rubber

(Dow-Corning: SILASTIC 437) became brittle at high temperatures (23), probably due to attack by SO_2 (16).

Permeabilities of SO_2 in TFE Teflon are summarized on an Arrhenius plot in Figure 1. The high temperature permeabilities determined in the present study and by Rodes _et_. _al_. (23) are consistent with the permeability reported by Jordan (15) at a temperature presumably in the range 20-30°C. Values estimated from SO_2 permeation tube emission rate data (17) are substantially out of line with the other permeabilities, but the degree of uncertainty in the tube dimensions used to obtain these values is sufficient to account for the discrepancy.

An Arrhenius plot of SO_2 permeabilities in FEP Teflon is shown in Figure 2. A single line correlates the measured and estimated permeabilities reasonably well, except for values reported by Benarie and Bui-the-Chuong (1) and estimated from permeation tube emission rates reported by Stevens _et_. _al_. (36) and Metronics, Inc. (17). Permeabilities obtained for flat membranes 0.02-0.1 mm thick were consistently 5-20% higher than values obtained for cylindrical tubes with wall thicknesses in the range 0.3-0.7 mm.

Stern _et_. _al_. (35) indicate that a phase change occurs in FEP Teflon at 60°C which might affect its permeability. Figure 2 suggests that this effect is minimal, if it exists at all.

SO_2 permeabilities in silicone and fluorosilicone rubbers are shown in Figure 3. The permeability of SO_2 in these materials is between one and two orders of magnitude higher than that in Teflon, and the activation energy for permeation of the silicones is much lower than that of Teflon. High SO_2 permeabilities are also found for dimethyl silicone rubbers, which are discussed by Robb (22), Hodgson (13) and an undated General Electric brochure (11). Permeabilities calculated at high temperatures for a fluorosilicone rubber in the present study and by Rodes et. al. (23) do not agree particularly well; however, the material in question was not available commercially when the latter measurements were made and the differences in the permeabilities of different tubes might reflect a difference in fabrication methods from one batch to another.

SO_2 permeabilities in polyethylene are given by several authors (1,3, 7,12,15). The permeability reported by Jordan (15) appears far too high, assuming that it was obtained in the temperature range 20-30°C; the other values are shown on an Arrhenius plot in Figure 4.

Studies of SO_2 transport in polymers which are not referenced in Table 1 have been carried out by Sano and coworkers (27-30), Stoeckli (37), and Svoboda and coworkers (38-40). References 27-30 deal with the permeation of SO_2 through polyethylene and plasticized polyvinyl chloride membranes, Reference 37 with sorption of SO_2 on polyvinylidene chloride, and References 38-40 with penetration of SO_2 into alkyd resins.

EFFECT OF TEMPERATURE ON PERMEABILITY

The Arrhenius plots of Figures 1,2 and 4 for TFE Teflon, FEP Teflon and polyethylene have been fit by linear regression to obtain the pre-exponential factors and activation energies listed in Table 2. The following data points were excluded from the regressions: Figure 1 -- Metronics; Figure 2 -- Stevens et. al. and Benarie and Bui-the-Chuong; Figure 4 -- all but Brubaker and Kammermeyer. Also listed in Table 2 are published activation energies for permeation of SO_2 through polyvinyl fluoride, polyvinylidene fluoride and polyethylene.

The permeabilities of silicone and fluorosilicone rubbers shown in Figure 3 are too scattered to permit meaningful regressions; however, the following ranges for P and E_p may be deduced from the data:

$$\left.\begin{array}{l}\text{SILASTIC } 437^{\circledR}\text{silicone rubber}\\ \text{SILASTIC LS-63U}^{\circledR}\text{fluorosilicone rubber}\\ 50°\text{C} \le T \le 232°\text{C}\end{array}\right\} \begin{array}{l} 10^{-7} \le P \le 5\text{x}10^{-7}\ \dfrac{\text{cm}^3\text{(STP)}}{\text{s}\cdot\text{cm}\cdot\text{cm Hg}}\\ 0.1 \le E_p \le 2\ \text{kcal/g-mole}\end{array}$$

EFFECT OF PRESSURE ON PERMEABILITY

At low pressures gas permeabilities, diffusivities and solubilities are characteristically independent of pressure (34). The high temperature permeation measurements reported in Table 1 -- for which the total pressures were close to atmospheric and partial pressures of SO_2 were in the range 0.08-1.3 cm Hg -- show this behavior: plots of permeation rate vs. SO_2 partial pressure obtained by Rodes et. al. (23) and in the present study were linear, with correlation coefficients usually in excess of 0.99.

Under some circumstances, however, the effective permeability of a substance depends on the partial pressure of the permeating species and/or the total pressure on the high concentration side of the interface. The cause may be the departure of the solubility of the material from Henry's Law behavior, a concentration-dependent diffusivity, or the occurrence of permeation by a mechanism other than solution followed by activated diffusion.

Pressure-dependent SO_2 permeabilities have been observed by Davis and Rooney (7) for polyethylene, polycarbonate and polyamide membranes, and by Seibel and McCandless (32) for polyvinylidene fluoride (Kynar). Seibel and McCandless worked at total pressures of 100-500 psig -- pressures at which any or all of the factors indicated could cause the observed pressure dependence of the effective permeability.

Solubilities of SO_2 in polyethylene and polymethyl methacrylate reported by Jordan (15) show a considerable departure from Henry's law. Davis and Rooney (7) report a Henry's law dependence for SO_2 in polyethylene, deviations from this behavior in polycarbonate and polyamide, and concentration-dependent diffusivities for all three materials.

Davis and Rooney (7) and Perret _et_. _al_. (20) present diffusivity and solubility correlations for SO_2 in the range 0-25°C. In the equations that follow, p_{SO_2} is the SO_2 partial pressure in cm Hg, C_{SO_2} the absorbed SO_2 concentration in cm^3 SO_2(STP)/cm^3 polymer, and D the SO_2 diffusivity in cm^2/s.

1. Polyamide at 25°C (7)

$$C = \frac{0.98\, p_{SO_2}}{1.0 + 0.169\, p_{SO_2}} + 0.298\, p_{SO_2} \tag{3}$$

$$D\times10^{10} \left\{ \begin{aligned} &= 3.63\times(10)^{0.05\,C} && \text{(4a)} \\ & && \text{(Determinations by two different methods)} \\ &= 2.63\times(10)^{0.06\,C} && \text{(4b)} \end{aligned} \right.$$

2. Polycarbonate at 25°C (7)

$$C = \frac{2.44\, p_{SO_2}}{1.0 + 0.241\, p_{SO_2}} + 0.522\, p_{SO_2} \tag{5}$$

3. Polyvinyl chloride (20)

$$0°\text{C}: \quad C = 0.719\, p_{SO_2} + 2.155 \qquad p_{SO_2} > 3 \text{ cm Hg} \qquad (6)$$

$$20°\text{C}: \quad C = 0.393\, p_{SO_2} + 1.472 \qquad p_{SO_2} > 54 \text{ cm Hg} \qquad (7)$$

The sorption isotherms given by Eqs. (3), (5), (6) and (7) are consistent with the dual mode mechanism proposed by Michaels et. al. (18) for sorption in glassy polymers. According to this mechanism, sorption is a combination of ordinary Henry's law solution -- which leads to a linear component of the isotherm -- and microvoid or hole-filling, which gives rise to a Langmuir expression. Both components of the isotherm appear explicitly in Eqs. (3) and (5). At sufficiently high pressures the isotherm becomes linear, with a slope equal to the Henry's law constant and a positive intercept -- cf. Eqs. (6) and (7).

EFFECT OF HUMIDITY ON PERMEABILITY

Stannett (34) observes that humidity has little effect on the permeability of gases through polymers in which water is only slightly soluble, but when water is highly sorbed the gas permeation rate may be significantly increased by an increase in humidity.

The few reported studies of the effects of humidity on SO_2 permeation confirm this observation. Felder, Ferrell and Spivey (10) report that the SO_2 permeabilities of TFE Teflon, FEP Teflon and SILASTIC LS-63U® fluorosilicone rubber tubes measured for dry gases and gases containing up to 21% water by volume are statistically indistinguishable at temperatures up to 200°C. Hanousek and Herynk (12) found that the permeability of polyethylene at 25°C decreased by 10-30% and the permeabilities of several types of paper decreased or remained unchanged when the relative humidity was raised from 0% to 84%, while the permeability of a polyamide increased by 33% and that of polyvinyl chloride increased by 10% for the same change in humidity. On the other hand, both Hanousek and Herynk (12) and Simril and Hershberger (33) report increases of an order of magnitude or more in the permeability of cellulosic films when the humidity was raised from 0% to 84-100%.

EFFECT OF PLASTICIZERS ON PERMEABILITY

The presence of a plasticizer in polymeric materials may increase the solubility and hence the permeability of these materials to water (34). Seibel and McCandless (32) utilized this principle to fabricate SO_2 - permeable membranes by adding sulfolane (an SO_2 solvent) as a plasticizer to polyvinylidene fluoride films. The addition of the sulfolane increased the permeability of SO_2 relative to that of N_2, with the separation factor increasing with decreasing temperature.

Sano has been the author or co-author of several patents and papers on the separation or removal of SO_2 by polyvinyl chloride membranes plasticized with dioctyl phthalate and tricresyl phosphate (27-30).

SUMMARY

Permeabilities of SO_2 in various polymers have been measured or calculated from published permeation rate data. Activation energies for permeation have been determined by fitting Arrhenius functions to permeability data for TFE Teflon, FEP Teflon, silicone and fluorosilicone rubbers, polyvinyl fluoride (Tedlar), polyvinylidene fluoride (Kynar) and polyethylene.

The permeabilities of TFE and FEP have been found to be similar, contradicting published assertions that TFE is considerably more permeable than FEP. Silicone and fluorosilicone rubbers are 10 to 100 times more permeable than Teflon, but they are also subject to embrittlement and attack by acid mist.

A transport model based on Henry's law for solution and Fick's law for diffusion correlates permeation data well for many materials at pressures of 1 atmosphere or less. At higher pressures deviations from these laws have been reported for polyethylene, polycarbonates and polyamides, polyvinyl chloride, polyvinylidene fluoride, and polymethyl methacrylate.

The observation of Stannett (34) that relative humidity affects the permeability of a gas through a polymer to the extent that the polymer absorbs water is borne out by the results of several experiments. As the humidity increases the permeabilities of TFE Teflon, FEP Teflon and fluorosilicone rubber tubes were unchanged, that of polyethylene decreased slightly, and those of a polyamide and of polyvinyl chloride increased slightly, while the permeabilities of cellulosic films increased substantially.

The addition of certain plasticizers to a polymer film may increase the permeability of the film to SO_2. This effect has been observed in sul-

folane-plasticized polyvinylidene fluoride and dioctyl phthalate and tricresyl phosphate - plasticized polyvinyl chloride films.

ACKNOWLEDGMENTS

This work was supported by Environmental Protection Agency Grant #801578. Mention of a commercial product or company name does not constitute endorsement by the Environmental Protection Agency.

The authors acknowledge with thanks assistance with the experiments provided by Mssrs. Chen-Chi Ma and Lanny C. Treece, helpful discussions with Professors Harold Hopfenberg and Vivian Stannett of North Carolina State University and Dr. James Homolya and Mr. Charles Rodes of the Environmental Protection Agency, and assistance with the manuscript preparation provided by Mrs. Mary Wade.

REFERENCES FOR APPENDIX A

1. Benarie, M. and Bui-the-Chuong, *Atm. Environ.*, *3*, 574 (1969).

2. Brocco, D. and Possanzini, M., *Inquimentato*, *14*, 21 (1972).

3. Brubaker, D. W. and Kammermeyer, K., *Ind. Eng. Chem.*, *46*, 733 (1954).

4. Chappuis, *Wied*. *Ann*., *19*, 21 (1883), referenced in Reychler (1921).

5. *Chemical Engineer's Handbook*, 5th Edition, R. H. Perry and C. H. Chilton, Editors, New York, McGraw-Hill (1973), p. 3-202.

6. Crank, J. and Park, G. S. in *Diffusion in Polymers*, J. Crank and G. S. Park, Editors, New York, Academic Press (1968), p. 1.

7. Davis, E. G. and Rooney, M. L., *Kolloid Z. Z. Poly*., *249*, 1043 (1971).

8. Dietz, R. N., Cote, E. A., and Smith, J. D., *Anal. Chem.*, *46*, 315 (1974).

9. *Federal Register*, *36*, 24890 (1971).

10. Felder, R. M., Ferrell, J. K., and Spivey, J. J., *Analysis Instrum.*, *12*, 35 (1974).

11. "General Electric Permselective Membranes," General Electric, Medical Development Operation, Chemical and Medical Division, Schenectady, N. Y.

12. Hanousek, J. and Herynk, L., *Chem. Listy*, *56*, 376 (1962).

13. Hodgson, M. E., *Filtr. and Sep.*, *10*, 418 (1973).

14. Hsieh, P. Y., *J. Appl. Polym. Sci.*, *7*, 1743 (1963).

15. Jordan, S., *Staub-Reinhalt Luft*, *33*, 36 (1973).

16. McIntyre, J. T., Dow Corning, Midland, Michigan, Private Communication (1974).

17. Metronics Product Bulletin No. 20-70, Metronics Associates, Inc., Palo Alto, California (1970).

18. Michaels, A. S., Vieth, W. R. and Barrie, J. A., *J. Appl. Phys.*, *34*, 13 (1963).

19. O'Keeffe, A. E. and Ortman, G. C., *Anal. Chem.*, *38*, 760 (1966).

20. Perret, E. A., Stoeckli, H. F., and Jeanneret, C., *Helv. Chim. Acta*, *55*, 1987 (1972).

21. Reychler, A., *J. Chim. Phys.* *8*, 617 (1910).

22. Robb, W. L., Ann. N. Y. Acad. Sci., 146, 119 (1968).

23. Rodes, C. E., Felder, R. M., and Ferrell, J. K., Environ. Sci. Technol., 7, 545 (1973).

24. Saltzman, B. E., Microfiche AD 727-516, Aerospace Medical Research Laboratory, Aerospace Division (1970).

25. Saltzman, B. E., Burg, W. R., and Ramaswamy, G., Environ. Sci. Technol., 5, 1121 (1971).

26. Saltzman, B. E., Feldmann, C. R. and O'Keeffe, A. E., Environ. Sci. Technol., 3, 1275 (1969).

27. Sano, H., Japanese Patent 19883 (1972).

28. Sano, H. and Otani, T., Osaki Kogyo Gijutsu Shikensho Kiho, 22, 24 (1971).

29. Sano, H. and Otani, T., Osaka Kogyo Gijutsu Shikensho Kiho, 22, 102 (1971).

30. Sano, H., Sakaguchi, S. and Tanaka, K., Japanese Patent 23785 (1972).

31. Scaringelli, F. P., Frey, S. A., and Saltzman, B. E., Am. Ind. Hyg. Assn. J., 28, 261 (1967).

32. Seibel, D. R. and McCandless, F. P., Ind. Eng. Chem. Proc. Des. Develop. 13, 76 (1974).

33. Simril, V. L. and Hershberger, A., Mod. Plast., 7, 95 (1950).

34. Stannett, V., in Diffusion in Polymers, J. Crank and G. S. Park, Editors, New York, Academic Press (1968), p. 41.

35. Stern, S. A., Sinclair, T. F., Gareis, P. J., Vahldieck, N. P., and Mohr, P. H., Ind. Eng. Chem., 57, 49 (1965).

36. Stevens, R. K., O'Keeffe, A. E., and Ortman, G. C., Environ. Sci. Technol. 3, 652 (1969).

37. Stoeckli, H. F., Helv. Chim. Acta, 55, 101 (1972).

38. Svoboda, M., Klicova, H., and Knapek, B., Prot. Steel Str. Atmos. Corr., Proc. Event. Eur. Fed. Corros., 57th 1970, 2, 343 (1971).

39. Svoboda, M., Knapek, B., and Smrckova, J., Farbe und Lack, 71, 809 (1965).

40. Svoboda, M., Knapek, B., and Smrckova, J., Farbe und Lack, 74, 659 (1968).

41. van Amerongen, G. J., J. Appl. Phys., 17, 972 (1946).

42. Venable, C. S. and Fuwa, T., J. Ind. Eng. Chem., 14, 139 (1922).

43. Ward, W. J., III, U. S. Patent 3625734, Dec. 1971.

Table I. SO_2 Permeabilities, Diffusivities, and Solubilities

Material	Temperature (°C)	Px10^{10}(a)	Dx10^{10}(b)	S(c)	Source
TFE Teflon tube OD=0.959 cm ID=0.806 cm	99	64.7	-	-	Present study
	128	107.	-	-	"
	131	105	-	-	"
	154	157.[d]	-	-	Felder *et*. *al*. (10)
	154	147.[d] (21.1% H_2O)	-	-	"
	173	212.	-	-	Present study
	175	242.	-	-	"
	175	249.	-	-	"
	179	221.[d]	-	-	Felder *et*. *al*. (10)
	179	231.[d] (21.1% H O)	-	-	"
	202	407.[d]	-	-	"
	230	473.	-	-	Present study
	241	557.	-	-	"
TFE Teflon tube OD=0.604 cm ID=0.544 cm	52	14.9	-	-	"
	68	17.7	-	-	"
	87	34.9	-	-	"
	127	55.2	-	-	"

Note: Footnotes on last page of table.

Table I (Cont'd)

Material	Temperature (°C)	Px10^{10} (a)	Dx10^{10} (b)	S (c)	Source
TFE Teflon tube heat-shrunk on a porous sintered stainless steel tube	152	145.	-	-	Present study
	175	197.	-	-	"
	201	285	-	-	"
TFE Teflon	20	11.4^{j,k}	-	-	Metronics (17)
	25^{l}	5.1	1300.	0.04	Jordan (15)
	30	17.8^{j,k}	-	-	Metronics (17)
	40	26.5^{j,k}	-	-	"
	93.3	29.9	-	-	Rodes *et*. *al*. (23)
	121	53.9	-	-	"
	121	57.6	-	-	"
	149	92.3	-	-	"
	177	181.	-	-	"
	177	154.	-	-	"
	204	234.	-	-	"
	232	448.	-	-	"
	232	427.	-	-	"
FEP Teflon tubes	127	60.	-	-	Present study
	158	124.	-	-	"
	175	256.^{d}	-	-	Felder *et*. *al*. (10)
	175	262.	-	-	Present study
	180	203.^{d}	-	-	Felder *et*. *al*. (10)
	201	384.^{d}	-	-	"

Table I (Cont'd)

Material	Temperature (°C)	$\mathrm{Px10}^{10}$(a)	$\mathrm{Dx10}^{10}$(b)	S(c)	Source
FEP Teflon heat-shrunk on a porous sintered stainless steel tube	126	68.4	-	-	Present study
	127	73.9	-	-	"
	152	128.	-	-	"
	181	242.	-	-	"
	196	316.	-	-	"
FEP Teflon tube heat-shrunk on a stainless steel coil	211.5	457.	-	-	"
FEP Teflon tube heat-shrunk with no support	124	62.4	-	-	"
	125	65.5	-	-	"
	150	120.	-	-	"
	179	219.	-	-	"
	194	285.	-	-	"
FEP Teflon Membrane 0.00263 cm thick	24	5.84	-	-	"
	47	11.9[j]	-	-	"
	48	13.6	-	-	"
	73	26.5[j]	-	-	"
	85	37.4 (32.5% H_2O)	-	-	"
	94	50.9	-	-	"
	97	44.7 (32.5% H_2O)	-	-	"
	115	91.7	-	-	"
	122	85.0	-	-	"

Table I (Cont'd)

Material	Temperature (°C)	$Px10^{10(a)}$	$Dx10^{10(b)}$	$S^{(c)}$	Source
FEP Teflon Membrane 0.0144 cm thick	74	22.3	-	-	Present study
	122	96.8	-	-	"
	147	103.	-	-	"
	149.5	179.	-	-	"
FEP Teflon	13.8	1.6^{k}	-	-	O'Keefe & Ortman (19)
	20	2.6^{k}	-	-	Scaringelli *et*. *al*. (31)
	20	3.2^{k}	-	-	"
	20	$2.3^{j,k}$	-	-	Metronics (17)
	20.1	2.4^{k}	-	-	O'Keeffe and Ortman (19)
	20.3	46.8^{k}	-	-	Stevens *et*. *al*. (36)
	22	65.8	70	0.922	Benarie & Bui-the-Chuong (1)
	25	$3.3^{j,k}$	-	-	Saltzman *et*. *al*. (26)
	25	$3.4^{j,k}$	-	-	"
	25	$4.0^{j,k}$	-	-	"
	25	4.2	-	-	"
	25	$4.0^{j,k}$	-	-	"
	25	$4.0^{j,k}$	-	-	"
	25	$3.3^{j,k}$	-	-	"
	25	$3.5^{j,k}$	-	-	"
	29.1	3.6^{k}	-	-	O'Keeffe and Ortman (19)
	30	$7.1^{j,k}$	-	-	Dietz *et*. *al*. (8)
	30	$3.8^{j,k}$	-	-	Metronics (17)
	30	4.5	-	-	"
	40	$5.8^{j,k}$	-	-	"

Table 1 (Cont'd)

Material	Temperature (°C)	$Px10^{10}$ (a)	$Dx10^{10}$ (b)	S (c)	Source
	40	$7.4^{j,k}$	-	-	Metronics (17)
	50.5	$17.4^{j,k}$	-	-	Dietz et. al. (8)
	60	$24.6^{j,k}$	-	-	"
Tecsil (silicone rubber)	22	11,800	-	-	Benarie & Bui-the-Chuong (1)
Silastic LS-63® (silicone rubber)	121	2,620	-	-	Rodes et. al. (23)
	177	2,810	-	-	"
	204	3,130	-	-	"
	232	3,480	-	-	"
Dimethyl Silicone (25%)	25	11,450	-	-	General Electric (11)
	25	13,730	-	-	Robb (22)
Dimethyl Silicone Peroxide cured, silica filler	25^{l}	$43,630^{j}$	-	-	Hodgson (1973)
Silastic LS-63U® (fluorosilicone rubber) ube OD=0.929 cm. ID=0.521 cm.	129	3,180	-	-	Present study
	160	3,330	-	-	"
	175	$3,130^{d}$	-	-	Felder et. al. (10)
	177	$3,240^{d}$ (21.1% H_2O)	-	-	"
	183	3,350	-	-	Present study
	195	$3,290^{d}$	-	-	Felder et. al. (10)
	195	$3,350^{d}$ (21.1% H_2O)	-	-	"
	225	$3,340^{d}$	-	-	"
	225	$3,430^{d}$ (21.1% H_2O)	-	-	"

Table I (Cont'd)

Material	Temperature (°C)	$Px10^{10}$(a)	$Dx10^{10}$(b)	S(c)	Source
Silastic LS-63U® tube	27	2,720	-	-	Present study
OD=0.848 cm.	44	2,950	-	-	"
ID=0.744 cm.	68	3,290	-	-	"
	100	3,350	-	-	"
	129	3,650	-	-	"
Silastic LS-63U tubes	121	2,360	-	-	Rodes et. al. (23)
	149	2,580	-	-	"
	177	2,880	-	-	"
	204	3,160	-	-	"
Polyvinyl fluoride (Tedlar) membrane	70	15.5	-	-	Present study
	80	23.7	-	-	"
	88	31.4	-	-	"
0.006196 cm thick	100.5	61.5	-	-	"
	104	54.1	-	-	"
Polyvinylidene fluoride (Kynar) membrane 0.00417 cm thick	39	3.20	-	-	Present study
	45	4.62	-	-	"
	55	7.56	-	-	"
	65	12.2	-	-	"
(Kynar)	23	2.51 (100 psig)[j]	-	-	Seibel & McCandless (32)
		2.68 (200 psig)[j]	-	-	"
		2.28 (300 psig)[j]	-	-	"
		3.47 (400 psig)[j]	-	-	"
		9.49 (500 psig)[j]	-	-	"

Table I (Cont'd)

Material	Temperature (°C)	Px10^{10}(a)	Dx10^{10}(b)	S(c)	Source
(Kynar + 8.2% Sulfolane)	13	7.29 (300 psig)^{j}	-	-	Seibel & McCandless (32)
		15.9 (400 psig)^{j}	-	-	"
	23	3.79 (100 psig)^{j}	-	-	"
		5.36 (200 psig)^{j}	-	-	"
		13.7 (300 psig)^{j}	-	-	"
		19.4 (400 psig)^{j}	-	-	"
		36.1 (500 psig)^{j}	-	-	"
	32	16.4 (300 psig)^{j}	-	-	"
		26.4 (400 psig)^{j}	-	-	"
		42.3 (500 psig)^{j}	-	-	"
	42	18.2 (300 psig)^{j}	-	-	"
		24.2 (400 psig)^{j}	-	-	"
		38.1 (500 psig)^{j}	-	-	"
	47	16.4 (300 psig)^{j}	-	-	"
		27.8 (400 psig)^{j}	-	-	"
		38.8 (500 psig)^{j}	-	-	"
	64	29.3 (300 psig)^{j}	-	-	"
		32.6 (400 psig)^{j}	-	-	"
		47.2 (500 psig)^{j}	-	-	"
	73	31.9 (300 psig)^{j}	-	-	"
		38.8 (400 psig)^{j}	-	-	"
		47.9 (500 psig)^{j}	-	-	"
Polycarbonate (Lexan)	25	22.4	-	Eq. (5) in text	Davis & Rooney (7)

Table I (Cont'd)

Material	Temperature (°C)	$P \times 10^{10(a)}$	$D \times 10^{10(b)}$	$S^{(c)}$	Source
Polyethylene (Visqueen)	6.5	9.0	-	-	Brubaker & Kammermeyer (3)
	11.5	13.0	-	-	"
	13	13.0	-	-	"
	15	17.0	-	-	"
	20.5	24.0	-	-	"
(Polyane)	22	43.4	30.	1.45	Benarie & Bui-the-Chuong (1)
(Visqueen)	23	28.0	-	-	Brubaker & Kammermeyer (3)
	25	20.9^{e}	1120	0.0191	Davis & Rooney (7)
	25	16.2^{f}	854^{g}	-	"
	25^{l}	840.0	1800	0.47	Jordan (15)
(NSR)	25	24.5 (0% RH)^{m}	-	-	Hanousek & Herynk (12)
	25	21.8 (84% RH)^{m}	-	-	"
(CSSR)	25	31.6 (0% RH)^{m}	-	-	"
	25	21.3 (84% RH)^{m}	-	-	"
(Visqueen)	30	42.0	-	-	Brubaker & Kammermeyer (3)
	41.5	70.0	-	-	"
	42	70.0	-	-	"
Polypropylene (Maurylene)	22	6.18	3.5	1.71	Benarie & Bui-the-Chuong (1)
Polyvinyl chloride	0	-	-	Eq. (6) in text	Perret et. al. (20)
	20	-	-	Eq. (7) in text	"
	22	132.	400.	0.329	Benarie & Bui-the-Chuong (1)
	25^{l}	0.042	1.4	0.03	Jordan (15)

Table I (Cont'd)

Material	Temperature (°C)	$Px10^{10(a)}$	$Dx10^{10(b)}$	$S^{(c)}$	Source
	25	412 (0% RH)^{m}	-	-	Hanousek & Herynk (12)
	25	45 (84% RH)^{m}	-	-	"
Copolymer of vinylidene chloride & vinyl chloride	25	0.201	-	-	Davis & Rooney (7)
Polyamide (Rilsan)	22	21.1	10.	1.84	Benarie & Bui-the-Chuong (1)
(Nylon 11)	25	6.58	-	Eqs. (3) & (4) in text	Davis & Rooney (7)
(CSSR)	25	8.54 (0% RH)^{m}	-	-	Hanousek & Herynk (12)
	25	11.4 (84% RH)^{m}	-	-	"
Vinyril 11 Rilsan and Saran (copolymer of vinyl and vinylidene chloride)	22	1.18	0.6	1.97	Benarie & Bui-the-Chuong (1)
Vulcanized Natural Rubber	0	-	-	0.528	Chappuis (4)
	18.5	-	-	0.322	Reychler (21)
	20-22	-	-	0.256	Venable & Fuwa (42)
	22	1,450	10,000	0.158	Benarie & Bui-the-Chuong (1)
	25	-	-	0.311	van Amerongen (41)
	43	-	-	0.153	"
Buna S	25	-	-	0.227	van Amerongen (41)
	43	-	-	0.129	"

Table I (Cont'd)

Material	Temperature (°C)	$P\times10^{10(a)}$	$D\times10^{10(b)}$	$S^{(c)}$	Source
Perbunan	25	-	-	0.632	van Amerongen (41)
	43	-	-	0.310	"
Neoprene G	25	-	-	0.239	van Amerongen (41)
	43	-	-	0.138	"
Polyisobutene (Oppanol B 200)	25	-	-	0.047	van Amerongen (41)
	43	-	-	0.032	"
Polymethyl methacrylate (Plexiglass)	22	0.132	-	-	Benarie & Bui-the-Chuong (1)
	25^{l}	2.6	6.2	0.42	Jordan (15)
Polyethylterephthalate (Mylar)	22	5.27	1.6	3.29	Benarie & Bui-the-Chuong (1)
Cellulose Films	22	52.7	27.0	1.98	Benarie & Bui-the-Chuong (1)
(Cellafan, CSSR)	25	0.256 (0% RH)^{m}	-	-	Hanousek & Herynk (12)
	25	7.14 (84% RH)^{m}	-	-	"
(Cellofen, English)	25	2.43 (0% RH)^{m}	-	-	Hanousek & Herynk (12)
	25	20.4 (84% RH)^{m}	-	-	"
(Ethylcellulose)	25	264	530^{h}	0.498^{h}	Hsieh (14)
			734^{i}	0.360^{i}	"
(Nitrocellulose)	25	176	7.9^{h}	0.222^{h}	Hsien (14)
			18.0^{i}	0.0977^{i}	"

Table I (Cont'd)

Material	Temperature (°C)	$Px10^{10(a)}$	$Dx10^{10(b)}$	$S^{(c)}$	Source
(Nomex)	22	0.132	-	-	Benarie & Bui-the-Chuong (1)
Regenerated Cellulose Film	28.1	$0.77x10^{-7}$	-	-	Simril & Hershberger (33)
	24.5	$0.77x10^{-7}$	-	-	"
	24.5	0.00169 (100% RH)	-	-	"
(22% glycerol plasticizer)	24-25	$33.6x10^{-7}$	-	-	"
Paper Imp II	25.	3.09 (0% RH)^{m}	-	-	Hanousek & Herynk (12)
	25.	3.03 (84% RH)^{m}	-	-	"
Paper PLP II	25.	6.74 (0% RH)^{m}	-	-	"
Paper PLP I	25.	1.31 (84% RH)^{m}	-	-	"
Chlorinated Polyether (Penton)	25.^{1}	$< 10^{-15}$	-	0.01	Jordan (15)
Polyethylene glycol liquid membrane:porous polymer backing of solvinert coated with TFE dispersion	100.	81,300.	-	-	Ward (43)

Footnotes for Table I.

[a] Permeability, $cm^3(STP)/s \cdot cm \cdot cm\ Hg$

[b] Diffusivity, cm^2/s

[c] Solubility, $cm^3(STP)/cm^3 \cdot cm\ Hg$

[d] Values published by Felder, et. al. (1974) were based on a nominal cylinder span gas concentration reported by the supplier. A more accurate concentration has since been obtained, and the given value reflects the correction.

[e] SO_2 partial pressure > 25 cm Hg

[f] Calculated as $(DS)_{P_{SO_2} \to 0}$

[g] SO_2 partial pressure → 0

[h] Author measures S by a volumetric method and calculates $D = P/S$

[i] Author measures S by a gravimetric method and calculates $D = P/S$

[j] Rough estimate

[k] Deduced from permeation tube emission rate

[l] Speculation -- author did not report a temperature

[m] Speculation -- author did not report time units

Table II. Arrhenius Parameters for SO_2 Permeability

Material	$\ln P_o$	$S.D^{(a)}$	$P_o \times 10^5$ $^{(b)}$	E_p $^{(c)}$	$S.D^{(a)}$	Source
TFE Teflon	-10.39	0.27	3.07	6.54	0.23	Regression on Figure 1
	-	-	-	6.99	0.83	Rodes et. al. (23)
FEP Teflon	-9.54	0.20	7.23	7.18	0.14	Regression on Figure 2
	-	-	-	7.14^e	-	Dietz et. al. (8)
	-	-	-	9.08^e	-	Saltzman et. al. (26)
	-	-	-	9.08^e	-	Brocco and Possanzini (2)
	-	-	-	8.45^d	0.86^d	"
Silastic LS-63U® (fluorosilicone rubber)	-14.65	0.13	0.0435	0.253	0.118	Present study
	-14.01	0.13	0.0826	0.651	0.088	"
	-	-	-	1.33	0.38	Rodes et. al. (23)
Silastic LS-63® (silicone rubber)	-	-	-	0.94	0.87	"
PVF (Tedlar) Membrane	-6.49	0.28	152.	9.39	0.20	Present study
Polyvinylidene fluoride (Kynar) + 8.2% sulfolane						
(300 psig)	-13.24^d	0.97^d	0.178^d	4.32^d	0.60^d	Seibel and McCandless (32)
(400 psig)	-15.51^d	0.51^d	0.0183^d	2.67^d	0.32^d	"
(500 psig)	-17.62^d	0.55^d	0.00223^d	1.07^d	0.35^d	"
Polyethylene	-2.44^d	0.56^d	$8700.^d$	10.2^d	0.33^d	Regression on Figure 4

Footnotes for Table II.

[a] Standard deviation

[b] cm^3(STP)/s·cm·cm Hg

[c] kcal/gmole

[d] Calculated from data reported by author

[e] Calculated by subtracting a heat of evaporation ΔH_{evap} = 5.46 kcal/g-mole (5) from the published activation energy, which was for the combined processes of evaporation and permeation.

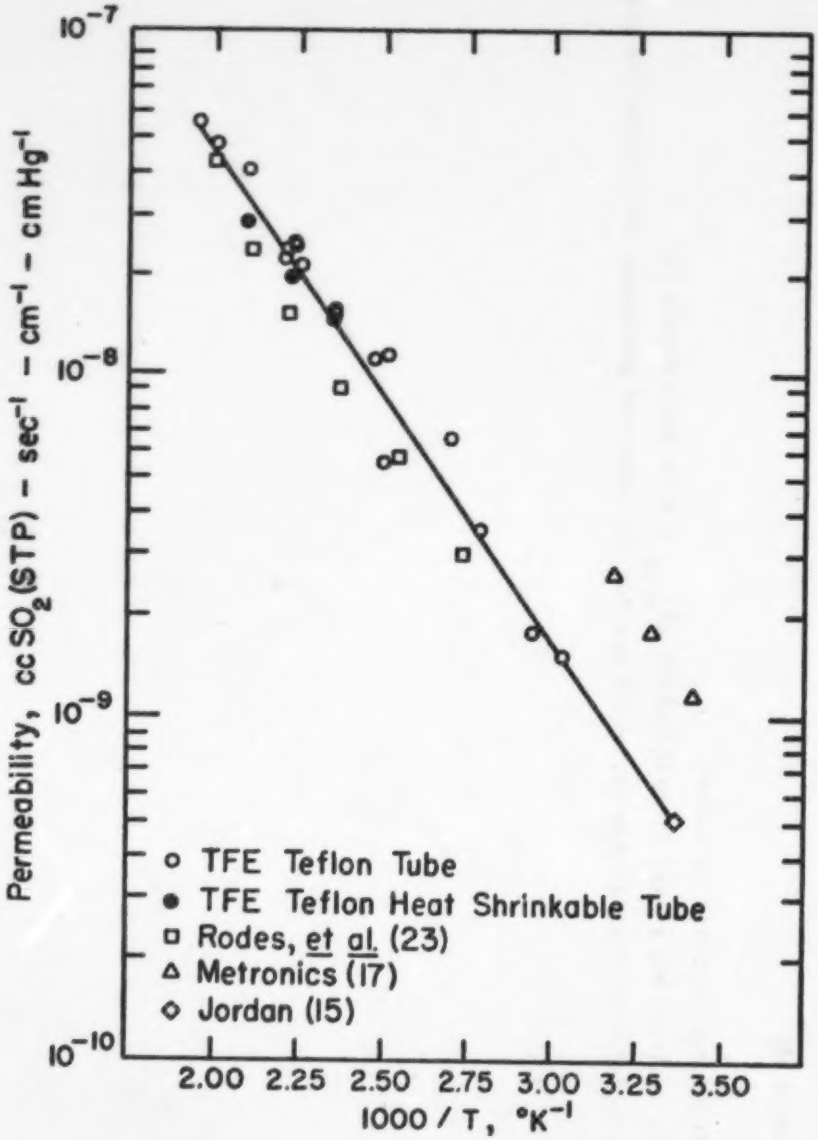

Figure 1. SO_2 Permeabilities of TFE Teflon.

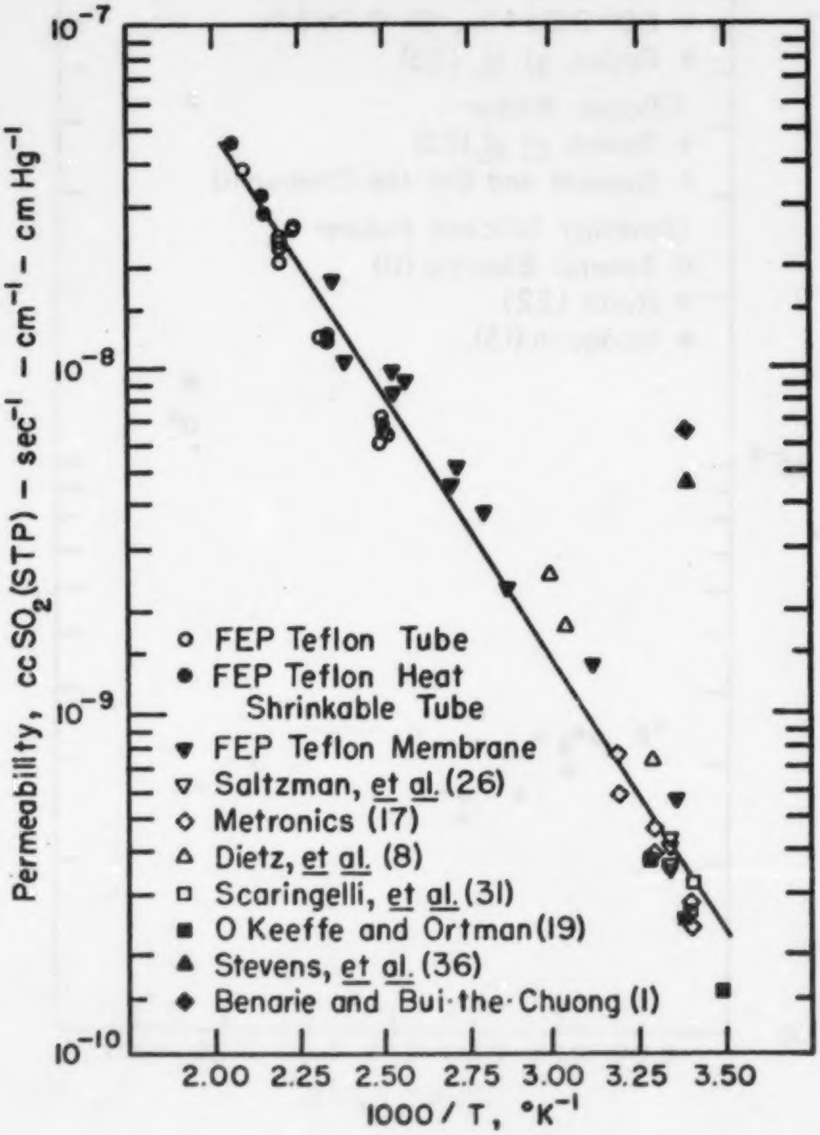

Figure 2. SO_2 Permeabilities of FEP Teflon.

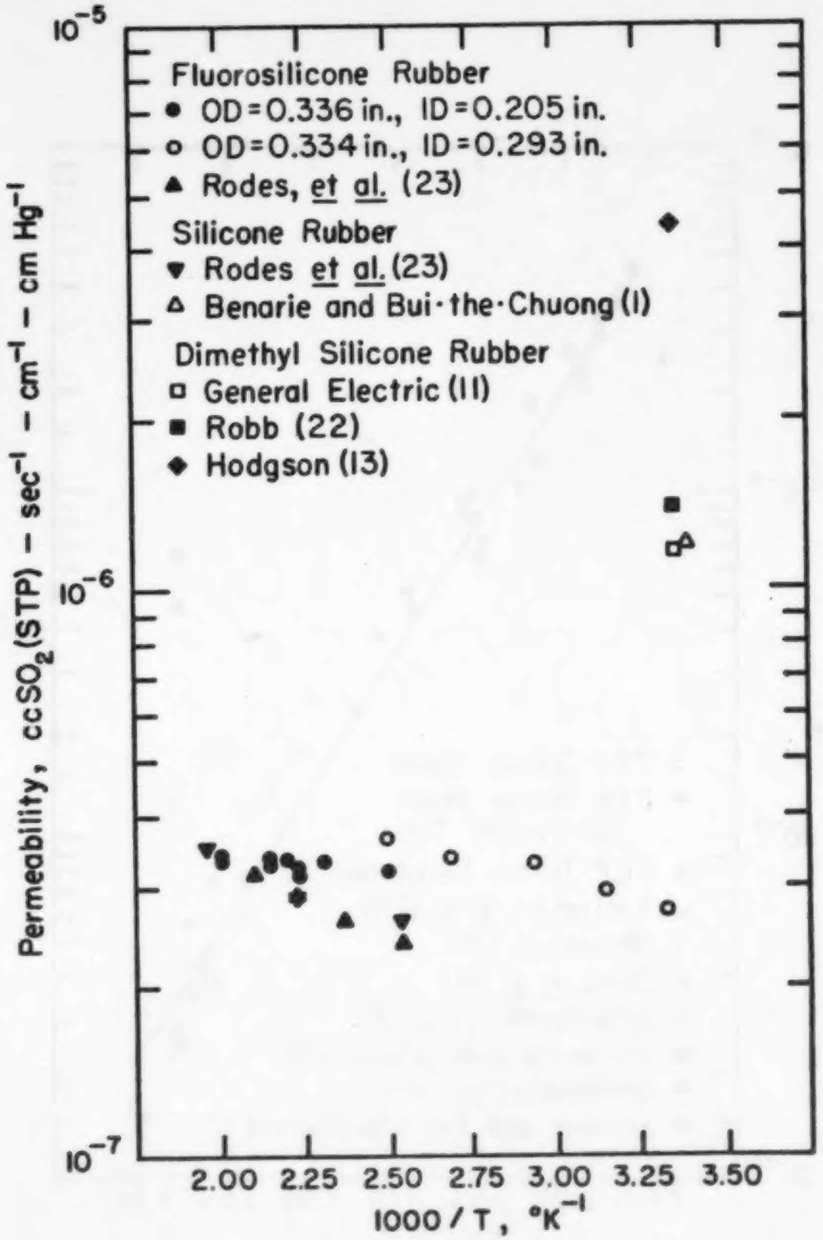

Figure 3. SO$_2$ Permeabilities of Silicone Rubbers.

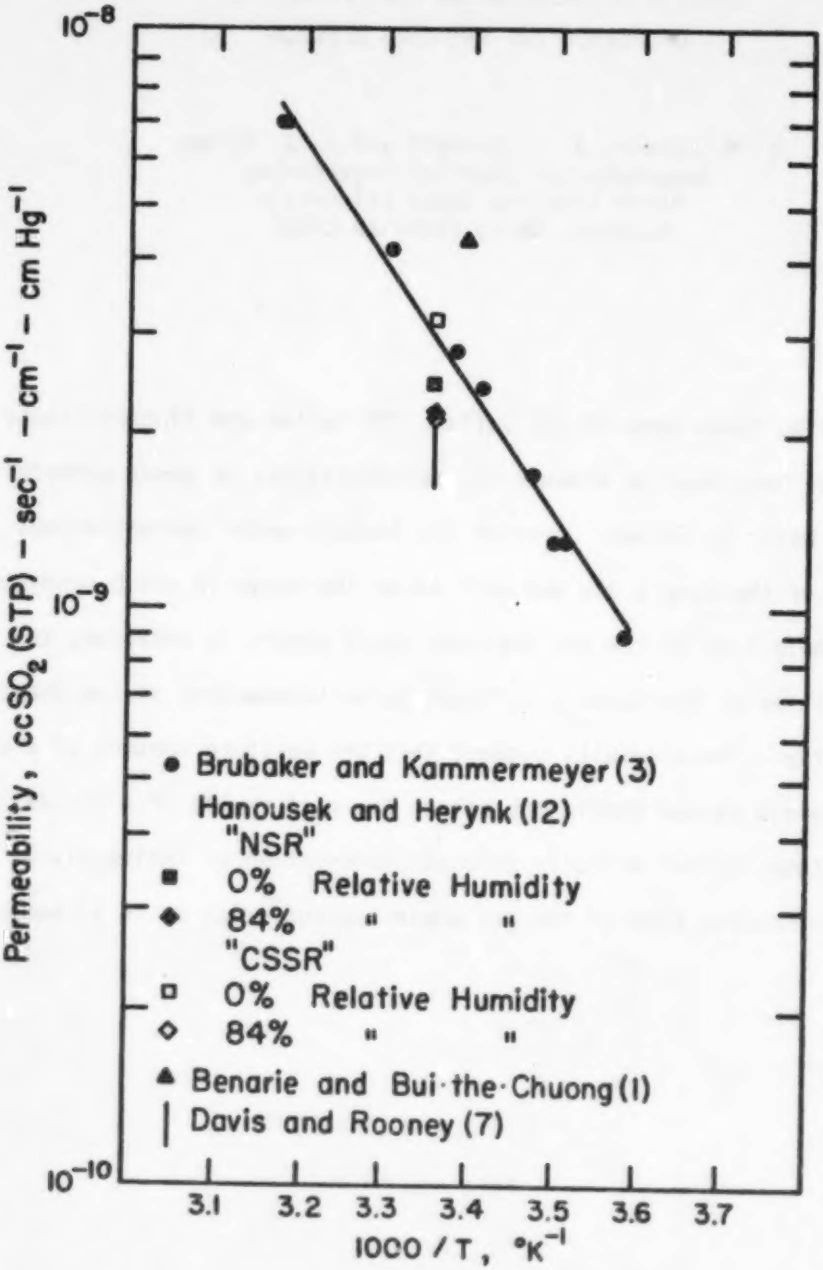

Figure 4. SO_2 Permeabilities of Polyethylene.

APPENDIX B

EFFECTS OF MOISTURE ON THE PERFORMANCE* OF PERMEATION SAMPLING DEVICES

R. M. Felder, J. K. Ferrell and J. J. Spivey
Department of Chemical Engineering
North Carolina State University
Raleigh, North Carolina 27607

ABSTRACT

Sampling tubes made of TFE Teflon, FEP Teflon and fluorosilicone rubber have been used to measure SO_2 concentrations in gases containing up to 21% water by volume. Even at the highest water concentrations, the dew point of the sample gas was well below the range in which condensation in the sample line or the gas analyzer could occur; in addition, the SO_2 permeabilities of the tubes were found to be independent of the chamber gas humidity. These results suggest that the moisture content of a stack gas or process stream should not affect the performance of a permeation sampling tube, either directly through condensation or indirectly by altering the permeation rate of the gas whose concentration is to be measured.

---

*Published as Analysis Instrumentation 12, 35 (1974). Reprinted by permission of the Instrument Society of America.

INTRODUCTION

Continuous stack gas monitoring has a variety of process industry applications. It can be used to verify that a process is operating at a desired steady-state level, to provide feedback signals to a control element in the event of undesired changes in operating conditions, to evaluate the performance of an add-on pollution control device, and to determine compliance with federal regulations relating to source emissions.

A number of factors such as high particulate loadings and high stack humidities can complicate the analysis of a gas sample drawn from a stack. To minimize the effects of these factors on the performance of a continuous monitoring device, the sample must be conditioned before being analyzed: particulates must be filtered out, and water must be removed.

Most sample conditioning methods involve the use of particulate filters and cold traps or water adsorption columns, devices which require relatively frequent servicing; these methods are consequently not ideally suited to long-term continuous monitoring. Rodes, Felder and Ferrell(2) recently reported on the use of polymeric sampling tubes for SO_2 monitoring, a technique suggested by O'Keeffe(1). A U-shaped tube which is permeable to SO_2 (or whatever gas is to be monitored) is inserted into the stack, and a clean carrier gas is passed through the inside of the tube; the resulting SO_2 concentration gradient from the outside of the tube to the inside leads to permeation of the SO_2 through the tube wall into the carrier gas, which then passes out of the stack to an analyzer.

Rodes et al.(2) studied the performance of TFE Teflon, silicone rubber and fluorosilicone rubber tubes, and showed that the concentration of SO_2 in the carrier gas could be easily and well correlated with the SO_2 concentration in the stack. A subsequent study by Spence, Felder, Ferrell and Rodes(3) showed that TFE tubes can effectively screen out particulates under heavy particulate loading conditions.

A major question regarding the feasibility of polymeric sampling interfaces is the effect of stack humidity on their performance. A high stack moisture content can have two possible deleterious effects: (1) water might permeate into the tube and subsequently condense, leading to erroneous analyzer readings; (2) water dissolved in the sampling tube could alter the tube permeability to the gas being monitored, so that a correction for stack humidity would have to be applied to the analyzer reading to determine the stack gas concentration. This paper reports on studies of stack humidity effects on the performance of TFE Teflon, FEP Teflon and fluorosilicone rubber sampling tubes, and indicates the extent to which these two negative phenomena are likely to affect the performance of these devices in continuous SO_2 monitoring.

EXPERIMENTAL

A schematic diagram of the experimental apparatus used in this study is shown in Figure 1.

A chamber of simulated stack gases was constructed by bolting two six-inch square end plates to the ends of a 12-inch long, 3-inch I.D. Type 316 stainless steel chamber. Each end plate was tapped to accept a .125-inch thermocouple fitting, a .125-inch pipe fitting, and a .375-inch pipe fitting. All fittings were of Type 316 stainless steel. Each of the .375-inch fittings was drilled internally to allow a section of .375-inch O.D. stainless steel tubing to pass through the end plate to the interior of the chamber. The sampling tube was connected to these sections of stainless steel tubing and supported by a stainless steel rod. The chamber assembly was then placed inside a thermostatically controlled oven with a temperature adjustable to 250°C.

A mixture of 5000 ppm SO_2 in air and a dilution stream consisting of air which had been passed through an activated charcoal column were fed through rotameters into a tee. The combined stream passed through an access port in the oven to one of the 0.125-inch taps in the chamber end plate. When desired, water was introduced into the chamber gas by metering liquid water fed from a constant head tank into a tee in the chamber gas line prior to its entry into the oven. The tee was packed with sintered stainless steel, and the tee and the line from the tee to the oven were heated gently by a heating tape controlled by a variable transformer; the stainless steel packing provided sufficient surface area to evaporate the water without abrupt dropwise flashing. The water vapor concentration in the chamber was calculated from the metered flow rates of liquid water and of the SO_2-air mixture, and was checked by a hygrometer. After leaving the chamber, the gas passed through a sodium hydroxide scrubber, and the scrubbed gas was vented.

Purified air was also used as the sampling tube carrier gas. The air passed through a rotameter and a .375-inch stainless steel tube into the sampling tube, and upon leaving the tube, flowed through a stainless steel line to a Meloy Labs flame photometric detector (Model SA-160) which measured the SO_2 concentration in the gas. When the carrier gas water vapor concentration was to be measured, the flow was diverted to a Panametrics hygrometer (Model 2000). Strip chart recorders permitted continuous monitoring of both SO_2 and water in the exit gas.

Two thermocouples were used to monitor the temperature in the chamber, and the temperatures of the carrier and chamber gases were monitored by thermocouples placed just prior to the chamber. The absolute pressure of the carrier gas and the pressure inside the chamber were measured using water manometers.

The flame photometric detector was calibrated using purified air passed over an SO_2 permeation tube with a known emission rate, varying the flow rate of the air to generate a series of gases with known SO_2 concentrations. This procedure was performed before and after each set of sampling runs at each temperature. The drift in the analyzer calibration during any set of measurements was never greater than 3%.

At the outset of a run the sampling tube inner and outer diameter and length were measured. The tube was placed in the stainless steel chamber and the lines inside the oven were connected to it. The oven thermostat was set, and the chamber temperature was monitored until steady-state was achieved. The chamber was then purged with gas containing the desired concentration of SO_2 and/or water, and the pressures of the carrier gas and the purge gas were regulated by throttling the appropriate lines downstream of the oven.

The pressure of the carrier gas was kept slightly higher than that of the purge gas to assure that a pinhole in the sampling tube would not lead to a large bulk flow from the purge gas to the carrier gas. The carrier gas flow was then adjusted to the desired value, and was directed from the outlet of the oven to either the flame photometric detector or the hygrometer. When the recorder trace indicated that steady-state diffusion of SO_2 or water vapor had been achieved, the recorder signal was noted and background concentrations of the diffusing gases were subtracted. (The concentration of SO_2 in the purified air was approximately .02 PPM, while the water vapor background concentration was approximately 50 PPM.) The fluxes of the permeating gases could then be calculated from the corrected concentrations of these gases in the carrier gas stream, the carrier gas flow rate, and the length of the sampling tube.

DATA ANALYSIS

The rate of permeation of a gas through the walls of a tube may be expressed as

$$F = \frac{2\pi P(p_2-p_1)}{\ln (b/a)} \qquad (1)$$

where

F = permeation rate, cm^3 (STP)/sec·cm length

P = permeability (product of diffusivity and solubility), cm^3 (STP)/sec·cm·cm Hg

p_1, p_2 = partial pressures of the permeating species in the carrier gas (inside the tube) and chamber gas (outside the tube), cm Hg.

a,b = inner and outer tube diameters, cm.

The principal assumptions which lead to Equation (1) are Fickian diffusion in the tube with a constant diffusivity, and Henry's law of solubility. In addition, if both the diffusivity and solubility follow an Arrhenius law temperature dependence, then

$$P = P_o \exp(-E_p/R_gT) \tag{2}$$

where

P_o = a pre-exponential factor, units of P
E_p = activation energy for permeation, kcal/g-mole
R_g = gas constant, kcal/g-mole·°K
T = absolute temperature, °K

Equation (1) predicts that a plot of F (obtained by multiplying the measured concentration of the permeating species in the carrier gas by the carrier gas volumetric flow rate) vs. $2\pi(p_2-p_1)/\ln (b/a)$ at a fixed temperature should be a straight line through the origin, with the slope equal to the permeability P at that temperature. Equation (2) predicts that an Arrhenius plot of ln P vs. 1/T should be linear, with the negative of the slope equal to the activation energy E_p divided by the gas constant R_g.

The experiments consisted of adjusting chamber concentrations of SO_2 and/or H_2O, measuring the permeation rates of these gases through the sampling tube walls, and plotting the data as indicated above. In this manner, permeabilities of the tube materials to SO_2 and to water could be determined at different temperatures.

RESULTS AND DISCUSSION

Sulfur Dioxide Permeation

Permeation measurements were made on TFE Teflon, FEP Teflon, and Silastic LS-63U® fluorosilicone rubber tubes, the latter manufactured by the Dow-Corning Corporation. In all of the permeation runs, the partial pressure of the SO_2 in the chamber (p_2 of Equation (1)) was several orders of magnitude greater than the partial pressure in the carrier gas (p_1); consequently, the permeability could be calculated from a plot of permeation rate (F) vs. $2\pi p_2/\ln(b/a)$.

Figure 2 shows plots of SO_2 permeation rates into a TFE Teflon tube vs. $2\pi p_{SO_2}/\ln(b/a)$ at three temperatures. Data points are shown both for dry chamber gases and chamber gases containing 21.1% water by volume (dew point = 61.5°C = 142°F).

Two principal points emerge from an inspection of Figure 2.

1. As predicted by Equation (1), the isotherms are straight lines through the origin. The assumed model therefore correlates the permeation rate data, and Equation (1) may accordingly be used for the design of permeation sampling tubes and the interpretation of data obtained with these devices.
2. The data obtained for dry and highly humid chamber gases are statistically indistinguishable, indicating that the presence of water in the chamber gas does not affect the permeability of TFE Teflon to sulfur dioxide. This is an encouraging result: it implies that for at least this material, permeation stack sampling data need not be corrected for variations in the stack gas humidity, so that there is no need to measure this quantity as a routine part of the stack monitoring procedure.

Figure 3 shows the results obtained using a fluorosilicone rubber tube. The results are qualitatively similar to those obtained for TFE: the plots are linear, and water in the stack gas has no discernible effect on the permeation rate of SO_2. The differences are that the SO_2 permeability of the fluorosilicone tube is roughly an order-of-magnitude greater than that of the Teflon tube, and is much less sensitive to temperature. Permeation rate plots for FEP Teflon are similar to those shown for TFE.

SO_2 permeabilities obtained by least-squares fitting of lines through the origin to permeation rate plots are listed in Table 1. The fluorosilicone permeabilities agree quite closely with those given by Rodes et al.(2) while the TFE permeabilities are roughly 60% higher than those reported in the earlier study, a discrepancy which we cannot now explain. Arrhenius plots of log P_{SO_2} vs. 1/T for TFE, FEP and fluorosilicone rubber are linear, as predicted by Equation (2); however, the temperature range of the data obtained so far is too small and the data points are too few in number to permit a meaningful calculation of activation energies for permeation.

Water Permeation

Permeation rates of water through the three tube materials were also measured. The results obtained for a TFE tube are shown in Figure 4. As was the case for SO_2 permeation, the data points for specific temperatures can be reasonably well correlated by straight lines through the origin, although the scatter in the water permeation data is greater than that for SO_2. Plots for FEP and fluorosilicone are similar to those of Figure 4, with the differences paralleling those reported for SO_2 permeation: the permeability of TFE at a given temperature is approximately equal to that of FEP and is an order-of-magnitude less than that of fluorosilicone, and the permeability of fluorosilicone is considerably less temperature-sensitive than are the permeabilities of TFE and FEP.

The permeabilities determined by least-squares fitting of lines through the origin to water permeation rate plots are listed in Table 2. Again, the temperature range and number of data points do not provide an adequate base for accurate estimation of Arrhenius plot slopes.

The results are adequate to establish one of the principal desired results of this study, however -- namely, that a polymeric permeation sampling device can provide a sample gas with a dew point well below the point at which condensation in the line leading to the analyzer could occur. For example, if the fluorosilicone tube used in this study were used to monitor a stack at 177°C with a stack gas dew point of 61°C, the dew point of a carrier gas flowing at 655 cm^3 (STP)/min (a representative figure for SO_2 monitoring) would be -29.5°C, and the carrier gas dew point would be even lower if a Teflon tube were used.

Studies are currently in progress to extend the temperature range of both the SO_2 and water permeation measurements so that activation energies for permeation may be determined with a reasonable degree of precision, to perform permeation tests on additional single and composite tube materials, to extend the tests to NO_x permeation measurements, to study the effects of mists (as opposed to water vapor) in the stack gas on the performance of permeation sampling tubes, and to field-test prototype devices in process and power-plant stacks.

CONCLUSIONS

The principal results of this study are as follows:

1. Stack sampling tubes made of TFE Teflon, FEP Teflon and fluorosilicone rubber all provide sample gases with dew points well below normal ambient temperatures.
2. The permeation rates of SO_2 through the tube materials tested are independent of the stack gas humidity.

Considered together, these results suggest that the moisture content of a stack gas or process stream should not affect the performance of a permeation sampling tube used to monitor SO_2, either directly through condensation in the line to the analyzer or indirectly by altering the rate of permeation of SO_2 into the tube.

REFERENCES

1. O'Keeffe, A., U. S. Patent Appl., December 1970.

2. Rodes, C. E., Felder, R. M. and Ferrell, J. K., 1973, "Permeation of Sulfur Dioxide Through Polymeric Stack Sampling Interfaces," Environ. Sci. Technol. 7, p. 545.

3. Spence, R. D., Felder, R. M., Ferrell, J. K. and Rodes, C. E., 1973, "A Polymeric Interface for Monitoring SO_2 Emission from Stationary Sources," paper presented at a National Meeting of the American Institute of Chemical Engineers, New Orleans, Louisiana, March 1973.

TABLE 1. SO_2 Permeabilities

Material	Temperature, °C	SO_2 Permeability $P \times 10^7$ (cm^3(STP)/sec·cm·cm Hg
TFE Teflon	154	0.162
	179	0.245
	202	0.359
FEP Teflon	171	0.207
	175	0.220
	180	0.217
	197	0.294
	201	0.318
Fluoro-silicone Rubber	153	2.92
	175	3.02
	200	3.18
	225	3.23

TABLE 2. Water Permeabilities

Material	Temperature, °C	Water Permeability $P \times 10^7$ (cm^3(STP)/sec·cm·cm Hg)
TFE Teflon	127	0.340
	171	0.711
	191	1.10
	217	1.36
FEP Teflon	171	0.443
	180	0.580
	197	0.755
Fluoro-silicone Rubber	130	7.94
	156	9.54
	177	11.28

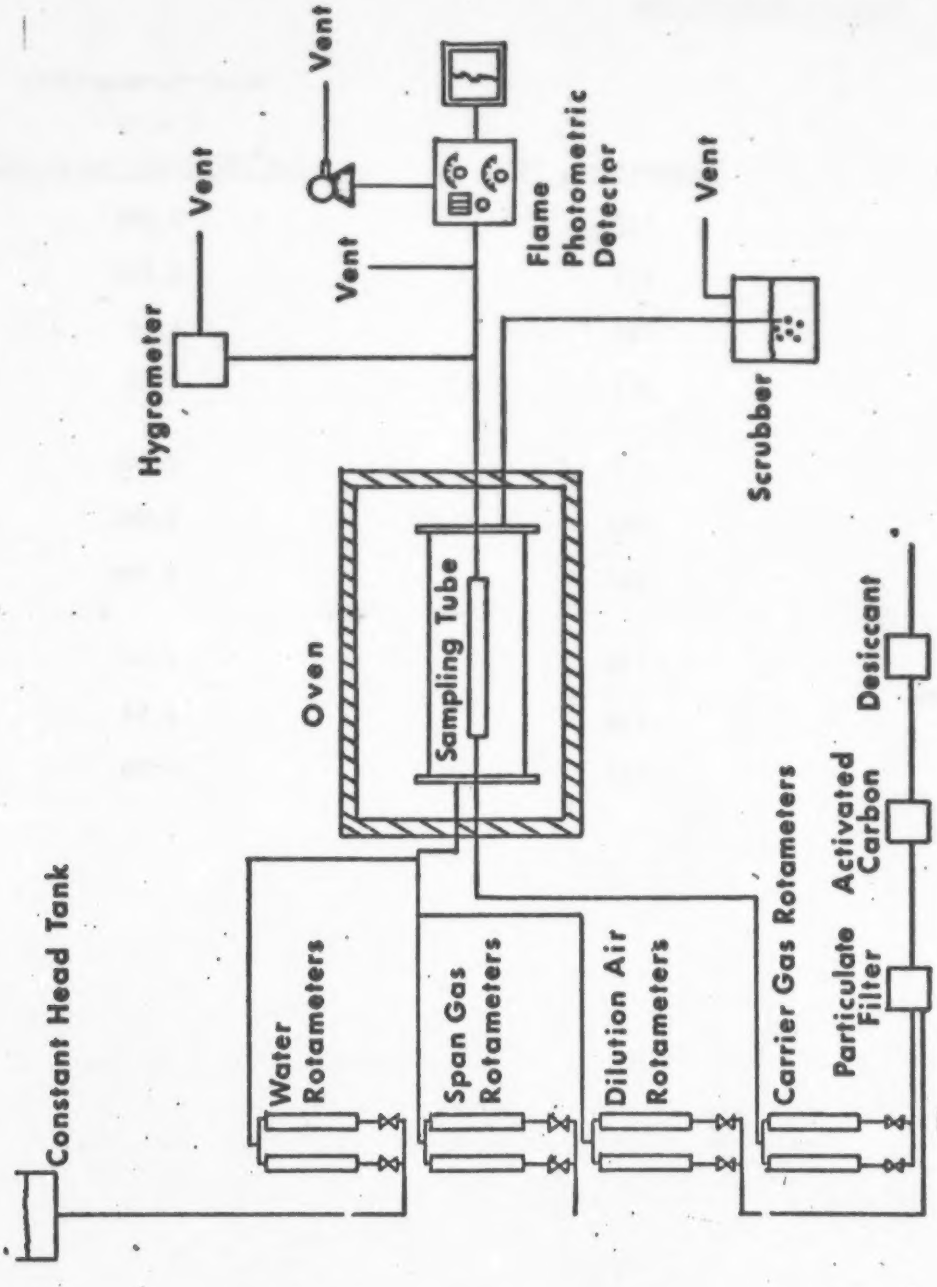
Constant Head Tank
Water Rotameters
Span Gas Rotameters
Dilution Air Rotameters
Carrier Gas Rotameters
Particulate Filter
Activated Carbon
Desiccant
Oven
Sampling Tube
Hygrometer
Vent
Vent
Vent
Flame Photometric Detector
Vent
Scrubber

Figure 1. Experimental Apparatus.

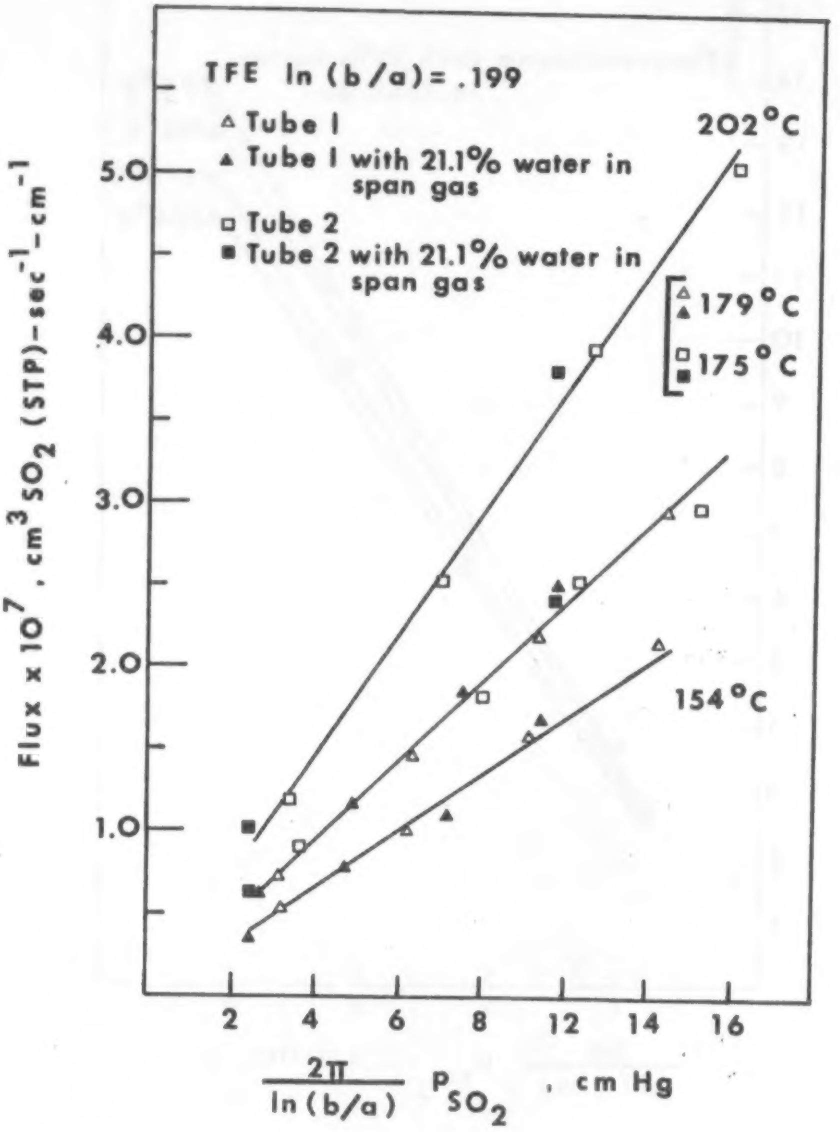

Figure 2. Permeation rates: SO_2 through TFE Teflon.

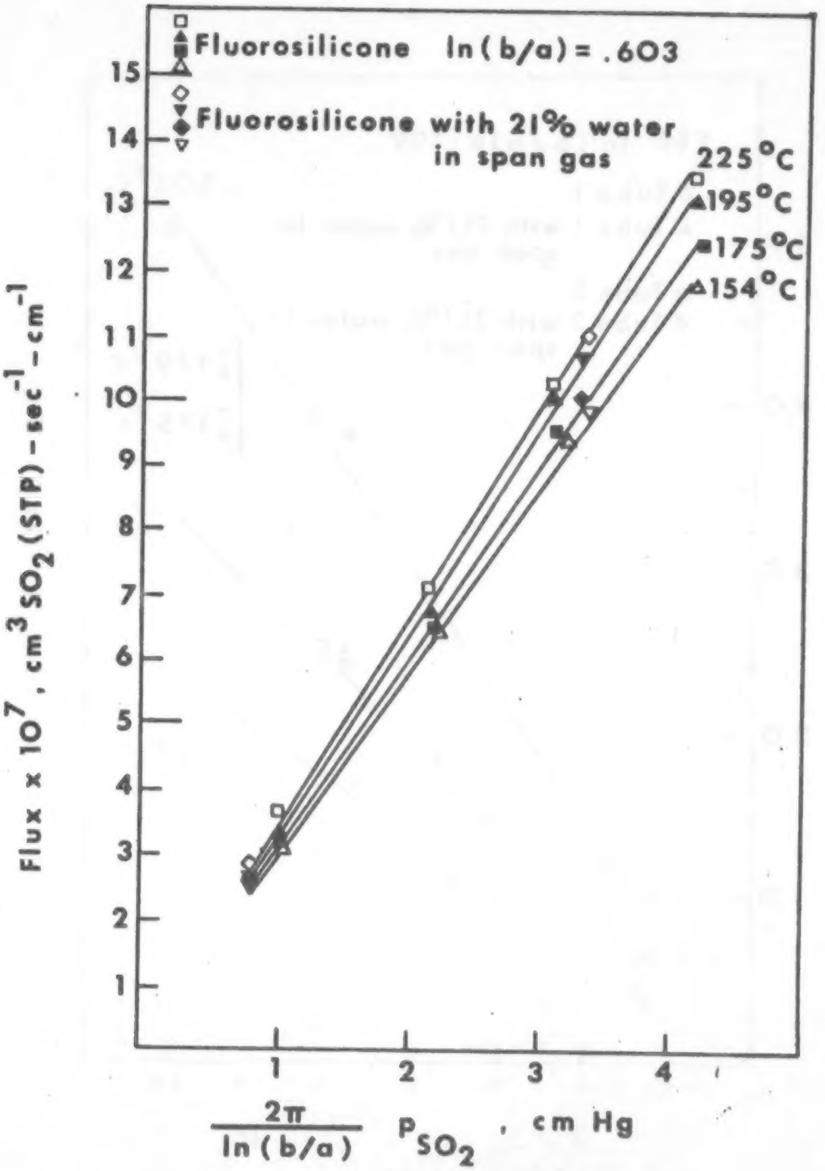

Figure 3. Permeation rates: SO_2 through Fluorosilicone Rubber.

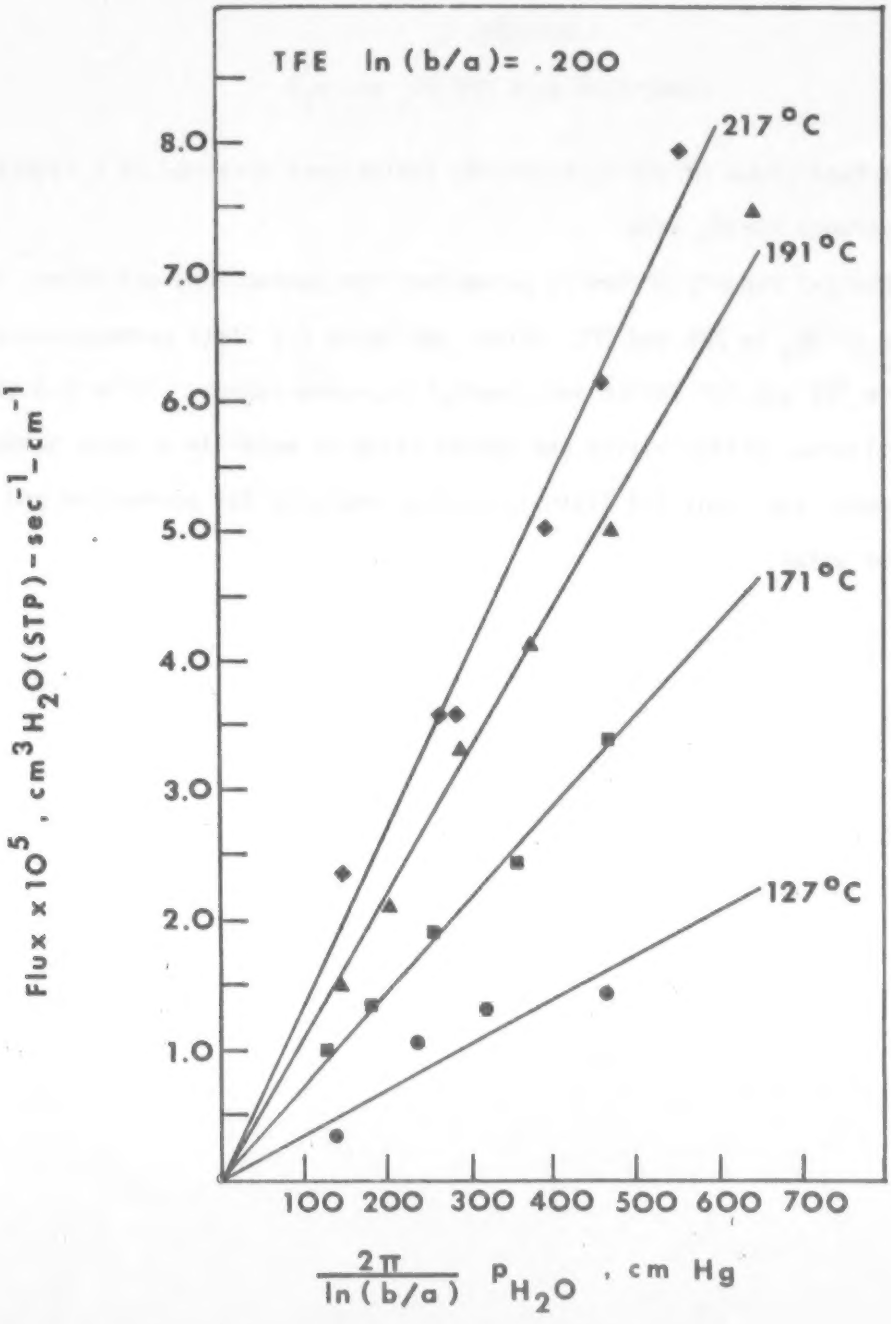

Figure 4. Permeation rates: Water through TFE Teflon.

APPENDIX C

PERMEATION DATA FOR NO_x and H_2O

The data given in the accompanying tables were obtained in a literature search through April, 1974.

Table C-1 reports Arrhenius parameters for permeation, diffusion, and sorption of NO_x in FEP and TFE Teflon, and Table C-2 lists permeabilities of NO_x in TFE and FEP Teflon and dimethyl silicone rubber. Table C-3 gives permeabilities, diffusivities and solubilities of water in a large number of polymers, and Table C-4 lists activation energies for permeation and diffusion of water.

Table C1. NO_x Arrhenius Parameters

Material	$P_o \times 10^5$ [(a)]	E_p [(b)]	D_o [(c)]	E_D [(b)]	$S_o \times 10^{10}$ [(d)]	ΔH_s [(b)]	Source
TFE Teflon							
(NO_2)	0.0116	2.55	70.	14.0	16.6	-11.4	Pasternak et al. (1970)
(N_2O_4)	0.00013	-0.5	-	-	-	-	"
$(NO_2-N_2O_4)$	-	9.91[e]	-	-	-	-	Dietz et al. (1970)
$(NO_2-N_2O_4)$	-	-	0.4	9.54	10,900.	-6.55	Johnson (1969)
FEP Teflon							
$(NO_2-N_2O_4)$	-	10.1[e]	-	-	-	-	Saltzman et al. (1971)
$(NO_2-N_2O_4)$	-	-	56.	13.5	3,800	-7.15	Johnson (1969)

---

[a] $cm^3(STP)/s \cdot cm \cdot cm\ Hg$

[b] kcal/gmole

[c] cm^2/s

[d] $cm^3(STP)/cm^3 \cdot cm\ Hg$

[e] Calculated by subtracting a heat of evaporation, $\Delta H_{evap} = 4.45$ kcal/gmole (Yaws and Hopper, 1974) from the published activation energy, which was for the combined processes of evaporation and permeation.

Table C2. Effective Permeabilities of Nitrogen Oxides

Material	Temperature (°C)	$P_e X10^{10}$ [(a)]	$(p_{NO_2} + p_{N_2O_4})$ [(b)]	Source
TFE Teflon				
(Permeation tubes)	20	207[c,d]	73.0	Metronics (1970)
(Film)	21	175[c,d]	76.0	Bazarre and Petriello (1970)
(Sprayed dispersion)	21.4	193[d]	76.8	Stanford (1963)
	"	202[d]	"	"
	"	268[d]	"	"
	"	289[d]	"	"
	"	268[d]	"	"
	"	176[d]	"	"
	"	362[d]	"	"
(Permeation tubes)	30	242[c,d]	116.3	Metronics (1970)
	30.4	75[d]	117.0	Dietz et.al. (1974)
	39.8	102[d]	177.1	"
	40	291[c,d]	177.8	Metronics (1970)

---

[a] Effective permeability, cm^3(STP)/s·cm.cm Hg; for NO_2 -N_2O_4 cm^3(STP)NO_2

[b] Vapor pressure, cm Hg, of NO_2 - N_2O_4 equilibrium (Handbook of Chemistry and Physics, 1969)

[c] Rough estimate

[d] Calculated from published flux using Eq. (3) or (4)

[e] Published value

[f] Speculation -- author did not report a temperature

Material	Temperature (°C)	$P_e \times 10^{10}$(a)	$(p_{NO_2} + p_{N_2O_4})$(b)	Source
FEP Teflon	13.8	40.8[d]	53.2	O'Keeffe and Ortman (1966)
(Permeation tubes)	20.	51.0[c,d]	73.0	Metronics (1970)
	20.	41.5[c,d]	"	"
	20.1	54.5[d]	"	O'Keeffe and Ortman (1966)
(film type A)	21.4	36.7[d]	76.8	Stanford (1963)
	"	32.0[d]	"	"
	"	52.3[d]	"	"
	"	35.7[d]	"	"
	"	11.1[d]	"	"
	"	14.2[d]	"	"
	"	2.36[d]	"	"
(film type 506)	"	16.3[d]	"	"
	"	14.6[d]	"	"
	"	54.8[d]	"	"
	"	45.4[d]	"	"
	"	71.0[d]	"	"
	"	44.3[d]	"	"
(Permeation tubes)	25.[f]	80.5[d]	92.7	Saltzman *et.al*.(1971)
	25.[f]	80.9[d]	92.7	"
	29.1	74.4[d]	110.2	O'Keeffe and Ortman (1966)
	30.	74.7[c,d]	116.3	Metronics (1970)
	30.	59.8[c,d]	116.3	"
	40.	115.[c,d]	177.8	"
	40.	90.6[c,d]	177.8	"
TFE and FEP Teflon				
Sprayed dispersion	21.4	42.7[d]	76.8	Stanford (1963)
	"	48.2[d]	"	"
	"	55.6[d]	"	"
	"	67.7[d]	"	"
	"	56.1[d]	"	"
	"	57.4[d]	"	" 1963)

Material	Temperature (°C)	$P_e \times 10^{10}$ (a)	$(p_{NO_2} + p_{N_2O_4})$ (b)	Source
TFE and FEP Teflon Codispersion				
(100% TFE)	21.	52.5^d	76.0	Petriello (1968)
(90% TFE)	"	52.5^d	"	"
(80% TFE)	"	38.6^d	"	"
(70% TFE)	"	17.5^d	"	"
(50% TFE)	"	$7.^d$	"	"
(0% TFE, 100% FEP)	"	$7.^d$	"	"
Laminate	"	38.6^d	"	"
	"	$94.5^{c,d}$		Bazarre and Petriello (1970)
Dimethyl Silicone Rubber (25%)				
(Permeability to NO_2)	25.	$5820.^e$	-	General Electric (undated)
(" " NO)	"	$458.^e$	-	"
(" " N_2O)	"	$3340.^e$	-	"
(" " NO_2)	"	$6960.^e$	-	Robb (1968)
(" " NO)	"	$550.^e$	-	"
(" " N_2O)	"	$3990.^e$	-	"

Table C3. Permeabilities, Diffusivities and Solubilities of Water in Polymers

Material	Temperature (°C)	Px10^{10}[a]	Dx10^{10}[b]	S[c]	Source
TFE					
(Teflon)	20	24.0	-	-	Korte-Falinski (1962)
	20	-	-	0.0709[q]	Barrie (1968)
	23	46.4	-	-	Toren (1965)
	30	33.6	-	-	Korte-Falinski (1962)
(Halon G-183)	38	8.45	-	-	Hadge et.al. (1972)
(Teflon)	40	38.4	-	-	Korte-Falinski (1962)
(Halon G-183)	50	14.9	-	-	Hadge et.al. (1972)
	60	13.5-28.6[d]	-	-	"
(Teflon)	127	340.	-	-	Felder et.al. (1974)
	171	711.	-	-	"

---

[a] Permeability, cm^3(STP)/s·cm.cm Hg

[b] Diffusivity, cm^2/sec

[c] Solubility, cm^3(STP)/cm^3·cm Hg

[d] Permeability depended on membrane thickness

[e] Permeability determined with liquid water at one surface

[f] Permeability determined with water vapor at one surface

[g] Calculated from the reported rate data and a driving force equivalent to the saturated vapor pressure.

[h] Data from unoriented film

[i] Data from oriented film

[j] Data from laboratory cast film

[k] Data from commercial film

[l] Data from calendared film

[m] Data from cast film

[n] Speculation -- permeability calculated based on an inferred membrane thickness

[p] Speculation -- author did not report a temperature

[q] Units are $\frac{\text{cc(STP)}}{\text{g polymer}\cdot\text{cm Hg}}$

Material	Temperature(°C)	$Px10^{10}$[a]	$Dx10^{10}$[b]	S^c	Source
TFE(Cont'd)					
(Teflon)	191	1,100.	-	-	Felder *et.al*. (1974)
(Teflon heat-shrunk on porous s.s)	213	1,340.	-	-	"
(Teflon)	217	1,360.	-	-	"
FEP					
	21	21.3	-	-	Woolley(1967)
	23	19.4	-	-	Toren (1965)
	25	480.[e]	-	-	Sivadjian and Riberio (1964)
	25	250.[f]	-	-	"
	35	26,400.[e]	-	-	"
	35	7,700.[f]	-	-	"
	39.5	42.9	-	-	DuPont
	45	66,000.[e]	-	-	Sivadjian and Riberio (1964)
	45	52,500.[f]	-	-	"
	55	75,500.[e]	-	-	"
	55	72,000.[f]	-	-	"
	65	118,000.[e]	-	-	"
	65	108,000.[f]	-	-	"
	75	290,000.[e]	-	-	"
	75	274,000.[f]	-	-	"
	85	898,000.[e]	-	-	"
	85	860,000.[f]	-	-	"
	95	1,560,000.[e]	-	-	"
	95	1,540,000.[f]	-	-	"

Material	Temperature (°C)	Px10^{10}[a]	Dx10^{10}[b]	S[c]	Source
FEP (Cont'd)					
(Teflon)	171	443.	-	-	Felder et.al. (1974)
	180	580.	-	-	"
	197	755.	-	-	"
Chlorotrifluoroethylene					
(Kel-F)	23	2.67	-	-	Toren (1965)
	23	2.00	-	-	"
	30	0.29	-	-	Barrie (1968)
(Halon)	38	3.63	-	-	Hadge et.al. (1972)
Ethylene/Chlorotrifluoroethylene					
(Halar)	30	14.8	-	-	Hadge et.al. (1972)
	45	24.1	-	-	"
	60	42.1	-	-	"
Polyvinyl fluoride					
(Tedlar)	25	4,023.[e]	-	-	Sivadjian and Riberio (1964)
	25	3,291.[f]	-	-	"
	35	34,700.[e]	-	-	"
	35	31,800.[f]	-	-	"
	38	34.	-	-	Hadge et.al. (1972)
	39.5	41.	-	-	Barrie (1968)
	39.5	1,070,000.	-	-	DuPont (undated)
	45	95,100.[e]	-	-	Sivadjian and Riberio (1964)
	45	75,300.[f]	-	-	"
	50	86.8	-	-	Hadge et.al. (1972)
	55	365,000.[e]	-	-	Sivadjian and Riberio (1964)
	55	357,000.[f]	-	-	"
	60	181.4	-	-	Hadge et.al. (1972)
	65	809,000.[e]	-	-	Sivadjian and Riberio (1964)
	65	537,000.[f]	-	-	"

Material	Temperature(°C)	$Px10^{10}$[a]	$Dx10^{10}$[b]	S[c]	Source
Polyvinyl fluoride (cont'd)					
(Tedlar)	75	1,600,000.[e]	-	-	Sivadjian and Riberio (1964)
	75	833,000.[f]	-	-	"
	85	3,330,000.[e]	-	-	"
	85	3,070,000.[f]	-	-	"
	95	5,030,000.[e]	-	-	"
	95	4,880,000.[f]	-	-	"
Fluoroplastic					
(32L, type N)	25	178.[g]	7,800	-	Shirokshina et.al.(1970)
(32L, type V)	25	175.[g]	8,000	-	"
(32L, type N)	40	119.[g]	10,300	-	"
(32L, type V)	40	116.[g]	12,000	-	"
(32L, type N)	50	75.[g]	10,200	-	"
(32L, type V)	50	78.[g]	10,300	-	"
Silicone Rubbers					
(dimethyl silicone)	25	33,000	-	-	Robb (1968)
	25	27,450	-	-	General Electric(undated)
(dimethyl silicone, peroxide cured, silica filler)	25	104,700.[n]	-	-	Hodgson (1973)
(5601)	25	15,300	-	-	Kass and Andrzejewski (1973)
(dimethyl silicone)	35	4,300	~70,000	-	Barrie (1968)
	38	1,111	-	-	Hadge et.al. (1972)
(5601)	48	13,070	-	-	Kass and Andrzejewski (1973)
(dimethyl silicone)	65	3,280	100,000	-	Barrie (1968)
(5601)	76	11,570	-	-	Kass and Andrzejewski
	100	10,430	-	-	" " (1973)
(Fluorosilicone Silastic LS-63U)	130	7,940	-	-	Felder et.al. (1974)
	156	9,540	-	-	" "
	177	11,280	-	-	" "

Material	Temperature(°C)	Px10^{10}[a]	Dx10^{10}[b]	S[c]	Source
Polycarbonate					
(Lexan)	21	2,800	-	-	Woolley (1967)
	23	778	-	-	Toren (1965)
(Unstretched)	23	1,456	-	-	Ito (1962)
(Uniaxial stretched)					
	23	1,120	-	-	Ito (1962)
	25	2,197.[g]	84,000	-	Shirokshina *et.al.* (1970)
(Kimfol)	25[p]	760	-	-	Woodgate (1971)
(Kimfol & Makrofol)	25[p]	370	-	-	Spivack (1970)
	25	1,170	350	3.34	Rust and Herrero (1969)
(Lexan)	25	14,000	6,800	2.22	Norton (1963)
	40	1,047.[g]	93,000	-	Shirokshina *et.al*. (1970)
(Unstretched)	40	1,207	-	-	Ito (1962)
(Uniaxial stretched)					
	40	933	-	-	Ito(1962)
	50	648.[g]	96,500	-	Shirokshina *et.al*. (1970)
(Lexan)	100	-	600	-	Norton (1963)
Polyethylene					
	0	7.5[l]	-	-	Doty et.al. (1946)
	15	24.5[l]	-	-	" "
	20	32.[l]	-	-	" "
	20	76.8	-	-	Korte-Falinski (1962)
	21	90.6	-	-	Woolley (1967)
	22	36.[m]	-	-	Doty *et.al*. (1946)
	25	61.[l]	-	-	" "
(Suprathen NR 100)	25	73.6	820	0.0898	Rust and Herrero (1969)
(Plastin)	25	39.8	122	0.326	Rust and Herrero (1969)
	25	12	-	-	Barrie (1968)
	25	25	-	-	"
	25	90	80	-	"
	30	124	-	-	"

Material	Temperature(^{o}C)	Px10^{10a}	Dx10^{10b}	S^{c}	Source
Polyethylene(Cont'd)					
	30	120.^{l}	-	-	Korte-Falinski (1962)
	32	86	-	-	Doty et.al. (1946)
	38	110.5^{l}	-	-	" "
	40	199	-	-	Korte-Falinski (1962)
	40	79.1^{m}	-	-	Doty et.al. (1946)
	60	222.^{m}	-	-	" "
	80	500.^{m}	-	-	" "
Polypropylene					
(Udel)	23	39.9	-	-	Toren (1965)
	25	22.9	49	0.467	Rust and Herrero (1969)
	25^{p}	39	-	-	Spivack (1970)
(Block 75-80,000 M.W.)	25	2,925.^{g}	111,000	-	Shirokshina et.al. (1970)
(Emulsion 250,000 M.W.)	25	3,216.^{g}	124,000	-	" "
	25	51	2,400	-	Barrie (1968)
	30	68	4.1	-	"
(Block 75-80,000 M.W.)	40	1,213.^{g}	110,000	-	Shirokshina et.al. (1970)
(Emulsion 250,000 M.W.)	40	1,457.^{g}	131,000	-	" "
(Block)	50	962.^{g}	143,000	-	" "
(Emulsion)	50	1,043.^{g}	154,000	-	" "
Polystyrene					
(Kardel)	23	>632	-	-	Toren (1965)
	25	1,130	1,400	0.807	Rust and Herrero (1969)
	25	970	-	-	Barrie (1968)
	25	895.^{h}	-	-	Doty et.al. (1946)
	25	835.^{i}	-	-	" "
	32	800.^{h}	-	-	" "
	32	840.^{i}	-	-	" "

Material	Temperature(^{o}C)	Px10^{10}[a]	Dx10^{10}[b]	S[c]	Source
Polystyrene (Contd)					
(Kardel)	38	870.[h]	-	-	Doty et.al. (1946)
	38	835.[i]	-	-	" "
	45	820.[h]	-	-	" "
	50	1,070	-	-	Barrie (1968)
Polyvinyl chloride					
(Geon 101)	0	86.[j]	-	-	Doty et.al. (1946)
	0	109.[j]	-	-	" "
	10	115.[j]	-	-	" "
	10	122.[j]	-	-	" "
(Vynan)	20	240.	-	-	Korte-Falinski (1962)
(Geon 101)	25	116.[j]	-	-	Doty et.al. (1946)
	25	123.[j]	-	-	" "
(Emulsion Genotherm U.G.)	25	257.	36	7.14	Rust and Herrero (1969)
(Plasticizer 100-75)	25	2,000	-	-	Barrie (1968)
(Chlorinated)	25	207	-	-	"
(Geon 101)	30	149.[j]	-	-	Doty et.al. (1946)
(Vynan)	30	259	-	-	Korte-Falinski (1962)
	30	-	230	-	Barrie (1968)
(Plasticizer 100-30)	30	340	170	-	"
(Geon 101)	35	155.[j]	-	-	Doty et.al. (1946)
(Vynan)	40	274	-	-	Korte-Falinski (1962)
(Geon 101)	45	187.[j]	-	-	Doty et.al. (1946)
(Plasticizer 100-75)	50	3,790	-	-	Barrie (1968)
(Chlorinated)	50	235	-	-	"
(Geon 101)	55	203.[j]	-	-	Doty et.al. (1946)
Polyvinyl chloride- acetate copolymer					
(Vinylite)	0	199.[j]	-	-	Doty et.al. (1946)
	10	222.[j]	-	-	" "

Material	Temperature(°C)	Px10^{10}(a)	Dx10^{10}(b)	S(c)	Source
Polyvinyl chloride (Vinylite)(Contd)	25	288[j]	-	-	Doty et.al. (1946)
	25	325[k]	-	-	"
(VYNS 90-10)	25[p]	210	-	-	Spivack (1970)
	32	-	600	-	Barrie (1968)
(Vinylite)	32	382[k]	-	-	Doty et.al. (1946)
	38	324[j]	-	-	"
	38	438[k]	-	-	"
Polyvinylidene Chloride - Vinyl Chloride Copolymer (Saran)	21	12.1	-	-	Woolley (1967)
	25	2.0	-	-	Doty et.al. (1946)
	32	5.2	-	-	"
	38	8.2	-	-	"
Polyvinylidene Chloride	30	1.4-10	-	-	Barrie (1968)
Polyvinylidene Chloride Acrylonitrile Copolymer	25	16	3.2	-	Barrie(1968)
Polyvinyl acetate	25	-	430.	-	"
	40	6,000.	1,500.	-	"
Polyvinyl alcohol	20	182,000.	-	-	Korte-Falinski (1962)
	25	19.	0.51	-	Barrie (1968)
	25	96.	12.5	-	"
	30	177,000.	-	-	Korte-Falinski (1962)
	40	144,000.	-	-	"
Polyvinyl formal-acetate-alcohol (Formvar)	25[p]	575.	-	-	Spivack (1970)
Polyvinylbutyral	25	1,850.	130	-	Barrie (1968)

Material	Temperature (^{o}C)	Px10^{10}(a)	Dx10^{10}(b)	S(c)	Source
Polyesters					
(Terephane)	20	221	-	-	Korte-Falinski (1962)
(Mylar)	21	115	-	-	Woolley(1967)
(Celanese)	23	142	-	-	Toren(1967)
(Kodar)	23	130	-	-	"
(Mylar)	23	167	-	-	"
(3-M)	23	146	-	-	"
(Hostaphan R50)	25	153	27.	5.67	Rust and Herrero(1969)
(Polyethylene Terephthlate)	25	175	39.	-	Barrie (1968)
(Mylar)	25^{p}	60	-	-	Spivack(1970)
(Terephane)	30	226	-	-	Korte-Falinski (1962)
	40	230	-	-	"
Polymethyl Methacrylate	50	2,500	1,300	-	Barrie (1968)
Polyethyl Methylacrylate	25	~3,500	1,050	-	"
	90	~6,000	35,000	-	"
Polymethacrylate	25	-	1,200	-	Barrie(1968)
(Emulsion)	25	3,391.^{g}	135,000.	-	Shirokshina et.al. (1970)
	40	1,491.^{g}	132,000.	-	"
	50	1,161.^{g}	177,000.	-	"
Polyarylate					
(F-1)	25	2,241.^{g}	85,000.	-	Shirokshina et.al. (1970)
(ITD 50:50)	25	5,908.^{g}	230,000.	-	"
(F-1)	40	1,207.^{g}	107,000.	-	"
(ITD 50:50)	40	2,876.^{g}	261,000.	-	"
(F-1)	50	910.^{g}	135,000.	-	"
(ITD 50:50)	50	1,860.^{g}	284,000.	-	"
Polyamide					
(Nylon MB2)	20	9,400	-	-	Korte-Falinski (1962)
(Rilsan)	20	235	-	-	"

Material	Temperature(°C)	Px10$^{10(a)}$	Dx10$^{10(b)}$	S$^{(c)}$	Source
Polyamide(Cont'd)					
(Nylon 6)	25	400	9.7	-	Barrie (1968)
	25	1,400	-	-	"
(Rilsan)	30	302	-	-	Korte-Falinski (1962)
(Nylon MB2)	30	8,980	-	-	"
(Rilsan)	40	403	-	-	"
(Nylon MB2)	40	8,400	-	-	"
(Nylon 6)	60	1,900	80.	-	Barrie (1968)
Poly(chloro-p-xylylene) (Parylene C)	25^{μ}	20	-	-	Spivack (1970)
Poly(-p-xylylene) (Parylene N)	25^{μ}	57	-	-	"
Polyethylene-tetrasulphide	21	60	-	-	Barrie (1968)
Diallyl phthalate (Diall 51-21)	38	116	-	-	Hadge et.al. (1972)
Phenolic (Phenall 8700)	60	14.7	-	-	Hadge et.al. (1972)
Epoxy (Competitive)	37	83.9	-	-	Hadge et.al. (1972)
(Experimental)	38	21.6	-	-	"
(Epiall 1970)	38	34	-	-	"
(Competitive)	50	129	-	-	"
(Experimental)	50	35	-	-	"
(Competitive)	60	155	-	-	"
(Experimental)	60	49.7	-	-	"
(Epiall 1970)	60	82.2	-	-	"
Bakelite	25	1,660	-	-	Barrie (1968)
Ethyl Cellulose					
	25	21,000	1,800	-	Barrie (1968)
	25	23,800	-	-	"

Material	Temperature(°C)	Px10^{10}(a)	Dx10^{10}(b)	S(c)	Source
Ethyl Cellulose (Cont'd)					
	80	11,000	12,000	-	Barrie (1968)
Regenerated Cellulose					
(Cellophane Impermeable IS)	20	1,870	-	-	Korte-Falinski (1962)
(Cellophane Permeable N)	20	14,600	-	-	"
(Cellophane)	21	44,000	-	-	Woolley (1967)
	25	1,900	-	-	Barrie (1968)
	25	3,580	-	-	"
	25	17,000	<10.	-	"
(Cellophane Imp. IS)	30	1,920	-	-	Korte-Falinski (1962)
(Cellophane Perm. N)	30	14,400	-	-	"
(Cellophane Imp. IS)	40	2,110	-	-	"
(Cellophane Perm. N)	40	13,800	-	-	"
Cellulose Acetate					
(Triacetate KC)	20	12,300	-	-	"
(Diacetate K41)	20	15,800	-	-	"
	20	16,500	-	-	"
	21	8,130	-	-	Woolley (1967)
	25	62,100	-	-	Barrie (1968)
	25	150,000	-	-	"
(Triacetate)	25	12,700	-	-	"
	30	6,000	170	-	"
(Triacetate KC)	30	12,500	-	-	Korte-Fatinski (1962)
(Diacetate K41)	30	16,100	-	-	"
	30	17,800	-	-	"
(Triacetate KC)	40	12,500	-	-	"

Material	Temperature(°C)	Px10^{10}[a]	Dx10^{10}[b]	S[c]	Source
Cellulose Acetate (Cont'd)					
(Diacetate K41)	40	16,300	-	-	Korte-Falinski (1962)
	40	19,200	-	-	"
(Triacetate)	50	13,800	-	-	Barrie (1968)
Rubber hydrochloride					
(Pliofilm)	20	10.2	-	-	Doty et.al. (1946)
	25	12.4	-	-	"
	25	14	4.1	-	Barrie (1968)
	30	20.8	-	-	Doty et.al. (1946)
	38	41	-	-	"
	43.5	43.5	-	-	"
	47.5	51.5	-	-	"
	52	87	-	-	"
Natural Rubber					
(Soft, Vulcan.)	25	2,290	-	-	Barrie (1968)
Polyisobutene	30	71-224.4	-	-	"
	37.5	110	-	-	"

Table C4. Activation Energies for Permeation and Diffusion of Water

Material	E_P (kcal/gmole)	E_D (kcal/gmole)	Source
Dimethyl Silicone	-	∿ 3	Barrie (1968)
Polyethylene	8.0	-	Doty et.al. (1946)
	10.2	-	"
	-	19.2	Spencer (1965)
	-	14.2	"
	8.0	14.2	Barrie (1968)
Polystyrene	0	-	Doty et.al. (1946)
Polypropylene	-	16.4	Spencer (1965)
	10.0	16.4	Barrie (1968)
Polyamide (Nylon)	-	13.3	Spencer (1965)
(Nylon 6)	-	6.5	Barrie (1968)
"	-	12.5	"
Polyethylene-Terephthalate	0.5	10.4	Barrie (1968)
Polyvinyl chloride	-	42	Spencer (1965)
	2.35	10	Barrie (1968)
	2.35	-	Doty et.al. (1946)
Polyvinyl chloride-acetate	2.35	-	Doty et. al. (1946)
	4.0	-	"
	-	7.7	Spencer (1965)
	-	19.6	"
Polyvinyl alcohol	-	14.3	Spencer (1965)
Polyvinyl acetate	-	15.0	Spencer (1965)

Material	E_P kcal/gmole	E_D kcal/gmole	Source
Polyvinyl acetate (Cont'd)			
	-	12.5	Barrie (1968)
	-	15	"
Polyvinylidene chloride	17.5	-	Doty *et.al.* (1946)
Polyvinylidene chloride-acrylonitrile	10.3	20.2	Barrie (1968)
Polyvinyl Butyral	-2.1	10.9	"
Polymethylacrylate	-	11.0	Spencer (1965)
Polymethylmethacrylate	-	11.6	Barrie(1968)
	-	11.6	Spencer(1968)
Polyethylmethacrylate	0.5	8.7	Barrie (1968)
	4.3	15.1	"
Cellulose Acetate	-	12.0	Spencer (1965)
	-	5.6	"
Ethyl Cellulose	-	6.6	"
	-	14.0	"
	-1.5	6.3	Barrie (1968)
	-2.8	9.5	"
Rubber Hydrochloride	12.8	-	Doty *et.al.* (1946)
	-	17.2	Spencer (1965)
	-	14.0	"

References for Appendix C

1. Barrie, J. A. in Diffusion in Polymers, J. Crank and G. S. Park, Editors, New York, Academic Press (1968), p. 259.
2. Bazarre, D. F. and Petriello, J., Plating, 57, 1025 (1970).
3. Dietz, R. N., Cote, E. A., and Smith, J. D., Anal. Chem., 46, 315 (1974).
4. Doty, P. M., Aiken, W. H., and Mark, H., Ind. Eng. Chem., 38, 788 (1946).
5. DuPont Tedlar PVF Film Bulletins TD-1A, TD-2, TD-3, and TD-6, E.I.DuPont de Nemours and Co., Inc., Film Dept., Wilmington, Del.
6. Dupont Teflon FEP fluorocarbon film bulletins T-1C, T-2D, T-3D, E.I.DuPont de Nemours and Co., Inc., Plastics Dept., Fluorocarbon Div., Wilmington, Del.
7. Felder, R. M., Ferrell, J. K., and Spivey, J. J., Anal. Instrum., 12, 35 (1974).
8. "General Electric Permselective Membranes," General Electric, Medical Development Operation, Chemical and Medical Division, Schenectady, N. Y.
9. Getman, F. H. and Daniels, F., Physical Chemistry, New York, John Wiley and Sons, Inc. (1946), p. 297.
10. Hadge, R. G., Riddell, M. N., and O'Toole, J. L., Soc. of Plast., Eng. Tech. Pap., 18, 545 (1972).
11. Handbook of Chemistry and Physics, Fiftieth Edition, R. C. Weast, Editor, Cleveland, Chemical Rubber Co. (1969), Sect. D, p. 145.
12. Ito, Yukio, Kobanshi Kagaku, 19, 413 (1962).
13. Johnson, R. L., NASA Ascension No. 5, N70-23369 and N70-33154. Contract No. NAS7-505 (1969).
14. Kass, W. J. and Andrzejewski, W. J., SLA-73-718, 1973 Report NTIS.
15. Korte-Falinski, M., J. Chem. Phys., 59, 27 (1962).
16. Metronics Product Bulletin No. 20-70, Metronics Associates, Inc., Palo Alto, Calif. (1970).
17. Norton, F. J., J. Appl. Poly. Sci., 7, 1649 (1963).
18. O'Keeffe, A. E. and Ortman, G. C., Anal. Chem., 38, 760 (1966).
19. Pasternak, R. A., Christensen, M. V., and Heller, J., Macromolecules, 3 366 (1970).

20. Petriello, J. V., AIAA and Aerospace Corp. Joint Symposium, Los Angeles, Calif., May 1968, Proceedings, North Hollywood, Calif., Western Periodicals, p. 119 (1968).

21. Robb, W. L., Ann. N. Y. Acad. Sci., 146, 119 (1968).

22. Rust, G. and Herrero, F., Materialpruf, 11, 166 (1969).

23. Saltzman, B. E., Burg, W. R., and Ramaswamy, G., Environ. Sci. Tech. 5, 1121 (1971).

24. Shirokshina, Z. V., Suykovskaya, N. V., and Pogodayev, A. K., Opt. Tech., 37, 42 (1970).

25. Sivadjian, J. and Riberio, D., J. Appl. Polymer Sci., 8, 1403 (1964).

26. Spencer, H. G., Official Digest, 37, 757 (1965).

27. Spivack, M. A., Rev. Sci. Instrum., 41, 1614 (1970).

28. Stanford, H. B., NASA Ascension No. N66-23478. Jet Propulsion Laboratory TM No. 33-123, Cal. Tec., Pasadena, Calif. (1963).

29. Toren, P. E., Anal. Chem., 37, 922 (1965).

30. Woodgate, B. E., J. Physics E: Scient.Instr. , 4, 1073 (1971).

31. Woolley, J. T., Plant Physiol., 42, 641 (1967).

32. Yaws, C. L. and Hopper, J. R., Chem. Eng., 81, 99 (1974).

APPENDIX D

POLYMERIC INTERFACES FOR CONTINUOUS STACK MONITORING*

Lanny C. Treece, Richard M. Felder and James K. Ferrell
Department of Chemical Engineering
North Carolina State University
Raleigh, North Carolina 27607

ABSTRACT

Teflon tubes have been used as interfaces between stacks containing SO_2 and ambient-level SO_2 analyzers. Continuous monitoring runs were carried out in process and power plant stacks in which the SO_2 concentration varied from 85 ppm to 2000 ppm. The interfaces provided sample gases with SO_2 concentrations which varied linearly with the SO_2 concentrations in the stacks. The presence of acid mist and solid particulate matter in the stack gases had no effect on the performance of the interfaces, and fluctuations in the stack gas SO_2 concentrations were accurately mirrored in the analyzer responses. The use of such interfaces eliminates the need for frequent manual operations usually associated with sample conditioning, such as filter changes and cold trap or drying column replacements, and therefore makes possible continuous unattended monitoring for extended periods of time.

---

* Published as Env. Sci. & Technology 10, 457 (1976). Reprinted by permission of the American Chemical Society.

INTRODUCTION

A growing concern about the environmental impact of industrial waste emissions into the atmosphere led to the passage of the Clean Air Act of 1970, which specifies that air pollution control plans include emission standards and requirements for monitoring stationary sources. If emission standards are to be enforced uniformly, then methods which indicate the true emission rates of particular pollutants must be available. Furthermore, these methods must be relatively simple and inexpensive so that industries which are required to comply with the standards can do so without making large expenditures for monitoring equipment and trained personnel.

Stack gas analyses have traditionally been performed by drawing a sample through a small tube inserted in the stack, collecting and fixing the pollutant in a solution or on a solid by absorption or reaction, and using conductimetric, colorimetric, or photometric analysis to determine the concentration of the pollutant. Some of the techniques in current use are described in the Federal Register,[1] the Los Angeles Pollution Control District Source Sampling Manual,[2] and by Cooper and Rossano.[3]

More recently, methods have been developed which provide continuous records of pollutant concentrations. A review of instrumentation for continuous SO_2 monitoring has been compiled by Hollowell, et al.[4]

A gas sample withdrawn directly from a stack must usually be conditioned before passing to a continuous analyzer or a wet chemical sampling train. The conditioning entails removing condensible vapors, mists, and solid particulates, and chemical species which are known to interfere with the analysis of the desired pollutant. A typical sample conditioning procedure might involve heating the gas to maintain vapors above their dew point or cooling to condense and remove the vapors from the sample stream, filtering the sample to remove particulates, and bubbling the gas through a liquid solution which removes the undesired chemical species but allows the pollutant to pass through to the analyzer.

A. O'Keeffe of the National Environmental Research Center, E.P.A., proposed using a polymer tube as a stack sampling interface. In the proposed method, a carrier gas is passed continuously through a polymer tube mounted in the stack, and the pollutant permeates through the tube wall from the stack into the carrier gas stream, which then passes to a continuous ambient analyzer. This method has several potential advantages over traditional sample conditioning techniques: an average concentration across the stack can be measured, polymers can be used which do not pass interfering pollutants, vapors in the carrier gas stream should be well above their dew points, and particulate filters are not required.

Rodes, Felder, and Ferrell[5] investigated the feasibility of this technique. TFE Teflon and fluorosilicone rubber tubes were tested at temperatures from 93°C to 232°C with simulated SO_2 stack concentrations in the range 1,000 ppm - 10,000 ppm. The conclusions of the study were that the SO_2 flux through such tubes is a predictable function of the temperature and SO_2 concentration in the stack, and response times can be kept reasonably short by selecting a tube with a sufficiently thin wall.

Felder, Spence, and Ferrell[6] measured the permeabilities of SO_2 for several materials over a wide range of temperatures, and compiled a complete summary of these results and published SO_2 permeability data. Felder, Ferrell and Spivey[7] investigated the permeation of SO_2 and water through TFE Teflon, FEP Teflon, and fluorosilicone rubber tubes. SO_2 permeation rates were measured over a temperature range 125°C - 225°C for simulated stack humidities of up to 21 mole percent water. The polymer screened out water vapor to an extent sufficient to preclude the possibility of condensation in the carrier gas stream, and the presence of water vapor in the stack gas did not affect the SO_2 permeation rates.

The purpose of the present study was to develop an in-situ calibration technique for a permeation interface, and to test this technique using prototype sampling devices in several process and power plant stacks. A calibration technique was designed and successfully tested. FEP Teflon, TFE Teflon, and fluorosilicone rubber tubes were used as interfaces in continuous monitoring runs of several days duration in the atmospheric exhausts of two SO_3 absorption towers, and a wet chemical technique was also used to obtain intermittent measurements of the concentration of SO_2 in the stack gases for comparison with the continuous monitoring results. Another series of experiments was carried out in the stack of an oil-fired power plant boiler. This paper reports on the results of these field tests.

CALIBRATION FORMULAS

The rate of transport of a gas through a cylindrical polymer tube is given by the following equation (Crank and Park[8]):

$$F = \frac{2\pi P}{\ln(b/a)} (p_2 - p_1) \qquad (1)$$

where F = flux of the diffusing gas through the polymer, $cm^3(STP) \cdot sec^{-1} \cdot cm^{-1}$

P = permeability of the polymer to the diffusing gas, $cm^3(STP) \cdot cm^{-1} \cdot sec^{-1} \cdot cm^{-1}(Hg)$

a, b = inner and outer tube radii, respectively, cm

p_1, p_2 = inner and outer bulk partial pressures of the diffusing gas, cm(Hg)

The principle assumptions leading to Equation (1) are that diffusion is Fickian with a concentration-independent diffusivity and that the solubility of the gas in the polymer follows Henry's law.

The permeability follows an Arrhenius relationship over a moderate temperature range:

$$P = P_o \exp(-E_p/RT) \tag{2}$$

where E_p = activation energy for permeation, kcal · gmole^{-1}

R = gas constant, kcal · gmole^{-1} · °K^{-1}

P_o = pre-exponential factor, units of P

The validity of Eqs. (1) and (2) for SO_2 permeating through TFE Teflon and FEP Teflon has been demonstrated by Rodes et al.[5] and Felder et al.[7]

A material balance on the diffusing component in the carrier gas yields

$$y_{CG} = FL/\phi \tag{3}$$

where y_{CG} = volume fraction of the diffusing component in the carrier gas stream leaving the polymer tube

L = polymer tube length, cm

ϕ = carrier gas flow rate, cm^3(STP) · sec^{-1}

Substitution of Eq. (1) into Eq. (3) yields

$$p_2 - p_1 = \frac{\phi \ln(b/a)}{2\pi LP} y_{CG} \tag{4}$$

If desired, the function of Eq. (2) may be substituted for the permeability P in this equation.

Under normal operating conditions, the partial pressure of SO_2 in the stack or calibrating gas (p_2) is roughly two orders of magnitude greater than that in the carrier gas (p_1); the carrier gas SO_2 concentration is therefore directly proportional to the stack gas concentration, making possible a single point calibration procedure.

EXPERIMENTAL

A portable system was designed and constructed for use in field-testing polymeric interfaces. The system, which was a modified version of an apparatus designed by Charles E. Rodes of the Environmental Protection Agency, included a central control panel, a probe for supporting the polymer tube in the stack, an ambient SO_2 analyzer and recorder, a thermocouple, potentiometer and recorder, an air compressor and an analyzer calibration system.

The polymer tube to be tested was mounted on a probe assembly shown in Figure 1. All parts of the probe were made from 316 stainless steel or TFE Teflon. The assembly was mounted in the stack by means of a 1/4" x 6" x 6" plate clamped to a bolt flange located on the outside of the stack. A 1/4" tube which passed through the inside of the 1/2" support tube served as the carrier gas inlet. A 1" tube functioned as a movable sheath which could be positioned over the polymer tube or withdrawn to expose the tube to the stack gas. A span gas of known concentration (calibration gas) was introduced into the sheath and passed over the outside of the polymer tube during calibration.

A 24" x 24" x 4" enclosure constructed from 1/4" plywood formed the central control panel. Flow control valves, pressure gauges, and rotameters were mounted on the front and side panels, as shown in Figure 2. The connecting 1/4" polypropylene tubes and Swagelok fittings were mounted behind the front panel and were accessible through a hinged rear panel. A removable plywood enclosure could be attached to protect the rotameters during transport to and from the test site. A small carbon vane compressor served as the central air supply. The air was purified by passing it through a dessicant bed, activated charcoal, and a particulate filter.

The calibration gas was prepared by dilution of a compressed cylinder gas (5,000 ppm SO_2 in air) with a stream of purified air. Both the cylinder gas and dilution air were metered through rotameters located on the control panel. By varying the ratio of dilution air and cylinder gas flow rates, a range of SO_2 concentrations could be obtained.

Upon leaving the probe, the carrier gas passed through an ambient SO_2 analyzer. Two continuous ambient analyzers were used in this study: a Meloy Labs Model SA-160 flame photometric detector and an Environmetrics Model NS-300 electrochemical transducer. Both analyzers produced a continuous record of the carrier gas SO_2 concentration. Known concentrations of SO_2 for analyzer calibration were generated by passing purified air at a measured rate across a standard Dynacal SO_2 permeation tube. Either the carrier gas or the analyzer calibration gas could be passed through the analyzer, depending on the setting of a three-way valve on the control panel.

The stack temperature was measured using a 60-inch copper-constantan thermocouple inserted in the carrier gas line such that the tip was positioned in the center of the polymer tube. The output emf was determined with a potentiometer and strip chart recorder.

Measurement of low SO_2 stack concentrations (less than 500 ppm) required a tube with a thin wall. Since Teflon tubes with sufficiently thin walls were not available, an FEP Teflon membrane (0.002") was wrapped and heat sealed around a 0.40" O.D. 40μ porosity stainless steel tube. The heat sealing was performed by Livingstone Coating Corporation, Charlotte, N. C.

The general procedure for testing a polymer interface was as follows. A polymer tube was mounted in the probe and positioned in the stack with the sheath in the calibration position. The components of the testing system were connected and checked for leaks. After calibration of the analyzer, the polymer tube was exposed to a span gas containing the desired concentration of SO_2. The carrier gas flow rate was then adjusted to its desired value, and the flow was directed to the analyzer. When the recorder signal reached a steady level, the carrier gas SO_2 concentration was noted. A plot of span gas concentration vs. carrier gas concentration generated in this manner was used as a calibration curve for the subsequent stack monitoring. The polymer tube was then exposed to the stack by withdrawing the sheath, and the analyzer signal was recorded. The signal was corrected for variations in the stack temperature using Eq. (2), with an activation energy for permeation of 6.54 kcal/g-mole for TFE Teflon and 7.18 kcal/g-mole for FEP Teflon.[6]

FIELD TEST RESULTS

Monitoring runs were carried out in two process stacks and a power plant boiler stack. The stack conditions and operating parameters for these field tests are summarized in Table 1. The sections that follow outline and discuss the results.

Single Contact Process Sulfuric Acid Plant

A one-day monitoring run was carried out using an FEP Teflon sampling tube in the SO_3 absorption tower stack of a single contact process sulfuric acid plant. The stack gas contained approximately 2,000 ppm SO_2, and the stack temperature was approximately 80°C. To check the continuous monitoring results, gas samples were periodically withdrawn directly from the stack and subjected to analysis by Federal Register Method 6.[1]

Figure 3 shows a typical calibration plot obtained in the course of the run. As anticipated, the carrier gas SO_2 concentration varied linearly with the span gas concentration. Under normal circumstances a single calibration point should suffice, making automation of the calibration procedure relatively straightforward.

The results of the monitoring measurements are shown in Figure 4. There were no significant operating problems, and excellent agreement was obtained between the continuous monitoring results and those obtained by intermittent direct sampling and wet chemical analysis.

A heavy acid mist was present in the stack, and considerable dropwise condensation occurred on the tube during the run. To estimate the effect of the condensation on the interface performance, the tube permeability was calculated from the plot of Figure 3 and other calibration plots using Eq. (1), and the calculated values were compared with values obtained for clean tubes of the same material. Figure 5 shows the results. The permeabilities determined for the condensate-coated tubes in the stack come quite close to a regression line on an Arrhenius plot of FEP permeabilities reported by Felder, Spence and Ferrell,[6] indicating that the presence of the condensate on the tube did not alter the effective tube permeability.

In another experiment, the SO_2 permeability of a TFE Teflon tube was measured, after which the tube was left in the absorption tower stack for one year and the permeability was then remeasured. A permeability decrease of about 15% was observed. This change would appear as a span drift, and would easily be accounted for by periodic recalibration. This result suggests the potential usefulness of Teflon interfaces as tools for long-range unattended continuous monitoring.

A fluorosilicone rubber tube (Silastic LS-63U®, manufactured by Dow-Corning) was placed in the stack for a period of twelve hours. Upon removal from the stack the tube showed obvious signs of deterioration, indicating that unlike Teflon, this material is unsuitable for use in an acid mist environment.

Double Contact Process Sulfuric Acid Plant

Monitoring runs were carried out over a two-day period in the SO_3 absorption tower stack of a double contact process sulfuric acid plant. The average concentration of SO_2 in the stack gas was 85 ppm, and the stack temperature was 67°C. To obtain a permeation rate sufficiently high for the carrier gas SO_2 concentration to be within the operating range of the analyzer (0.02-0.5 ppm), a tube with a very thin wall had to be constructed. This was done by wrapping and heat-sealing a 2 mil FEP Teflon membrane about a porous stainless steel support. The continuous readings obtained using this device were compared with readings obtained with an on-stream stack gas analyzer operated by plant employees.

The results of these tests are shown in Figure 6. THe stack gas analyzer used in the normal operation of the process indicated 60 ppm on one day and 85 ppm the following day, while the continuous monitoring system indicated an average concentration of 85 ppm both days. Since no process changes were made during this two-day period, it can be speculated that the latter result is more likely to be correct. Moreover, the continuous record provided by the test system fluctuated less than the intermittent record obtained with the plant instrument.

These results and those obtained in the single contact process stack indicate that polymeric interfaces can be used to monitor stacks containing SO_2 at concentrations which vary over a wide range. The concentration in the first stack, ≈2,000 ppm, is typical of uncontrolled emissions from many process and power plant stacks, while that in the second stack, ≈85 ppm, is characteristic of a controlled emission. A system composed of two probes and a single analyzer might therefore be used to measure the effectiveness of an SO_2 removal process by monitoring both the inlet and outlet SO_2 concentrations.

Oil-Fired Power Plant Boiler Stack

Monitoring runs were carried out in an oil-fired power plant boiler at North Carolina State University. A #6 fuel oil containing 1.9% sulfur was burned, and the SO_2 content of the stack gas varied between 250 ppm and 1,045 ppm as the load on the boiler was changed. The stack temperature fluctuated between 170°C and 213°C.

On one day, the feed to the boiler was changed from natural gas with a negligible sulfur content to fuel oil, and 150 minutes later a change back to natural gas was carried out. Figure 7 shows the analyzer response during this period.

The ability of the sampling interface to follow changes in the SO_2 concentration in the stack is illustrated by Figure 7. Following each fuel change, the analyzer signal reached its final value in approximately 10 minutes. Most of this time lag is probably attributable to the time required for the stack gas SO_2 concentration to reach its final value rather than time lags of the sampling tube and analyzer. A better indication of the sampling system dynamics is seen in the response from 120 minutes to 135 minutes, where a momentary increase in the fuel feed rate was reflected almost instantly by a corresponding peak in the analyzer response. As in previous runs, good agreement was achieved between measurements made with the test system and others obtained by direct sampling and wet chemical analysis.

A four-day monitoring run was carried out in the same stack, with results shown in Figure 8. The breaks in the analyzer signal record (the lower curve) are due partially to periodic recalibrations, and partially to difficulties with the strip chart recorder which occurred during unattended periods of operation. The results are sufficiently complete, however, to show that the sampling interface-analyzer system provided accurate readings and responded rapidly to variations in the fuel feed rate (and hence in the stack gas SO_2 concentration).

A gross measurement of the particulate concentration in the stack using Federal Register Method 5[1] yielded a loading of 0.21 g/m^3. Inspection of the sampling tube at the conclusion of the tests revealed a slight powdery deposition on the tube surface, but recalibration measurements suggest that this layer had no effect on the SO_2 permeability of the tube. This result is consistent with previously reported results concerning the lack of particulate interference effects in tests of a TFE Teflon sampling tube in a coal-fired power plant boiler (Spence, Felder, Ferrell and Rodes[9]). Polymeric interfaces are thus able to provide clean samples for analysis regardless of the particulate loading in the stack, and to do so without a need for filters or other particulate removal devices in the sampling train.

CONCLUSIONS

Previous studies[5,7,9] have suggested the potential advantages of in-stack polymeric interfaces for continuous stack monitoring. The field tests discussed in this report provide additional evidence of the performance capability of such devices. Demonstrated features of TFE and FEP sampling tubes include the following.

1. Interfaces can be designed to monitor stack gases with SO_2 concentrations from tens to thousands of parts per million.
2. The presence of water vapor in the stack does not affect the rate of permeation of SO_2 through the interface, so that the analyzer reading need not be corrected for the stack humidity.[7] Moreover, Teflon is sufficiently impermeable to water to eliminate the possibility of condensation in the sample line or the analyzer.[7] There is consequently no need for heated sample lines, cold traps or sample drying columns in the sampling train.

3. The presence of liquid or solid particulate matter in the stack gas has had no measurable effect on the performance of sampling interfaces in tests carried out to date. Using such an interface in a sampling train therefore eliminates the need for frequent filter changes, making long-term unattended continuous monitoring a good possibility.
4. Responses obtained using polymer interfaces follow changes in the stack gas SO_2 concentration accurately and rapidly, suggesting the potential applicability of such devices as feedback control loop components.

ACKNOWLEDGMENTS

This work was carried out under Environmental Protection Agency Research Grant #801578. The authors wish to express their appreciation to James Homolya and Chen-Chi Ma for assistance with the experimentation. Particular thanks go to Roger Spence, who carried out the field tests in the power plant boiler stack and who has provided assistance throughout the entire program.

REFERENCES

1. "Standards of Performance for New Stationary Sources," Federal Register, 36, 24890, December 23, 1971.
2. Source Sampling Manual, Los Angeles Air Pollution Control District, Los Angeles, Calif., 1963.
3. H. B. H. Cooper and A. T. Rossano, Jr., Source Testing for Air Pollution Control, New York, McGraw-Hill (1971).
4. C. D. Hollowell, G. Y. Gee and R. D. McLaughlin, "Current Instrumentation for Continuous Monitoring for SO_2," Anal. Chem., 45, 63A (1973).
5. C. E. Rodes, R. M. Felder and J. K. Ferrell, "Permeation of Sulfur Dioxide through Polymeric Interfaces," Env. Sci. Technol., 7, 545 (1973).
6. R. M. Felder, R. D. Spence and J. K. Ferrell, "Permeation of Sulfur Dioxide through Polymers," Manuscript in preparation.
7. R. M. Felder, J. K. Ferrell and J. J. Spivey, "Effects of Moisture on the Performance of Permeation Sampling Devices," Analysis Instrum., 12, 35 (1974).
8. J. Crank and G. S. Park, Diffusion in Polymers, p. 5, New York, Academic Press (1968).
9. R. D. Spence, R. M. Felder, J. K. Ferrell and C. E. Rodes, paper presented at the National Meeting of the AIChE, New Orleans, La., March 1973.

Table I. Field Test Parameters

Stack Location	Single-Contact Process SO_3 Absorption Tower	Double-Contact Process SO_3 Absorption Tower	Oil-Fired Power Plant Boiler
Stack Conditions	≈ 2,000 ppm SO_2 ≈ 80°C	≈ 85 ppm SO_2 ≈ 67°C	250-1,045 ppm SO_2 170°C - 213°C
Interface	FEP Teflon Tube I.D. = 0.544 cm O.D. = 0.604 cm L = 75 cm	FEP Teflon Membrane (2 mils) on a porous stainless steel tube Support I.D. = 1.016 cm Support O.D. = 1.026 cm L = 44 cm	TFE Teflon Tube I.D. = 0.403 cm O.D. = 0.480 cm L = 70.5 cm
Analyzer	Electrochemical Transducer Range: 0-0.1 ppm SO_2	Flame Photometer Range: 0-0.5 ppm	Flame Photometer Range: 0-0.5 ppm
Carrier Gas Flow Rate	1250 cm^3/min @ 21.4°C, 1 atm	300 cm^3/min @ 21.4°C, 1 atm	500 cm^3/min @ 21.4°C, 1 atm

LIST OF FIGURES

Figure 1. Stack sampling probe.

Figure 2. Schematic of stack sampling apparatus.

Figure 3. Probe calibration plot.

Figure 4. Monitoring data: Single contact process stack.

Figure 5. Sampling tube permeabilities.

Figure 6. Monitoring data: Double contact process stack.

Figure 7. Monitoring data: Boiler stack, 1-day run.

Figure 8. Monitoring data: Boiler stack, 4-day run.

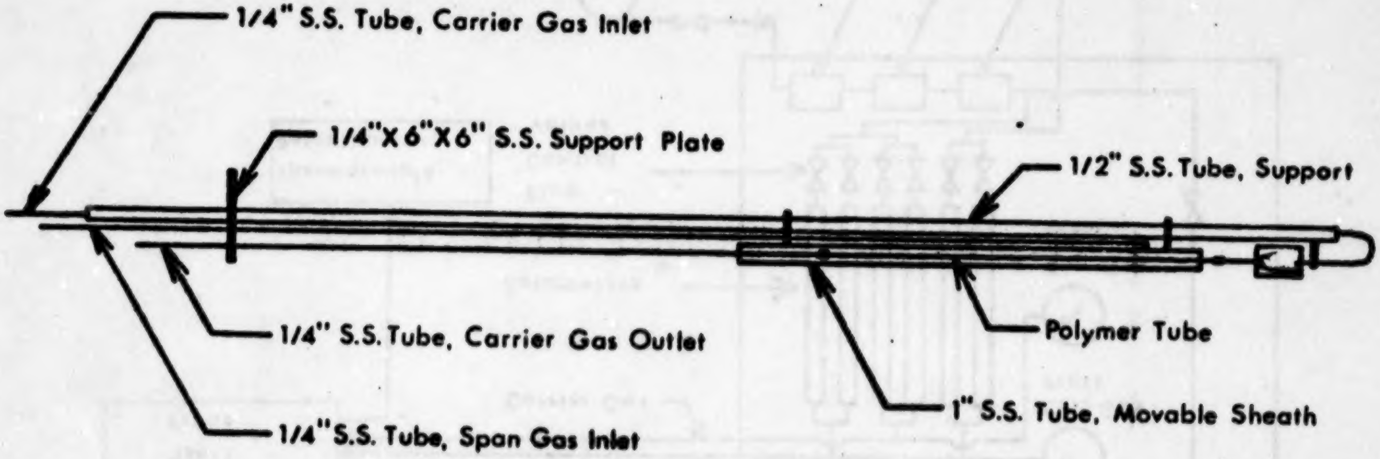
1/4" S.S. Tube, Carrier Gas Inlet
1/4"X 6"X 6" S.S. Support Plate
1/2" S.S. Tube, Support
1/4" S.S. Tube, Carrier Gas Outlet
1/4" S.S. Tube, Span Gas Inlet
Polymer Tube
1" S.S. Tube, Movable Sheath

Figure 1. Stack sampling probe.

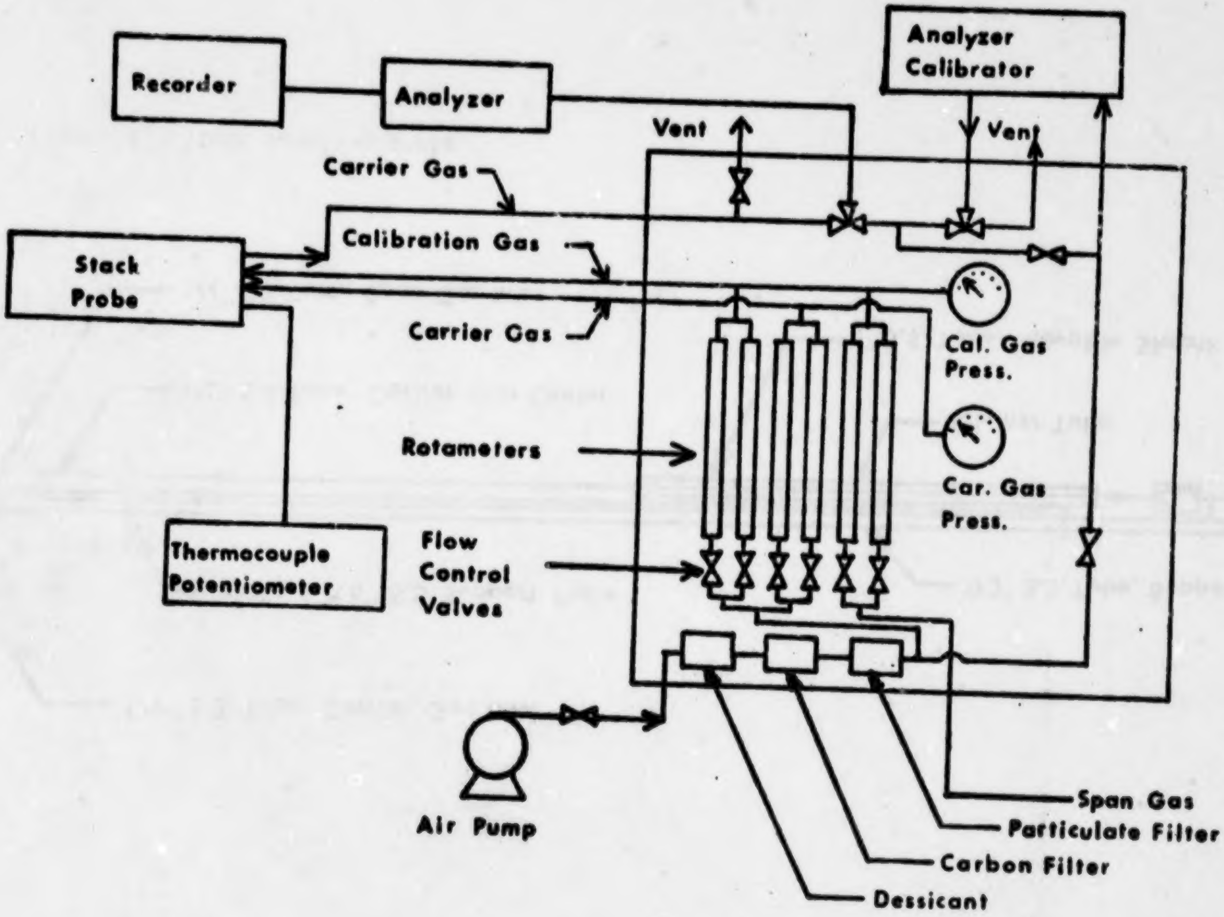
Recorder
Analyzer
Analyzer Calibrator
Vent
Vent
Carrier Gas
Calibration Gas
Stack Probe
Carrier Gas
Cal. Gas Press.
Rotameters
Car. Gas Press.
Thermocouple Potentiometer
Flow Control Valves
Air Pump
Span Gas
Particulate Filter
Carbon Filter
Dessicant

Figure 2. Schematic of stack sampling apparatus.

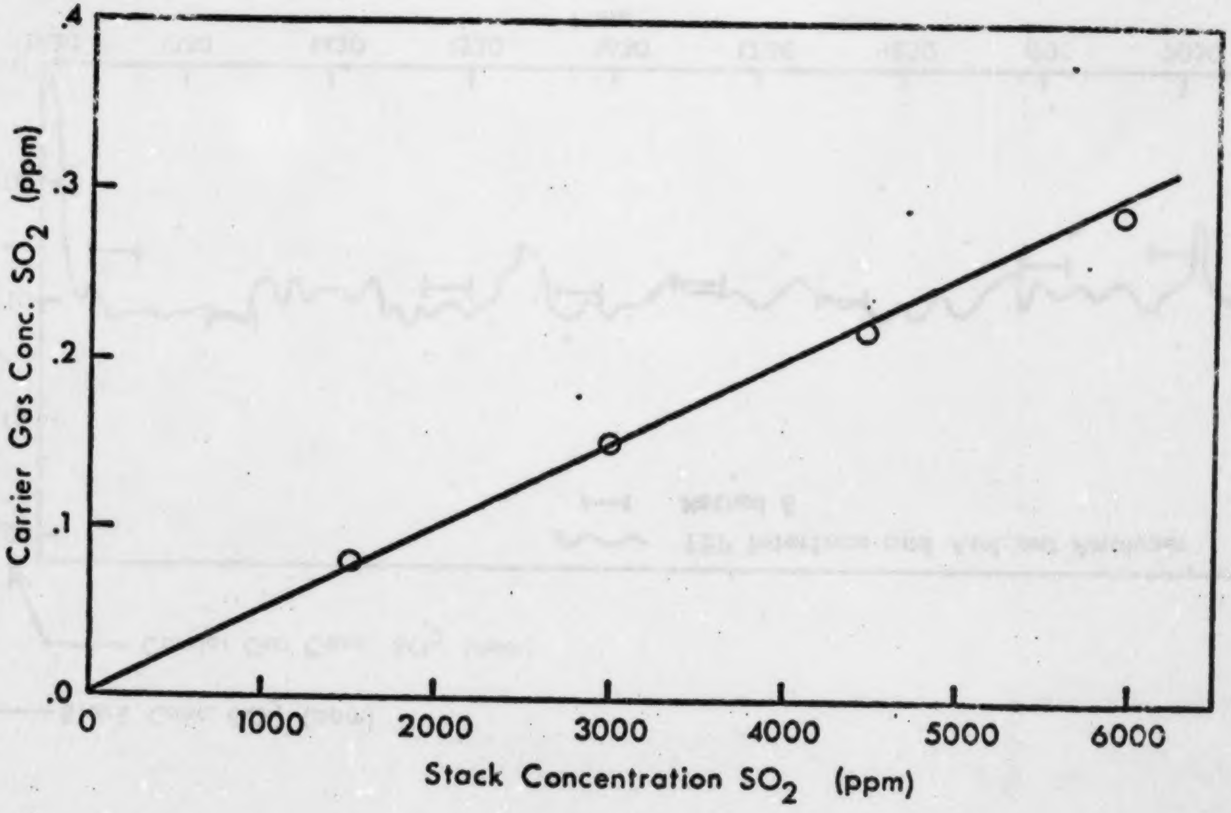

Figure 3. Probe calibration plot.

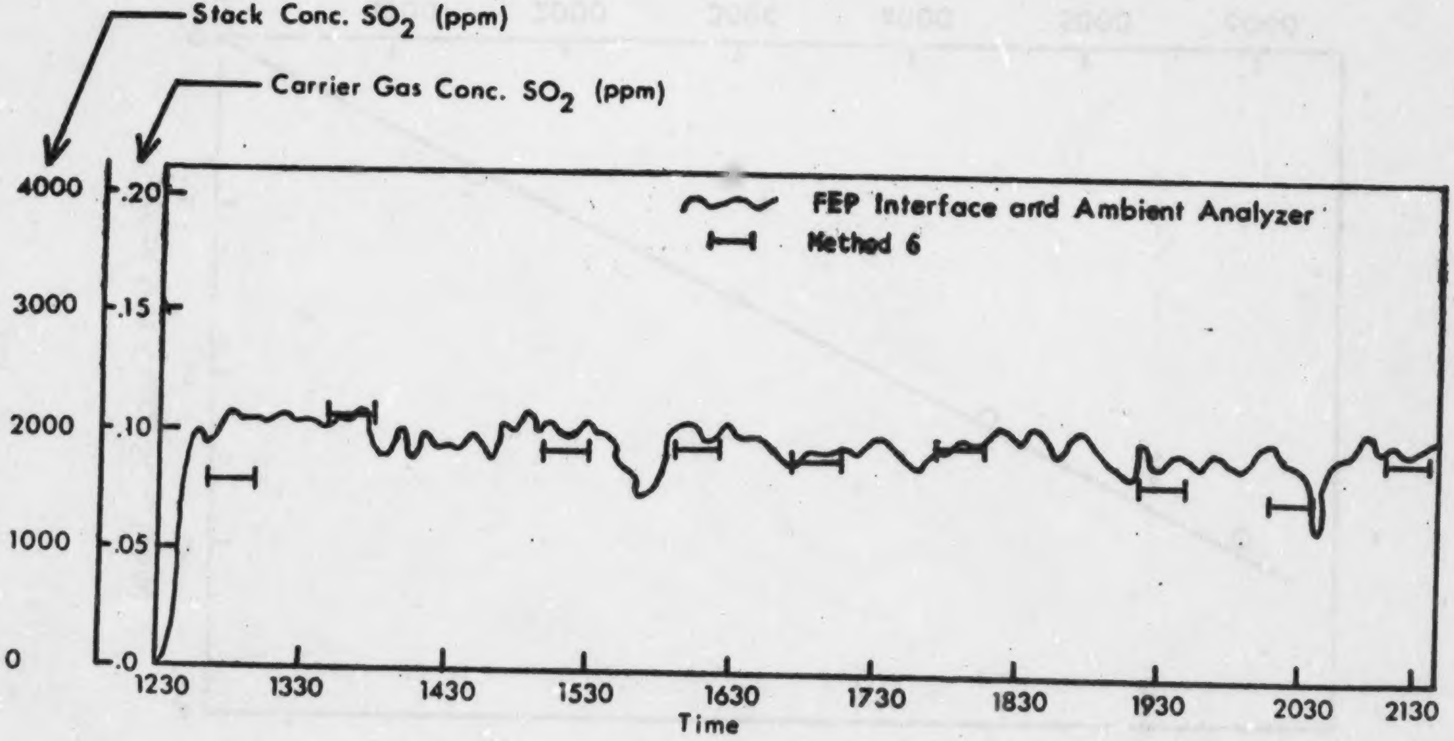

Figure 4. Monitoring data; Single contact process stack.

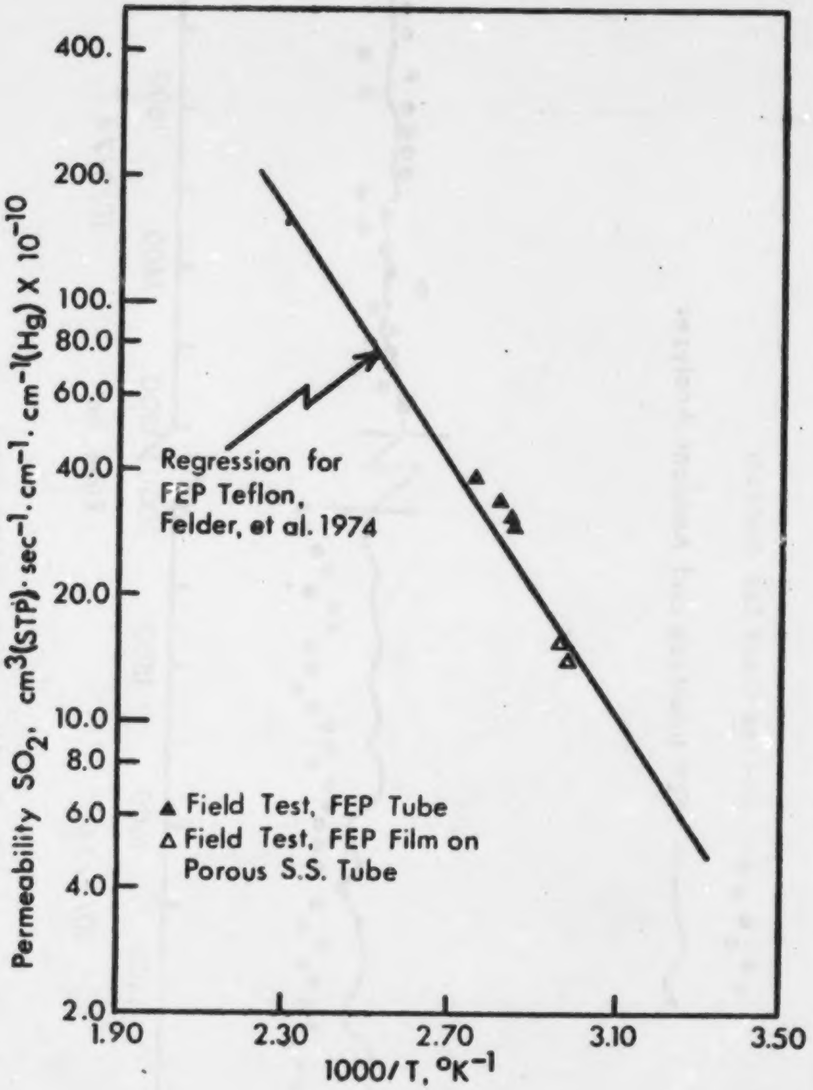

Figure 5. Sampling tube permeabilities.

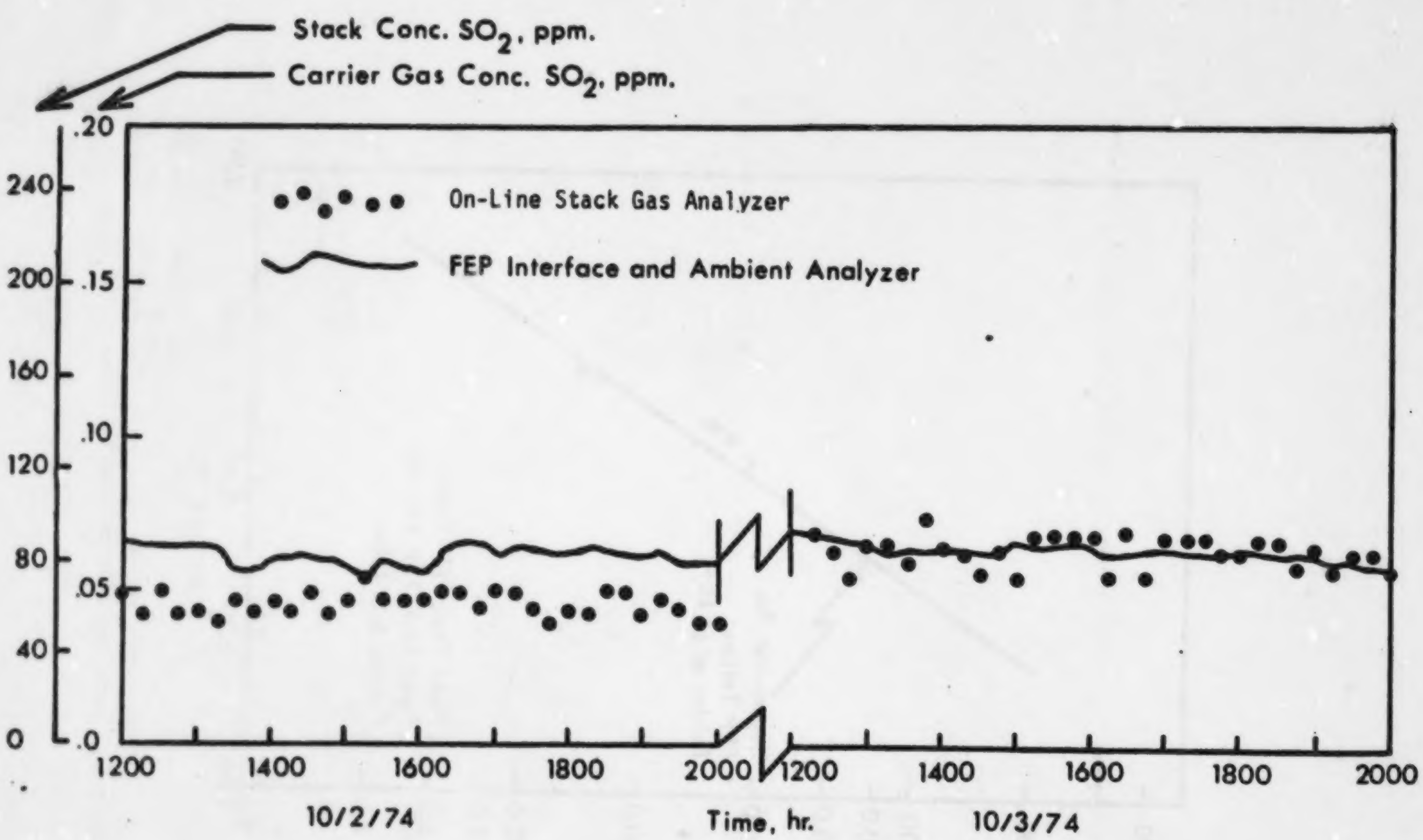

Figure 6. Monitoring data: Double contact process stack.

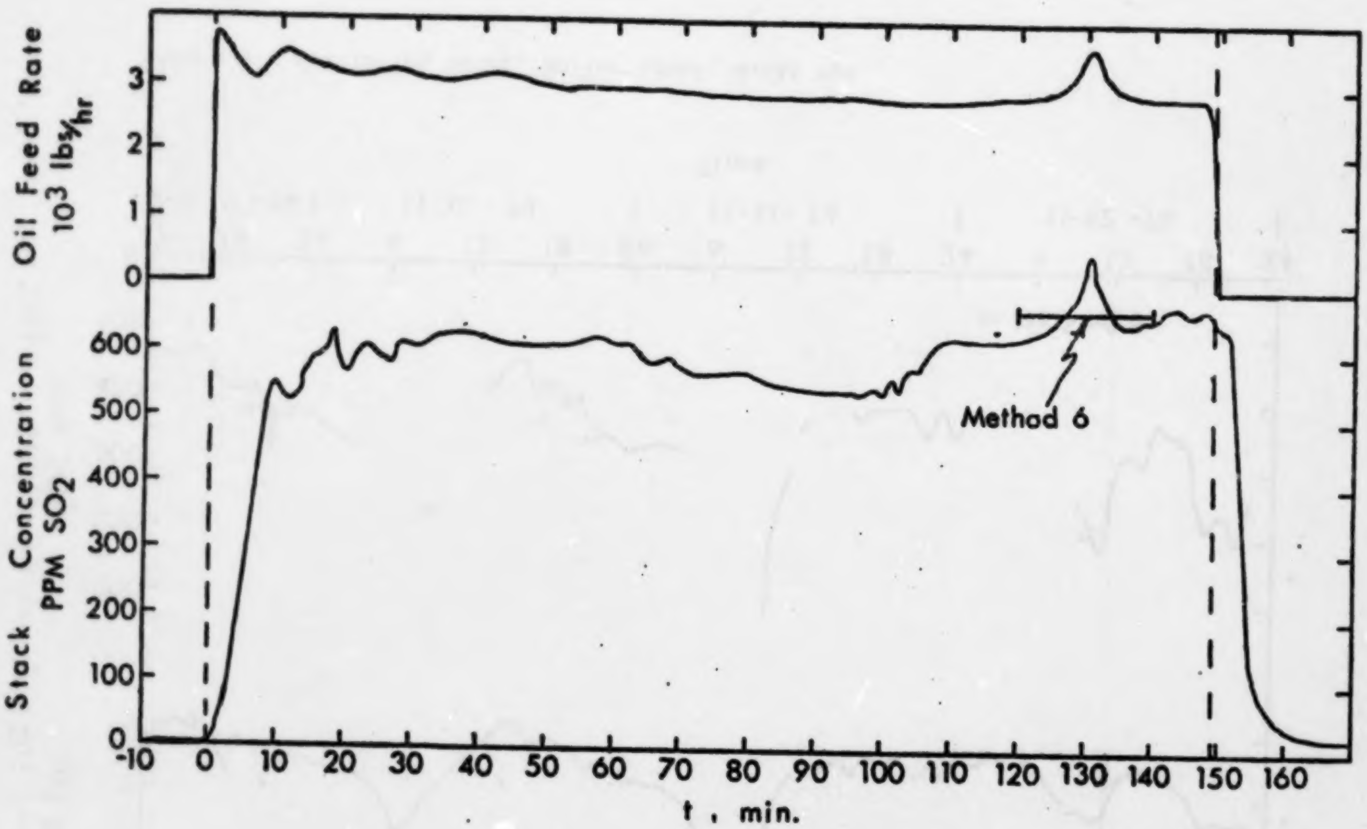

Figure 7. Monitoring data: Boiler stack, 1-day run.

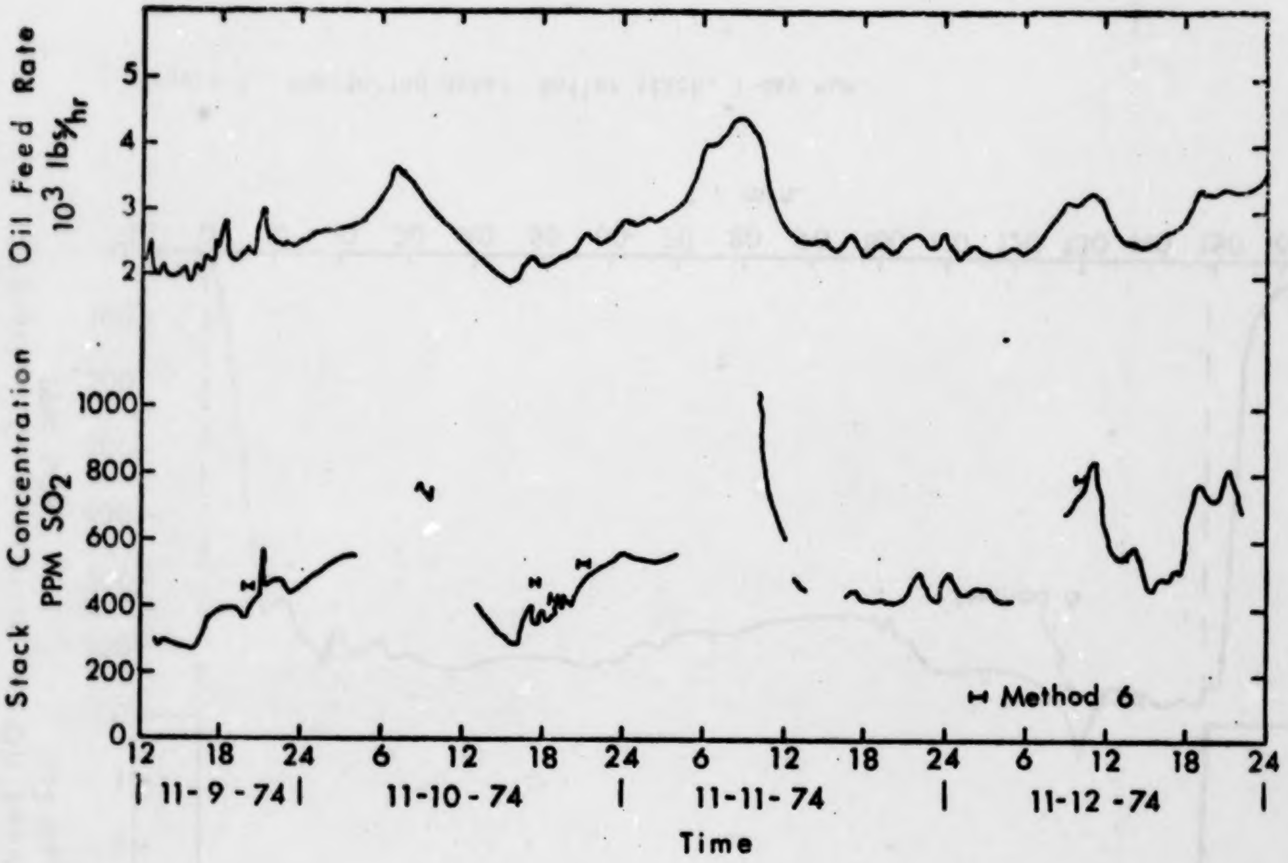

Figure 8. Monitoring data; Boiler stack, 4-day run.

APPENDIX E

A METHOD FOR THE DYNAMIC MEASUREMENT OF DIFFUSIVITIES OF GASES IN POLYMERS*

R. M. Felder, R. D. Spence and J. K. Ferrell
Department of Chemical Engineering
North Carolina State University
Raleigh, North Carolina 27607

ABSTRACT

A method is presented for determining the diffusivity of a gas in a polymer from the response to a step concentration change in a continuous flow permeation chamber. The outlined procedure has several advantages over techniques currently in use: it requires simple numerical integration rather than curve-fitting; it utilizes the complete response, rather than a portion of the response which falls within the region of validity of a short-time asympotic solution of the diffusion equation, and it is applicable both to flat membranes and cylindrical tubes. An illustration of the method is provided by the measurement of the diffusivity of sulfur dioxide in a PTFE tube at several temperatures.

---

[*] Published as J. Appl Polymer Sci. 19, 3193 (1975). Reprinted by permission of John Wiley & Sons, Inc.

INTRODUCTION

The determination of the permeability or diffusivity of a gas in a polymer commonly involves measuring the amount of the gas which permeates through, into or out of a sample of the polymer in a closed volume system.[1] Several problems are associated with experiments of this type. Measuring the cumulative amount rather than the instantaneous rate of permeation or sorption limits the precision of the data; moreover, in batch permeation experiments a pressure gradient is imposed across a membrane, and consequently elaborate membrane sealing and support provisions are required.[2,3]

An approach to permeation measurements in which a gas permeates through a membrane into a flowing stream avoids these problems. Steady-state operation can be achieved in such an experiment, thereby increasing the attainable precision, and equal pressures can be maintained in both compartments of the permeation chamber, minimizing the requirements for sealing and supporting the membrane.

The continuous permeation technique has been applied extensively to the measurement of permeabilities of gases in polymers (see, for example, References 2, 4, and 5). Pasternak, Schimscheimer and Heller[3] showed that the continuous technique may also be used to measure the diffusivity of a gas in a flat membrane. In the method proposed by Pasternak et al. a step change in the partial pressure of the penetrant is imposed on one side of the membrane, and the rate of permeation into the gas flowing past the other side is monitored continuously. The data are plotted such that a straight line is obtained for a portion of the response, with the slope of the line being a known function of the diffusivity. The method is effective, but being based on either a short-time or long-time asymptotic solution of the diffusion equation limits its applicability: when deviations from the anticipated straight line occur, it is difficult to determine whether they are due to experimental error, or to a violation of the assumptions of the diffusion model, or simply to the invalidity of the asymptotic solution in the range of response times where the deviations occur.

This paper outlines an alternative method for determining the diffusivity of a gas in a polymer from step response data obtained in a continuous permeation chamber. The proposed method has several advantages over that of Pasternak et al.: it requires simple numerical integration of response data, rather than curve-fitting; it utilizes the complete response, rather than a portion of the response which falls within the region of validity of an asymptotic solution of the diffusion equation, and it is applicable to cylindrical tubes as well as flat membranes. The method is illustrated by the experimental determination of the diffusivity of sulfur dioxide in a PTFE tube.

THEORETICAL

A continuous permeation chamber consists of two compartments separated by a membrane. At a time t=0 a penetrant is introduced into one compartment (the upstream compartment), and permeates through the membrane into a stream flowing through the other (downstream) compartment. The concentration of the penetrant in the gas leaving the downstream compartment is monitored continuously until steady-state is attained.

It is assumed that diffusion of the penetrant in the gas phase and absorption at the membrane surface are instantaneous processes, that diffusion in the membrane is Fickian with a constant diffusivity $D(cm^2/s)$, and that the concentration of dissolved gas at the downstream surface of the membrane is always sufficiently low compared to the concentration at the upstream surface that it may be set equal to zero. The diffusion equation and boundary conditions for a flat membrane of thickness h, and for a cylindrical tube with inner radius a and outer radius b with the penetrant introduced on the outside of the tube, are given below:

Flat Membrane | Cylinder

$$\frac{\partial C(t,x)}{\partial t} = D\frac{\partial^2 C(t,x)}{\partial x^2} \qquad \frac{\partial C(t,r)}{\partial t} = \frac{D}{r}\frac{\partial}{\partial r}\left(r\,\frac{\partial C}{\partial r}\right) \qquad (1)$$

$$C(0,x) = 0 \qquad C(0,r) = 0 \qquad (1a)$$

$$C(t,0) = C_1 \qquad C(t,a) = 0 \qquad (1b)$$

$$C(t,h) = 0 \qquad C(t,b) = C_1 \qquad (1c)$$

The solutions of these equations may be obtained by simplifying solutions given by Crank[6] for more general boundary conditions, and the resulting expressions for $C(t,x)$ and $C(t,r)$ may in turn be used to derive expressions for the rate at which the gas permeates through the downstream membrane surface. For a flat membrane with a surface area $A(\mathrm{cm}^2)$

$$\phi_{fm} = -DA\left(\frac{\partial C}{\partial x}\right)_{x=h}$$

$$= \frac{DAC_1}{h}\left\{1 + 2\sum_{n=1}^{\infty}(-1)^n \exp\left(-\frac{n^2\pi^2 Dt}{h^2}\right)\right\} \qquad (2)$$

and for a cylinder of length L

$$\phi_c = 2\pi DL\left(r\,\frac{\partial C}{\partial r}\right)_{r=a}$$

$$= \frac{2\pi DLC_1}{\ln(b/a)}\left\{1 + 2\ln(b/a)\sum_{n=1}^{\infty}\frac{J_o(\alpha_n a)\,J_o(\alpha_n b)}{J_o^2(\alpha_n a) - J_o^2(\alpha_n b)}\exp(-\alpha_n^2 Dt)\right\} \qquad (3)$$

where α_1, α_2, ... are the real positive roots of the equation

$$J_o(\alpha_n a)\,Y_o(\alpha_n b) - J_o(\alpha_n b)\,Y_o(\alpha_n a) = 0 \qquad (4)$$

ϕ_c is defined to be positive for flow in the negative r direction. In Eqs. (3) and (4), J_o and Y_o are the zero-order Bessel functions of the first and second kind. An expression for the permeation rate applicable to both geometries is

$$\phi(t) = \phi_{ss} \left[1 + K \sum_{n=1}^{\infty} b_n \exp(-\omega_n^2 Dt)\right] \tag{5}$$

where the steady-state permeation rate ϕ_{ss} is

$$\phi_{ss} = DAC_1/h \qquad \text{flat membrane} \tag{6a}$$

$$= 2\pi DLC_1/\ln(b/a) \qquad \text{cylinder} \tag{6b}$$

and the expressions for K, b_n and ω_n^2 may be deduced by inspection of Eqs. (2) and (3).

The total amount of the penetrant that has permeated through the membrane up to time t is

$$Q(t) = \int_0^t \phi(t)\, dt \tag{7}$$

Substituting the expression of Eq. (5) for $\phi(t)$ in Eq. (7) yields

$$Q(t) = \phi_{ss} t + \frac{\phi_{ss} K}{D} \sum_{n=1}^{\infty} \frac{b_n}{\omega_n^2} - \frac{\phi_{ss} K}{D} \sum_{n=1}^{\infty} \frac{b_n}{\omega_n^2} \exp(-D\omega_n^2 t) \tag{8}$$

As t becomes large the exponential terms become negligible and a plot of Q(t) vs. t approaches a straight line. The intersection of this line with the time axis -- the so-called time lag t_1 -- is obtained by setting the first two terms of Eq. (8) equal to zero and solving for t, with the result

$$t_1 = -\frac{K}{D} \sum_{n=1}^{\infty} \frac{b_n}{\omega_n^2} \tag{9}$$

Expressions for the time lag for planar and cylindrical membranes are given by Crank and Park[1]

$$(t_1)_{fm} = h^2/6D \tag{10}$$

$$(t_1)_c = \frac{a^2 - b^2 + (a^2 + b^2) \ln (b/a)}{4D \ln (b/a)} \; * \tag{11}$$

Eqs. (10) and (11) provide the basis for the determination of D from an experiment in which Q(t) is measured in a closed-volume system and t_1 is determined graphically. If instead $\phi(t)$ is measured in a continuous permeation apparatus the following analysis is pertinent.

The quantity $(1 - \phi/\phi_{ss})$ may easily be calculated from experimental response data and integrated numerically from t=0 to t=∞. If the value of this integral is designated M_o, then from Eq. (5)

$$M_o = \int_0^\infty [1 - \frac{\phi(t)}{\phi_{ss}}] \, dt = K \int_0^\infty \sum_{n=1}^{\infty} b_n \exp (- D\omega_n{}^2 t) \, dt \tag{12}$$

Interchanging the order of summation and integration yields

$$M_o = \frac{K}{D} \sum_{n=1}^{\infty} \frac{b_n}{\omega_n{}^2} \tag{13}$$

which by comparison with Eq. (9) is identical to the time lag, so that the expressions of Eqs. (10) and (11) may be equated to M_o as well as t_1. Thus, if

$$M_o = \int_0^\infty [1 - \frac{\phi(t)}{\phi_{ss}}] \, dt \tag{14}$$

then for a flat membrane

$$D = h^2/6 \, M_o \tag{15}$$

and for a cylinder

$$D = \frac{a^2 - b^2 + (a^2 + b^2) \ln (b/a)}{4 \, M_o \ln (b/a)} \tag{16}$$

---

*The expression for the cylinder given by Crank and Park[1] erroneously omits the D in the denominator. The correct form is given in the original derivation by Jaeger.[7] A formula for this quantity given by Crank[6] is incorrect, although it yields results which are numerically quite close to the correct values.

Experimental values of $\phi(t)$ or any measured quantity proportional to ϕ, such as the concentration of the penetrant in the gas stream flowing past the downstream side of the membrane, may be substituted into Eq. (14), and the value of M_0 may be obtained by numerical integration. The diffusivity D may then be calculated from Eq. (15) or (16).*

EXPERIMENTAL PROCEDURE AND RESULTS

The diffusivity of sulfur dioxide in PTFE (Teflon) was determined at 100°C. A PTFE tube with an inner radius a=0.403 cm and an outer radius b=0.480 cm was mounted in a chamber in a thermostatically-controlled oven. A stream of air containing less than 0.02 ppm SO_2 -- the carrier gas -- passed through the inside of the tube. At a time t=0 a gas containing 1.5% SO_2 by volume and the balance dry air -- the chamber gas -- was introduced into the chamber outside the polymer tube. SO_2 permeated through the tube wall into the carrier gas, which passed out to an electrochemical transducer SO_2 detector connected to a strip chart recorder. Additional details of the experimental apparatus are given by Rodes, Felder and Ferrell.[4]

The total time lag due to the residence time of the chamber gas in the upstream compartment, the residence time of the carrier gas between the permeation chamber and the detector, and the 90% response time of the detector, was estimated to be 17 seconds. Since the 90% rise time of the measured response was of the order of 30 minutes, the precise dynamic characteristics of the chamber, the carrier gas lines and the analyzer were not considered important, and the 17 second lag was for simplicity assumed to be a pure time delay. The measured response was accordingly shifted horizontally by this amount to obtain the transient response of the polymer tube alone.

---

*In process dynamics terminology, M_0 is the zeroth moment of the negative unit step response of the membrane, and the technique of estimating D from the calculated value of M_0 is an example of the method of moments.

The corrected response $R(t)$ normalized by its asymptotic (steady-state) value R_{ss} is shown in Figure 1 as a series of discrete points. The quantity M_o was evaluated from Eq. (14) by replacing ϕ/ϕ_{ss} with R/R_{ss} and using Simpson's rule with $\Delta t = 1$ minute. The calculated value of M_o, 17.9 minutes, was substituted into Eq. (16) to obtain $D = 9.1 \times 10^{-7}$ cm^2/second. This value was not highly dependent on the assumption of 17 seconds for the time lag of the system components other than the membrane: using 0 seconds or 34 seconds instead of 17 seconds made a difference of only 1.5% in the calculated diffusivity.

The theoretical curve of $\phi(t)/\phi_{ss}$ (= $R(t)/R_{ss}$) vs. t evaluated by substituting the tube dimensions and the calculated diffusivity into Eq. (3) is shown as the solid curve of Figure 1. The agreement between the experimental and theoretical responses is excellent, and confirms the validity of both the diffusion model and the technique used to estimate the diffusivity.

Diffusivities have been measured at several temperatures between 22°C and 121°C using this technique. Measurements were made using two PTFE tubes with different wall thicknesses, and two upstream SO_2 concentrations for each tube. The measured diffusivities are shown in an Arrhenius plot in Figure 2; the SO_2 percentages shown in the legend on this figure are the molar percentages of SO_2 in the upstream chamber gas. Also shown in Figure 2 is an SO_2 diffusivity reported by Jordan[8] for PTFE at a temperature presumed to be in the range 20°C-30°C. Jordan used a sorption technique, and calculated D as the quotient of a measured permeability and a measured solubility; the agreement between his value and the values obtained in the present study is reasonable, albeit not outstanding.

SO_2 diffusivities measured using thick and thin-walled PTFE tubes appear to differ by approximately 30-50%. The coincidence of data points obtained using two different upstream concentrations at a fixed temperature suggests the constancy of D under the prevailing experimental conditions. Least-squares fits to the data of Figure 2 yield an activation energy for diffusion of 8.45 ± 0.1 kcal/g-mole.

Future papers will report the results of diffusivity measurements for several penetrants and polymers, and will outline applications of the continuous measurement technique to the monitoring of gaseous pollutant emissions from stationary sources, the project which provided the impetus for this study.

DISCUSSION

Process Dynamic Considerations in Diffusivity Measurements

This study outlines a method for determining the diffusivity of a gas in a membrane from the response at one membrane surface to a step change in penetrant concentration at the other surface. What is actually measured, however, is the response of a series of system components including the chamber gas line, the chamber itself, the membrane, the carrier gas line leading to the analyzer, and the analyzer and recorder, each of which represents an additional lag or delay between the input signal and the measured response. An essential step in determining the diffusivity is to extract (deconvolute) the step response of the membrane from the response of the entire system.

In the experiment described in this paper, the mean residence times in the chamber and carrier gas lines and in the chamber were calculated by dividing each component volume by the volumetric flow rate of the chamber or carrier gas. The response of the analyzer to a step input of SO_2 was measured experimentally, and the 90% rise time was noted. The sum of the calculated residence times and the rise time of the analyzer in the experiment of Figure 1 was 17 seconds, which was sufficiently small on the time scale of the total response to justify approximating these lags as a single time delay.

In an experiment in which the membrane response is rapid -- as it might be, for example, in measurements on a thin membrane at a high temperature -- the dynamics of the system components other than the membrane must be taken into account more explicitly in the response analysis. A reasonable approach would be to characterize all connecting lines as pure time delays, and the permeation chamber and (possibly) the analyzer as first-order lags, all components being in series with the membrane. Standard deconvolution techniques could then be used to determine the step response of the membrane alone.

Measurement of Concentration - Dependent Diffusivities

Partial pressures of gases in continuous permeation chambers are usually 1 atm or less, under which condition the diffusivity of a penetrant is likely to be independent of the concentration of the penetrant dissolved in the membrane. This independence was confirmed in this study by carrying out runs with two significantly different penetrant partial pressures in the chamber gas and finding essentially the same diffusivity in both cases.

A possible extension of the continuous permeation technique to conditions at which the diffusivity varies with penetrant concentration is to pass a gas with a penetrant concentration C_0 on both sides of a membrane until equilibrium is achieved, and then to increase the concentration on one side (upstream) to C_1 and to measure the response on the other side (downstream). Provided that the dissolved penetrant concentration at the downstream surface of the membrane is not significantly changed from its initial value by the amount of gas that permeates, a simple variable transformation $C' = C - C_0$ reduces the mathematical analysis required to determine D to that given previously for the case when $C_0 = 0$. The calculated diffusivity would correspond to a concentration somewhere between the upstream and downstream concentrations C_1 and C_0. Several experiments of this type for different (C_0, C_1) pairs could in principle be used to generate a curve of D vs. C.

CONCLUSIONS

The diffusivity of a gas in a polymer membrane or a hollow cylindrical tube can be conveniently measured by integrating the response to a step change in penetrant concentration in a continuous permeation chamber. The proposed method has been used to measure the diffusivity of SO_2 in PTFE (Teflon) at temperatures from 22°C to 121°C, yielding an activation energy for diffusion of 8.45 ± 0.1 kcal/g-mole. A modified version of the method may be used to determine concentration-dependent diffusivities.

ACKNOWLEDGMENTS

This work was supported by Environmental Protection Agency Grant #801578. The authors acknowledge with thanks helpful discussions with Professors Harold Hopfenberg and Vivian Stannett of North Carolina State University, Department of Chemical Engineering, and assistance with the experimentation provided by Mssrs. Chen-chi Ma and Lanny Treece.

NOTATION

A = surface area of a flat membrane, cm^2

a,b = inner and outer radii of a hollow cylindrical tube, cm

b_n = coefficient in Eq. (5)

C = concentration of penetrant dissolved in a membrane, moles/cm^3

C_o,C_1 = initial concentration and concentration at the upstream membrane surface, moles/cm^3

D = diffusivity, cm^2/s

h = thickness of a flat membrane, cm

J_o = zero-order Bessel function of the first kind

K = coefficient in Eq. (5)

L = length of cylindrical tube, cm

M_o = quantity defined by Eq. (14)

$Q(t)$ = cumulative permeation up to time t, moles

$R(t)$ = measured variable proportional to $\phi(t)$

R_{ss} = asymptotic (steady-state) value of R

r = radial position coordinate in a cylindrical tube, cm

t = time from imposition of a step change in penetrant partial pressure, s

t_l = time lag, s

x = position coordinate in a flat membrane, cm. $x=0$ corresponds to the upstream surface of the membrane.

Y_o = zero-order Bessel function of the second kind

Greek Letters

α_n = nth real positive root of Eq. (4)

$\phi(t)$ = rate of permeation into the gas downstream of the membrane, moles/s

ϕ_{ss} = asymptotic (steady-state) value of ϕ

ω_n = coefficient in Eq. (5)

NOTATION (Cont'd)

Subscripts

c = cylinder

fm = flat membrane

REFERENCES

1. J. Crank and G. S. Park, Eds., Diffusion in Polymers, Academic Press, New York, 1968.
2. T. L. Caskey, Mod. Plastics, 45, 447 (1967).
3. R. A. Pasternak, J. F. Schimscheimer, and J. Heller, J. Polym. Sci. A-2, 8, 467 (1970).
4. C. E. Rodes, R. M. Felder, and J. K. Ferrell, Environ. Sci. Technology, 5, 1121 (1971).
5. R. M. Felder, J. K. Ferrell, and J. J. Spivey, Analysis Instrumentation, 12, 35 (1974).
6. J. Crank, The Mathematics of Diffusion, Clarendon Press, Oxford, 1956.
7. J. C. Jaeger, Proc. Roy. Soc. N.S.W., 74, 342 (1940).
8. S. Jordan, Staub-Reinhalt Luft, 33, 36 (1973).

LIST OF FIGURES

Figure 1. Experimental and Theoretical Step Responses of a PTFE Tube.

Figure 2. Arrhenius Plot of SO_2 Diffusivities in PTFE Tubes.

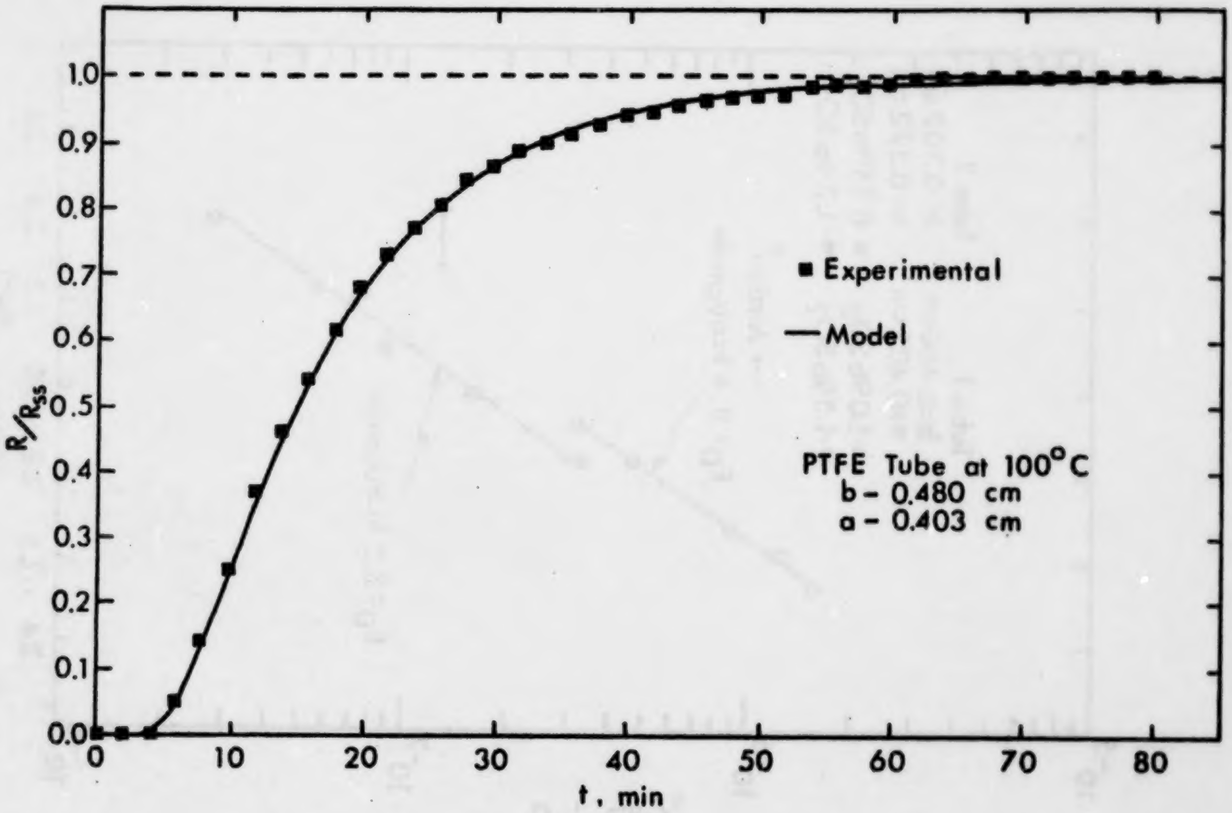

Figure 1. Experimental and Theoretical Step Responses of a PTFE Tube.

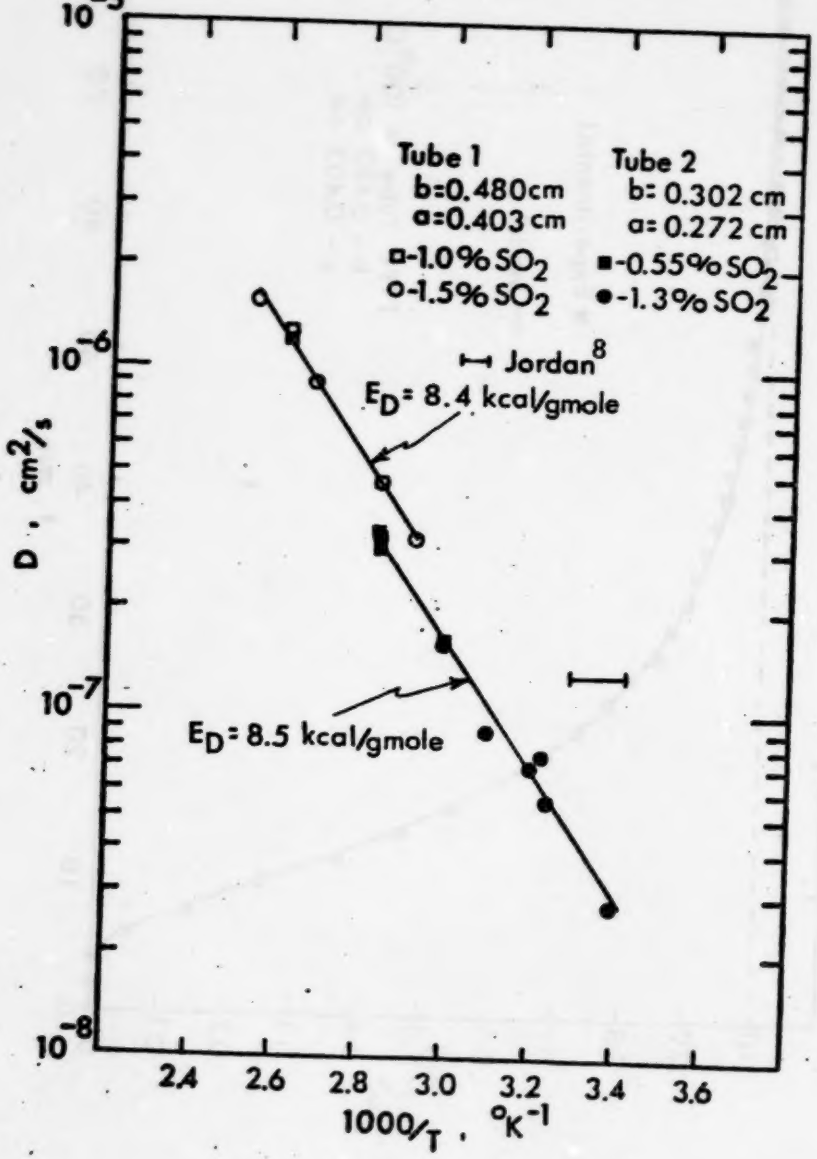

Figure 2. Arrhenius Plot of SO_2 Diffusivities in PTFE Tubes.

APPENDIX F

A METHOD OF MOMENTS FOR MEASURING DIFFUSIVITIES OF GASES IN POLYMERS*

R. M. Felder, C. C. Ma, and J. K. Ferrell
Department of Chemical Engineering
North Carolina State University
Raleigh, North Carolina 27607

ABSTRACT

A method of moments has been formulated for the determination of the diffusivity of a gas in a polymer from a step response in a continuous permeation chamber. Contributions of system components other than the polymer are easily factored out to determine the contribution of the polymer alone, and this contribution is then analyzed to calculate the diffusivity. The method has been applied to the measurement of the diffusivity of sulfur dioxide in PTFE (Teflon) and fluorosilicone rubber tubes over a wide temperature range.

---

* Published as AICHE J. 22, 724 (1976). Reprinted by permission of the American Institute of Chemical Engineers.

SCOPE

Traditional methods for measuring the diffusivity of a gas in a polymer involve either passage of the gas through a membrane into a closed chamber in which the pressure is monitored, or sorption of the gas in a small polymer sample suspended from a spring whose elongation is monitored. In either experiment, a substantial driving force is needed to achieve measurable penetration fluxes, thereby limiting the penetrant concentrations for which data may be obtained.

An approach in which a gas permeates through a membrane into a flowing stream overcomes many of the experimental problems associated with closed volume systems, and allows accurate measurements of gas transport properties for penetrant concentrations as low as tens of parts per million. This technique is not without its drawbacks, however. The complete solution of the time-dependent diffusion equation is at best an infinite series, and curve-fitting methods for estimating the diffusivity generally utilize either short-time or long-time asymptotic solutions. When deviations from the anticipated straight line behavior occur, it is difficult to determine whether they are due to experimental error, or to a violation of the assumptions of the diffusion model, or simply to the invalidity of the asymptotic solution in the range of response times where the deviations occur.

Felder, Spence and Ferrell (1975a) recently formulated a method for estimating the diffusivity of a gas in a polymer from a moment of a step response in a continuous permeation chamber. The method requires only numerical integration rather than curve fitting, and does not depend on the existence of a short-time or long-time asymptotic solution of the diffusion equation.

A problem associated with this technique (and with any other dynamic response technique) is that what is measured is the response of the entire system--connecting line, chamber, permeable membrane, and gas analyzer--to a step concentration change upstream of the chamber, while what is needed to evaluate the desired diffusivity is the step response of the membrane alone. This paper develops an extension of the moment technique which provides a simple but accurate resolution of this problem.

CONCLUSIONS AND SIGNIFICANCE

The method of moments for determining the diffusivity of a gas in a permeable material has been found to provide several advantages over traditional closed-volume and continuous measurement techniques.

1. The use of a continuous permeation chamber rather than the closed volume chamber of the standard time-lag experiment permits the attainment of a true steady state, and yields data which are less susceptible to cumulative errors.
2. Maintaining equal pressures on both sides of the membrane (which cannot be done in a closed volume chamber) minimizes the requirements for membrane support and sealing, and allows accurate measurements with very low penetrant concentrations.
3. The complete response to a step change in penetrant concentration is utilized, rather than a portion of the response which falls within the region of validity of a short-time or long-time asymptotic solution of the diffusion equation.
4. Simple numerical integration of response data rather than curve-fitting is required.
5. The method is applicable to cylindrical tubes as well as flat membranes.
6. The contributions of system components other than the membrane may be factored out of the measured response by simple subtraction of moments to obtain the contribution of the membrane alone.

The method has been applied to the measurement of the diffusivity of sulfur dioxide in fluorosilicone rubber and PTFE (Teflon) tubes at temperatures from 21°C to 227°C. Calculated diffusivities have in several cases been substituted into the analytical solution of the diffusion equation to regenerate the response curves from which the diffusivities were estimated. The close agreement between the measured and calculated responses validates both the estimation technique and the diffusion model upon which it is based.

THEORETICAL

Measurement of Transport Properties in a Continuous-Flow Permeation Chamber

In a continuous permeation experiment, a penetrant is introduced at a partial pressure p_1 (cm Hg) on one side of a flat membrane or on the outside of a hollow cylindrical tube, and permeates through the polymer into a gas stream flowing past the membrane or through the inside of the tube. The concentration of the penetrant in the exiting gas is monitored continuously until a steady state is attained.

The following assumptions are made:

1. Gas phase resistance to mass transfer is negligible.
2. Absorption of the penetrant at the polymer surface is an instantaneous process.
3. The concentration of the dissolved gas at the downstream membrane surface is negligible compared to that on the side where the penetrant was introduced.
4. The solubility of the penetrant in the polymer is independent of the penetrant concentration in the gas phase.
5. Diffusion in the polymer is Fickian with a constant diffusivity D(cm^2/s).

The diffusion equation may be solved for the rate of permeation of the gas through the polymer (see Appendix A), and the solutions may in turn be used to derive expressions for the diffusivity D. Let $\phi(t)$ (mole/s) be the measured permeation rate, ϕ_s, the asymptotic (steady state) value of this rate, and define

$$M_0 = \int_0^\infty \left[1 - \frac{\phi(t)}{\phi_s}\right] dt \tag{1}$$

Felder et al. (1975a) have shown that for a flat membrane with a surface area

$A(cm^2)$ and thickness $h(cm)$,

$$D = h^2/6M_o \tag{2}$$

and for a cylinder with inner radius a and outer radius b,

$$D = \frac{a^2 - b^2 + (a^2 + b^2)\ \ln(b/a)}{4M_o\ \ln(b/a)} \tag{3}$$

If diffusivities are measured at several temperatures, an Arrhenius plot of ln D vs. 1/T yields the activation energy for diffusion of the penetrant in the polymer (Stannett, 1968).

The analytical solution for the permeation rate $\phi(t)$ through the wall of a hollow cylindrical tube is given in Appendix A, along with a numerical technique for evaluating the infinite series which is a part of the solution.

Deconvolution of the Polymer Tube Response from the Total System Response

A difficulty associated with dynamic response measurements of the type just described is that what is measured is the response of the entire system -- connecting lines, chamber, polymer, and gas analyzer -- to a step concentration change upstream of the chamber, while what is needed to evaluate the diffusivity from Eqs. (1) and (2) or (3) is the response of the polymer alone.

In the experiments described by Felder et al. (1975) this problem was solved by assuming that the connecting lines, the chamber and the analyzer each acted as pure time delays, and the measured response was accordingly shifted horizontally by the total of these delays. The values of the delays for the lines and the chamber were taken to be the nominal mean residence times (volume/volumetric flow rate) of the gases flowing through these units, and the time delay attributed to the analyzer was arbitrarily set equal to the time required for the analyzer reading to reach 90% of its final value in calibration runs.

In previous diffusivity measurements, the time lag due to the polymer accounted for most of the total system response time, so that the particular method used to correct for the other contributions to the response was immaterial. However, if (for example) the diffusivity of a gas in a thin membrane at a high temperature is to be measured, the response times of the other system components may be equal to or even greater than that of the polymer. In such cases, representing all the time lags as pure delays would be a serious error; the analyzer, in particular, is unlikely to be a pure delay, or for that matter a pure first-order process or anything else that can easily be modeled.

Fortunately, the true dynamic characteristics of the system components may be taken into account in correcting the measured response, with little more effort than was required for the oversimplified method used previously. The procedure is to calculate as before the mean residence times of the gas in the line leading to the chamber (τ_1) and in the chamber itself (τ_2), and the mean residence time of the carrier gas in the line leading from the chamber to the analyzer (τ_3). Next, if $R_a(t)$ is the transient response of the analyzer to a step change in the penetrant concentration at its inlet (i.e. the response measured when the analyzer is calibrated) and R_{as} is the steady-state value of this response, then the time lag due to the analyzer may be determined by numerical integration as

$$\tau_a = \int_0^\infty [1 - \frac{R_a(t)}{R_{as}}] \, dt \qquad (4)$$

Finally, if $R(t)$ is the measured response of the entire system to a step concentration change (R is presumed to be proportional to the penetrant flux), R_s is the steady-state value of this response, and

$$M_o' = \int_0^\infty [1 - \frac{R(t)}{R_s}] \, dt \qquad (5)$$

then the correct value of M_o to use in the diffusivity formulas (Eqs. (2) and (3)) is

$$M_o = M_o' - (\tau_1+\tau_2+\tau_3+\tau_a) \qquad (6)$$

The theoretical justification for this procedure is given in Appendix B.

EXPERIMENTAL

Apparatus

A permeation chamber was constructed by clamping two 6-inch square stainless steel endplates with Teflon gaskets to the ends of a 3-inch I.D., 24-inch long stainless steel chamber. Each endplate was drilled and tapped to accept a 0.125-inch thermocouple bulkhead fitting, a 0.125-inch pipe fitting and a 0.375-inch pipe fitting. All fittings were stainless steel. Each of the 0.375-inch fittings was drilled internally to allow a length of 0.375-inch O.D. stainless steel tubing to pass through the endplate to the interior of the chamber. The polymer tube was connected between these internal fittings and supported by a stainless steel rod inserted inside the tube. The chamber assembly was then placed inside a thermostatically controlled oven.

A schematic diagram of the flow apparatus is shown in Figure 1. The feed to the chamber is a mixture of a cylinder gas containing roughly 1.5% SO_2 in air and air containing less than 0.03 ppm SO_2. The precise concentration of SO_2 in the cylinder gas is determined using EPA Method 6 -- absorption of the SO_2 in an isopropanol-hydrogen peroxide solution, and titration with a standardized barium perchlorate solution (Environmental Protection Agency, 1971). The dilution air is obtained by passing room air through a calcium chloride drying column, an activated charcoal column, and a particulate filter. The cylinder gas and dilution air are fed through rotameters into a tee, and the combined stream passes into the chamber on the outside of the polymer tube. A second stream of clean air (the carrier gas) is metered and fed into the inside of the tube; the SO_2 permeating through the tube wall is picked up by this stream, which passes out of the chamber to a Meloy Laboratories Model SA-160 flame photometric sulfur detector. The rate of permeation of SO_2 is calculated as the product of the concentration read by the detector and the known volumetric flow rate of the carrier gas.

Copper-constantan thermocouples are used to monitor the temperature at two locations near the outside surface of the polymer tube, and the pressures of the chamber and carrier gases are measured with manometers. Strip chart recorders are used to obtain continuous records of the signals from the SO_2 analyzer and from one of the thermocouples. The analyzer is calibrated before and after each run with a gas obtained by passing purified air at a measured rate over a calibrated SO_2 permeation tube.

This experimental system has been used to determine steady-state permeabilities of sulfur dioxide and water in a number of polymers (Rodes et al., 1973; Felder, Ferrell and Spivey, 1974; Felder, Spence and Ferrell, 1975b). Additional details about its design are given in these references.

Procedures for Diffusivity Measurements

The sample tube dimensions are measured before the tube is connected to the fitting in the chamber. The outer diameter of the tube is measured with a micrometer at several points around a circumference well away from an end, and an average value is calculated. A small length of the tube is then cut axially, and the wall thicknesses at several points are measured with the micrometer and averaged. The inner diameter is determined from the mean outer diameter and wall thickness.

The tube is mounted in the chamber and the chamber in turn is mounted in the oven. The oven thermostat is set, and the chamber temperature is monitored until it reaches a constant value. The flow rates of the cylinder gas and dilution air are adjusted to produce a chamber gas with a known SO_2 concentration, and the flow rate of the carrier gas is adjusted to provide a sample gas with an SO_2 concentration within the range of the flame photometric detector (ideally 0.1-1 ppm). The total pressure on both sides of the tube is maintained at approximately 1 atmosphere.

The flow of the cylinder gas commences at a time $t=0$, and the run continues until the measured concentration of SO_2 in the sample gas levels off and remains level for at least 15 minutes. The sample gas SO_2 concentration is multiplied by the volumetric flow rate of the sample gas to calculate the flow rate of SO_2 leaving the tube, and the relatively small flow rate of SO_2 in the entering air is subtracted to determine the SO_2 permeation rate $\phi(t)$. The time lags τ_1, τ_2, and τ_3 attributable to the connecting lines and the chamber are calculated from the known volumes of these components and volumetric flow rates of the chamber and carrier gases, and the analyzer time lag τ_a is determined from calibration data using Eq. (4). The total system time lag M_0' is obtained from $\phi(t)(\equiv R(t))$ using Eq. (5), and the lag due to the polymer alone is determined from Eq. (6). Finally, the diffusivity of SO_2 in the polymer is calculated from Eq. (3).

RESULTS AND DISCUSSION

Fluorosilicone Rubber Tubes

Diffusivities of SO_2 in a fluorosilicone rubber tube (Dow Corning: SILASTIC LS-63U®) were measured at temperatures between 74°C and 198°C, using three different chamber gas SO_2 concentrations. The results are shown on an Arrhenius plot in Figure 2. The near coincidence of the data points obtained for the different concentrations at a fixed temperature suggests the constancy of D at the SO_2 partial pressures of 10 mm Hg and less used in these measurements. The activation energy for diffusion obtained from Figure 2 is $E_d = 30.6 \pm 0.9$ kJ/mole.

As a test of the validity of the diffusivity estimation technique, the theoretical expression given in Appendix A for the permeation rate $\phi(t)$ was evaluated using diffusivities calculated at three different temperatures. Figure 3 shows plots of the resulting curves of $R/R_s(=\phi/\phi_s)$ vs. t, along with the experimental data. The close correspondence between the experimental and theoretical responses at each temperature provides evidence for the validity of both the diffusivity estimation technique and the diffusion model on which the technique is based.

PTFE Tubes

Diffusivities of sulfur dioxide in PTFE (Teflon) tubes have been measured at temperatures from 21°C to 227°C. Figure 4 shows an Arrhenius plot of the results obtained to date, along with a diffusivity measured by Jordan (1973) at a temperature presumed to be in the range 20-30°C. Straight lines can be fit quite well to the data for each individual tube, but noticeable variations occur from one tube to another. The diffusivity reported by Jordan is comparable to but higher than those measured in the present work, a result probably attributable to the substantially higher SO_2 concentrations used in Jordan's study.

A least-squares line has been fit to the data shown in Figure 4 to obtain the following estimation formula for the diffusivity of SO_2 in PTFE.

$$D(\mathrm{cm}^2/\mathrm{s}) = 0.238 \exp(-4760/T) \qquad (7)$$

The activation energy for diffusion should not be deduced from Eq. (7), since differences between the diffusivities of the thick-walled tubes used at the higher temperatures and those of the thin-walled tubes used at the lower temperatures introduce a bias in the slope of a line fit to all the data points. This point is the subject of continuing study.

ACKNOWLEDGMENT

This work was supported by Environmental Protection Agency Grant #801578. The authors acknowledge with thanks assistance provided by Dr. Roger Spence. A paper based on this work was presented at the 80th National Meeting of the American Institute of Chemical Engineers, Boston, Mass., September, 1975.

NOTATION

a = inner cylinder radius, cm

b = outer cylinder radius, cm

C = dissolved penetrant concentration, mole/cm^3

C_1, C_2 = penetrant concentrations at the upstream and downstream membrane surfaces, mole/cm^3

D = diffusivity, cm^2/s

E_D = activation energy for diffusion, kJ/mole

$F(t)$, F_s = transient step response of total system and its steady-state limit

$F_i(t)$, F_{is} = transient step response of ith system component and its steady-state limit

$G(s)$ = Laplace transform of $g(t)$

$G_i(s)$ = Laplace transform of $g_i(t)$

$g(t)$ = unit impulse response of total system

$g_i(t)$ = unit impulse response of ith system component

h = thickness of flat membrane, cm

J_n = nth-order Bessel function of the first kind

k_n = $\alpha_n a$

L = length of cylinder, cm

M_0 = zeroth moment of negative normalized step response of polymer, s

M_0' = zeroth moment of negative normalized step response of total system, s

$R(t)$, R_s = transient response to a step change in penetrant concentration, and its steady-state limit

$R_a(t)$, R_{as} = transient response of the analyzer alone to a step change at its inlet, and its steady-state limit

r = radial coordinate, cm

s = Laplace transform variable, s^{-1}

T = temperature, K

t = time, s

U_o = function defined by Eq. (A6)

x = b/a

$x_i(t)$ = signal at outlet of i^{th} system component

Y_n = n^{th}-order Bessel function of the second kind

Greek Letters

α_n = root of $U_o(\alpha_n a) = 0$

$\delta(t)$ = Dirac delta function, s^{-1}

μ_i = variable defined by Eq. (B1), s

τ = total system time lag, s

τ_i = time lag of i^{th} system component, s

$\phi(t)$, ϕ_s = transient permeation rate and its steady-state limit, mole/s

LITERATURE CITED

Abramowitz, M. and I. A. Stegun, eds., Handbook of Mathematical Functions, p. 16, National Bureau of Standards, Washington (1964).

Carslaw, H. S. and J. C. Jaeger, The Conduction of Heat in Solids, p. 489, Clarendon Press, Oxford (1959).

Crank, J., The Mathematics of Diffusion, p. 78, Clarendon Press, Oxford (1956).

Douglas, J. M., Process Dynamics and Control, Vol. I, Prentice-Hall, Englewood Cliffs (1972).

Environmental Protection Agency, Standards of Performance for New Stationary Sources, Federal Register 36, No. 247, Part II, pp. 24890-24893 (1971).

Felder, R. M., J. K. Ferrell, and J. J. Spivey, "Effects of Moisture on the Performance of Permeation Sampling Devices," Anal. Instrumentation 12, 35 (1974).

Felder, R. M., R. D. Spence and J. K. Ferrell, (a) "A Method for the Dynamic Measurement of Diffusivities of Gases in Polymers," J. Appl. Poly. Sci., 19, 3193 (1975).

Felder, R. M., R. D. Spence and J. K. Ferrell, (b) "Permeation of Sulfur Dioxide through Polymers," J. Chem. Eng. Data, 20, 235 (1975).

International Business Machines, System 360 Scientific Subroutine Package (360A-CM-03X), Version III, Form H20-0205-3 (1968).

Jordan, S., "Messungen der Permeabilität einiger Kunststoffe gegenüber Schwefeldioxid," Staub-Reinhalt, Luft, 33, 36 (1973).

Rodes, C. E., R. M. Felder, and J. K. Ferrell, "Permeation of Sulfur Dioxide through Polymeric Stack Sampling Interfaces," Environ. Sci. Technology, 7, 545 (1973).

Stannett, V. T., "Sample Gases," in Diffusion in Polymers, J. Crank and G. S. Park, eds., Academic Press, New York (1968).

APPENDIX A

Permeation of a Gas into a Hollow Cylinder.

At a time t=0 a penetrant is introduced on the outside of a cylindrical tube of length L, inner radius a and outer radius b. It is assumed that gas phase mass transfer resistance is negligible, diffusion in the polymer is Fickian with a constant diffusivity, and the partial pressure of the penetrant inside the tube is negligible compared to that outside the tube.

Let p be the partial pressure of the penetrant in the gas phase, C the concentration of penetrant dissolved in the polymer, D the diffusivity and $S = (C/p)_{surface}$ the solubility of the penetrant in the polymer. If the partial pressures outside and inside the tube are p_1 and p_2, the dissolved gas concentrations in the polymer in equilibrium with these partial pressures are $C_1(=Sp_1)$ and $C_2(=Sp_2)$, and the initial concentration of the penetrant in the polymer is C_o, then the diffusion equation and its boundary conditions are

$$\frac{\partial C}{\partial t} = \frac{D}{r} \frac{\partial}{\partial r} \left(r \frac{\partial C}{\partial r}\right) \tag{A1}$$

$$C(0,r) = C_o \tag{A2}$$

$$C(t,a) = C_2 \tag{A3}$$

$$C(t,b) = C_1 \tag{A4}$$

The solution of this equation is given by Crank (1956) as

$$C(t,r) = \frac{C_1 \ln(r/a) + C_2 \ln(b/r)}{\ln(b/a)} + \pi C_o \sum_{n=1}^{\infty} \frac{J_o(\alpha_n a) U_o(\alpha_n r)}{J_o(\alpha_n a) + J_o(\alpha_n b)} \exp(-\alpha_n^2 Dt)$$

$$- \pi \sum_{n=1}^{\infty} \frac{[C_1 J_o(\alpha_n a) - C_2 J_o(\alpha_n b)]\, J_o(\alpha_n a) U_o(\alpha_n r)}{J_o^2(\alpha_n a) - J_o^2(\alpha_n b)} \exp(-\alpha_n^2 Dt) \tag{A5}$$

where

$$U_o(\alpha_n r) = J_o(\alpha_n r)Y_o(\alpha_n b) - J_o(\alpha_n b)\, Y_o(\alpha_n r) \tag{A6}$$

and $\alpha_1, \alpha_2, \ldots$ are the real positive roots of the equation $U_o(\alpha_n a) = 0$. J_o and Y_o are the zero-order Bessel functions of the first and second kind.

In the system under consideration in this study $C_o = 0$ and $C_2 << C_1$, so that the solution simplifies to

$$C(t,r) = \frac{C_1 \ln(r/a)}{\ln(b/a)} - \pi C_1 \sum_{n=1}^{\infty} \frac{J_o^2(\alpha_n a)U_o(\alpha_n r)}{J_o^2(\alpha_n a) - J_o^2(\alpha_n b)} \exp(-\alpha_n^2 Dt) \tag{A7}$$

The rate at which the penetrant permeates into the tube interior equals the rate of diffusion at the inner surface

$$\phi(t) = 2\pi DL(r \frac{\partial C}{\partial r})_{r=a} \tag{A8}$$

(ϕ is defined to be positive if flow is in the negative r direction.) Substituting Eq. (A7) for C in this expression yields

$$\phi(t) = \frac{2\pi DL\, C_1}{\ln(b/a)} - 2\pi^2 DL\, C_1\, a \sum_{n=1}^{\infty} \frac{J_o^2(\alpha_n a) \exp(-\alpha_n^2 Dt)}{J_o^2(\alpha_n a) - J_o^2(\alpha_n b)} \left(\frac{dU_o(\alpha_n r)}{dr}\right)_{r=a} \tag{A9}$$

Differentiation of Eq. (A6) yields

$$\frac{dU_o(\alpha_n r)}{dr} = \alpha_n[J_o'(\alpha_n r)Y_o(\alpha_n b) - J_o(\alpha_n b)Y_o'(\alpha_n r)] \tag{A10}$$

where $J_o'(\alpha_n r) = dJ_o(\alpha_n r)/d(\alpha_n r)$. Since from the theory of Bessel functions $J_o' = -Y_1$ and $Y_o' = -J_1$,

$$\left(\frac{dU_o(\alpha_n r)}{dr}\right)_{r=a} = \alpha_n[J_o(\alpha_n b)Y_1(\alpha_n a) - J_1(\alpha_n a)Y_o(\alpha_n b)] \tag{A11}$$

By definition, $\alpha_1, \alpha_2, \ldots$ are the roots of the equation

$$J_o(\alpha_n a)Y_o(\alpha_n b)-J_o(\alpha_n b)Y_o(\alpha_n a) = 0 \qquad \text{(A12)}$$

from which

$$\frac{J_o(\alpha_n b)Y_o(\alpha_n a)}{J_o(\alpha_n a)} = Y_o(\alpha_n b) \qquad \text{(A13)}$$

Another result from the theory of Bessel Functions is (Carslaw and Jaeger, 1959)

$$J_o(\alpha_n a)Y_1(\alpha_n a)-J_1(\alpha_n a)Y_o(\alpha_n a) = -\frac{2}{\pi\alpha_n a} \qquad \text{(A14)}$$

If this equation is multiplied by the ratio $J_o(\alpha_n b)/J_o(\alpha_n a)$, and the quantity

$$J_o(\alpha_n a)Y_o(\alpha_n a)/J_o(\alpha_n a)$$

is replaced by $Y_o(\alpha_n b)$ according to Eq. (A13), the result is

$$J_o(\alpha_n b)Y_1(\alpha_n a)-J_1(\alpha_n a)Y_o(\alpha_n b) = -\frac{2}{\pi\alpha_n a}\frac{J_o(\alpha_n b)}{J_o(\alpha_n a)} \qquad \text{(A15)}$$

This expression may be substituted into Eq. (A11) to yield

$$\left(\frac{dU_o(\alpha_n r)}{dr}\right)_{r=a} = -\frac{2}{\pi a}\frac{J_o(\alpha_n b)}{J_o(\alpha_n a)} \qquad \text{(A16)}$$

which may in turn be substituted into Eq. (A9) to yield

$$\phi(t) = \frac{2\pi DL\,C_1}{\ln(b/a)}\left[1 + 2\ln(b/a)\sum_{n=1}^{\infty}\frac{J_o(\alpha_n a)J_o(\alpha_n b)}{J_o^2(\alpha_n a)-J_o^2(\alpha_n b)}\exp(-\alpha_n^2 Dt)\right] \qquad \text{(A17)}$$

The leading factor in Eq. (A17) is the steady-state permeation rate ϕ_s. It follows that

$$\phi(t)/\phi_s = 1 + 2\ln(b/a)\sum_{n=1}^{\infty}\frac{J_o(\alpha_n a)J_o(\alpha_n b)}{J_o^2(\alpha_n a)-J_o^2(\alpha_n b)}\exp(-\alpha_n^2 Dt) \qquad \text{(A18)}$$

where

$$\phi_s = \frac{2\pi LD}{\ln(b/a)} C_1 \tag{A19}$$

Felder et al. (1975a) showed that the integral

$$M_o = \int_o^\infty [1 - \frac{\phi(t)}{\phi_s}] \, dt \tag{A20}$$

is simply related to the diffusivity D through the relationship of Eq. (5), a relationship which involves no infinite series and none of the transcendental functions or roots of nonlinear equations which appear in Eq. (A18). To confirm the validity of the diffusivity estimation formula and of the assumptions that underly it, however, the estimated value of D must be substituted back into the full expression of Eq. (A18), and the calculated curve of $\phi(t)/\phi_s$ must be compared with the data used to estimate D.

The evaluation of the expression of Eq. (A18) poses two problems: finding the roots $\{\alpha_n\}$, and achieving convergence of the series. To perform the calculation, it is convenient to work with the series expressed in terms of the variables a and x =b/a rather than a and b. Since b = ax, the equation which defines $\{\alpha_n\}$ -- Eq. (A12) -- may be written in terms of modified roots $k_n = a\alpha_n$ as

$$J_o(k_n)Y_o(xk_n)-J_o(xk_n)Y_o(k_n) = 0 \tag{A21}$$

and the normalized permeation rate is

$$\phi(t)/\phi_s = 1+2 \ln x \sum_{n=1}^{\infty} \frac{J_o(k_n)J_o(xk_n)}{J_o^2(k_n)-J_o^2(xk_n)} \exp(-\frac{k_n^2 D}{a^2} t) \tag{A22}$$

Newton's rule is used to estimate the roots of Eq. (A19). If

$$U_o(k) = J_o(k)Y_o(xk)-J_o(xk)Y_o(k) \tag{A23}$$

then

$$dU_o/dk = U_o'(k) = J_o(xk)Y_1(k) - J_1(k)Y_o(xk)$$

$$+ x[J_o(k)Y_1(xk) - J_1(xk)Y_o(k)] \tag{A24}$$

A value of k is selected initially (the method of selection is discussed below), and subsequent values are calculated as

$$k_{new} = k_{old} - \frac{U_o(k_{old})}{U_o'(k_{old})} \tag{A25}$$

The procedure terminates when the relative change in k is less than one part in 10^6. Subroutines BESJ and BESY of the IBM 360 Scientific Subroutine Package (IBM, 1968) are used to evaluate the Bessel functions in the expressions for U_o and U_o'.

The following empirical formula has been found to be effective for estimating the value of the first root k_1:

$$\begin{aligned}(k_1)_o &= 1.0+\exp[0.595-1.71 \ln (x-1)-0.257 \ln^2(x-1)] && x < 3.5 \\ &= 1.0 && x \geq 3.5\end{aligned} \tag{A26}$$

First guesses for subsequent roots are made as follows:

$$(k_2)_o = 2k_1 \tag{A27}$$

$$(k_n)_o = 2k_{n-1} - k_{n-2} \ , \quad n \geq 3 \tag{A28}$$

Eq. (A28) appears to represent a true asymptotic relationship as n becomes large, although this has not been formally proved. The program which implements this root-finding procedure was checked using values of $k_n(x)$ tabulated on p. 330 of Crank (1956).

The series of Eq. (A22) converges rapidly for moderate to large values of t, but slowly or not at all for $(Dt/a^2) << 1$. The Euler transformation (Abramowitz and Stegun, 1964) has been found effective in achieving convergence at small times. The procedure is to evaluate and add terms successively to both the original and transformed series, and to terminate when either one converges to a present tolerance. The roots k_n are stored as they are calculated, so that each need be determined only once, regardless of the number of values of t for which $\phi(t)/\phi_s$ is evaluated.

Deconvolution of the Step Response of a Polymer in a Continuous-Flow Permeation Chamber.

In the experiments described in this paper, the input signal to the system is imposed by opening a valve which commences the flow of a gas containing the penetrant. The gas flows through a connecting line and enters the chamber on one side of the polymer; a portion of the penetrant dissolves in and diffuses through the polymer into a carrier gas, which passes to an analyzer where the penetrant concentration (the output signal) is measured.

Schematically, the system may be viewed as a series of process units, each with its own dynamic characteristics.

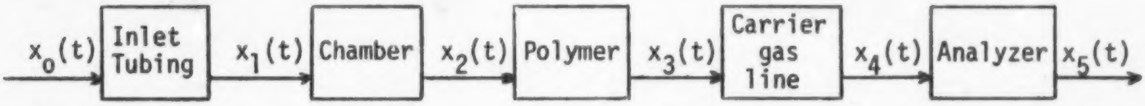

What is measured is the response $x_5(t)$ to a step input $x_0(t)$, whereas what is desired is related to the response of the polymer alone (x_3) to a step change in the chamber gas concentration (x_2). Standard process dynamics procedures are applicable to this problem, if it is assumed that each component behaves linearly. This assumption is valid for the polymer if the penetrant diffusivity and solubility are both independent of the penetrant concentration, and may or may not be valid for the analyzer. Most of the theoretical foundations for the development that follows may be found in the work of Douglas (1972).

The terms defined below will be used to obtain the desired result.

$g_i(t)$ = the unit impulse response of the i^{th} component ($i=1-5$); i.e., if $x_{i-1} = \delta(t)$, then $x_i(t) = g_i(t)$.

$g(t)$ = the unit impulse response of the overall system: if $x_0(t) = \delta(t)$, then $x_5(t) = g(t)$

μ_i = the zeroth moment of $g_i(t)$

$$\mu_i = \int_0^\infty g_i(t)dt \qquad \text{(B1)}$$

τ_i = the mean of g_i, which is also the mean residence time for the flow-through components ($i=1,2$ and 4). τ has the same significance for $g(t)$.

$$\tau_i = \frac{\int_0^\infty t\, g_i(t)dt}{\int_0^\infty g_i(t)dt} \quad ; \quad \tau = \frac{\int_0^\infty t\, g(t)dt}{\int_0^\infty g(t)dt} \qquad \text{(B2)}$$

$G_i(s)$ = the Laplace transform of $g_i(t)$, or the transfer function of the i^{th} component

$$G_i(s) = \int_0^\infty e^{-st}\, g_i(t)dt \ ; \ G(s) = \int_0^\infty e^{-st}\, g(t)dt \qquad \text{(B3)}$$

$F_i(t), F_{is}$ = the response of the i^{th} component to a step input, and the asymptotic value of this response as $t \to \infty$.

$F(t), F_s$ = the step response of the overall system and the asymptotic value of this response.

$$M_0{}' = \int_0^\infty \left[1 - \frac{F(t)}{F_s}\right]dt \qquad \text{(B4)}$$

$$M_o = \int_0^\infty \left[1 - \frac{F_3(t)}{F_{3s}}\right] dt \qquad (B5)$$

$$\tau_a = \int_0^\infty \left[1 - \frac{F_5(t)}{F_{5s}}\right] dt \qquad (B6)$$

The preceding notation follows that used in the main body of the paper: M_o' is calculated from the measured system response, M_o is the quantity needed to determine the diffusivity of the penetrant in the polymer, and τ_a is determined from analyzer calibration data. The result to be proved is that

$$M_o = M_o' - (\tau_1 + \tau_2 + \tau_4 + \tau_a) \qquad (B7)$$

According to Duhamel's principle the input and output for the i^{th} component satisfy the relationship

$$x_i(t) = \int_0^t x_{i-1}(t-t')\, g_i(t')dt' \qquad (B8)$$

If $x_{i-1}(t)$ is a unit step function ($x_{i-1} \equiv 1$ for $t \geq 0$) then from Eq. (B8)

$$F_i(t) = \int_0^t g_i(t')dt' \qquad (B9)$$

Letting $t \to \infty$ in Eq. (B9) and noting Eq. (B1) yields the result

$$F_{is} = F_i(\infty) = \mu_i \qquad (B10)$$

and differentiating Eq. (B9) with respect to t yields $g_i = dF_i/dt$, which for convenience in a future calculation may be rewritten as

$$g_i(t) = -\frac{d}{dt}[F_{is} - F_i(t)] \qquad (B11)$$

The quantity τ_i of Eq. (B2) may be rewritten with the aid of Eqs. (B1) and (B10) as

$$\tau_i = \frac{1}{F_{is}} \int_0^\infty t g_i(t)dt \qquad (B12)$$

Integrating by parts with $u=t$, $dv=g_i dt$, $du=dt$ and from Eq. (B11) $v = -(F_{is}-F_i)$, yields

$$\tau_i = (1/F_{is})\{-t[F_{is}-F_i(t)]_0^\infty + \int_0^\infty [F_{is}-F_i(t)]dt\} \qquad (B13)$$

Provided that

$$\lim_{t \to \infty} t[F_{is}-F_i(t)] = 0 \qquad (B14)$$

(which must be satisfied for any real process component), Eq. (B13) becomes

$$\tau_i = \int_0^\infty [1- \frac{F_i(t)}{F_{is}}]dt \qquad (B15)$$

It follows from Eqs. (B15) and (B4) - (B6) that

$$\tau = M_0' \qquad (B16)$$

$$\tau_3 = M_0 \qquad (B17)$$

$$\tau_5 = \tau_a \qquad (B18)$$

Next, a Taylor expansion of the exponential in Eq. (B3) for the transfer function $G_i(s)$ yields

$$G_i(s) = \int_0^\infty g_i(t)dt - s \int_0^\infty t g_i(t)dt + O(s^2) \qquad (B19)$$

from which

$$\lim_{s \to 0} G_i(s) = \int_0^\infty g_i(t)dt \qquad (B20)$$

$$\lim_{s \to 0} - \frac{dG_i}{ds} = \int_0^\infty t g_i(t)dt \qquad \text{(B21)}$$

and hence

$$\tau_i = \frac{\int_0^\infty t g_i(t)dt}{\int_0^\infty g_i(t)dt} = \lim_{s \to 0} \left\{- \frac{1}{G_i(s)} \frac{dG_i(s)}{ds}\right\} \qquad \text{(B22)}$$

The subscripts may be dropped to obtain the analogous result for the overall system. The condition for the validity of (B22) is simply that the integrals exist, which they must for any real process.

Finally, if G(s) is the overall system transfer function, then $G(s) = G_1(s)G_2(s) \ldots G_5(s)$. Taking logs of both sides of this equation, differentiating with respect to s and multiplying by -1 yields

$$- \frac{1}{G(s)} \frac{dG(s)}{ds} = - \sum_{i=1}^{5} \frac{1}{G_i(s)} \frac{dG_i(s)}{ds} \qquad \text{(B23)}$$

or from Eq. (B22)

$$\tau = \tau_1 + \tau_2 + \tau_3 + \tau_4 + \tau_5 \qquad \text{(B24)}$$

Substituting for τ, τ_3 and τ_5 from Eqs. (B16) - (B18) and solving the resulting equation for M_o yields

$$M_o = M_o' - (\tau_1 + \tau_2 + \tau_4 + \tau_a) \qquad \text{(B7)}$$

which is the desired result. (The time lag τ_4 has been relabeled τ_3 in Eq. (6), to avoid an unexplained omission in the sequence of subscripts shown in this equation.)

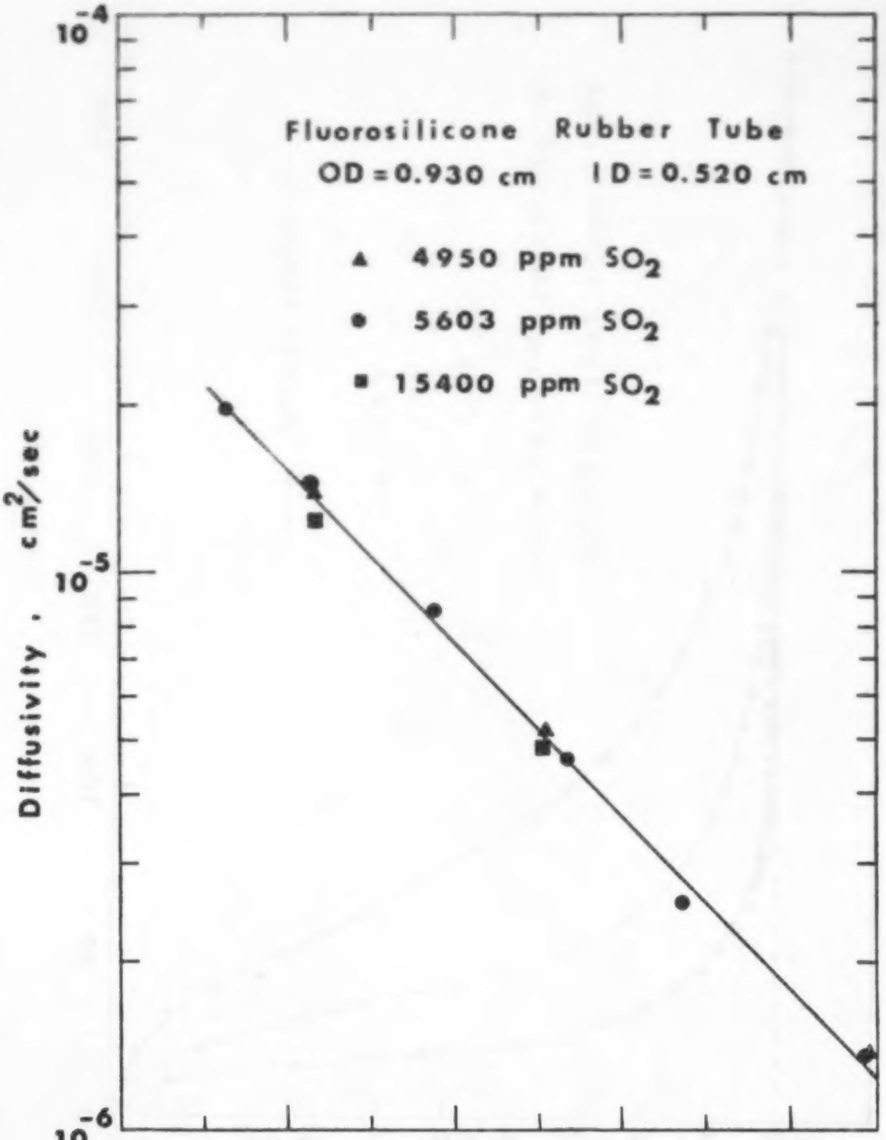

Figure 2. Diffusivities of SO_2 in a fluorosilicone rubber tube.

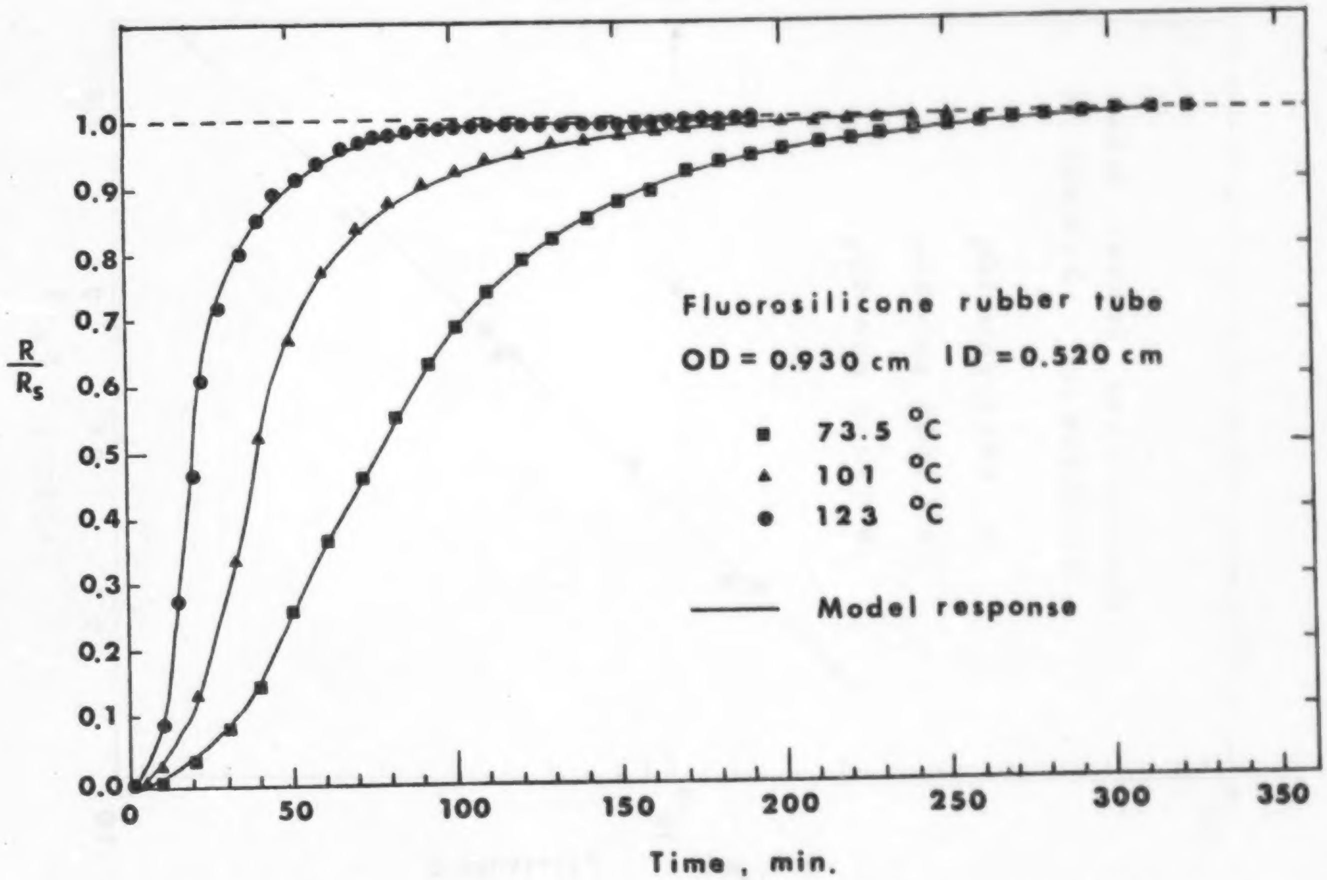

Figure 3. Theoretical and experimental transient response isotherms.

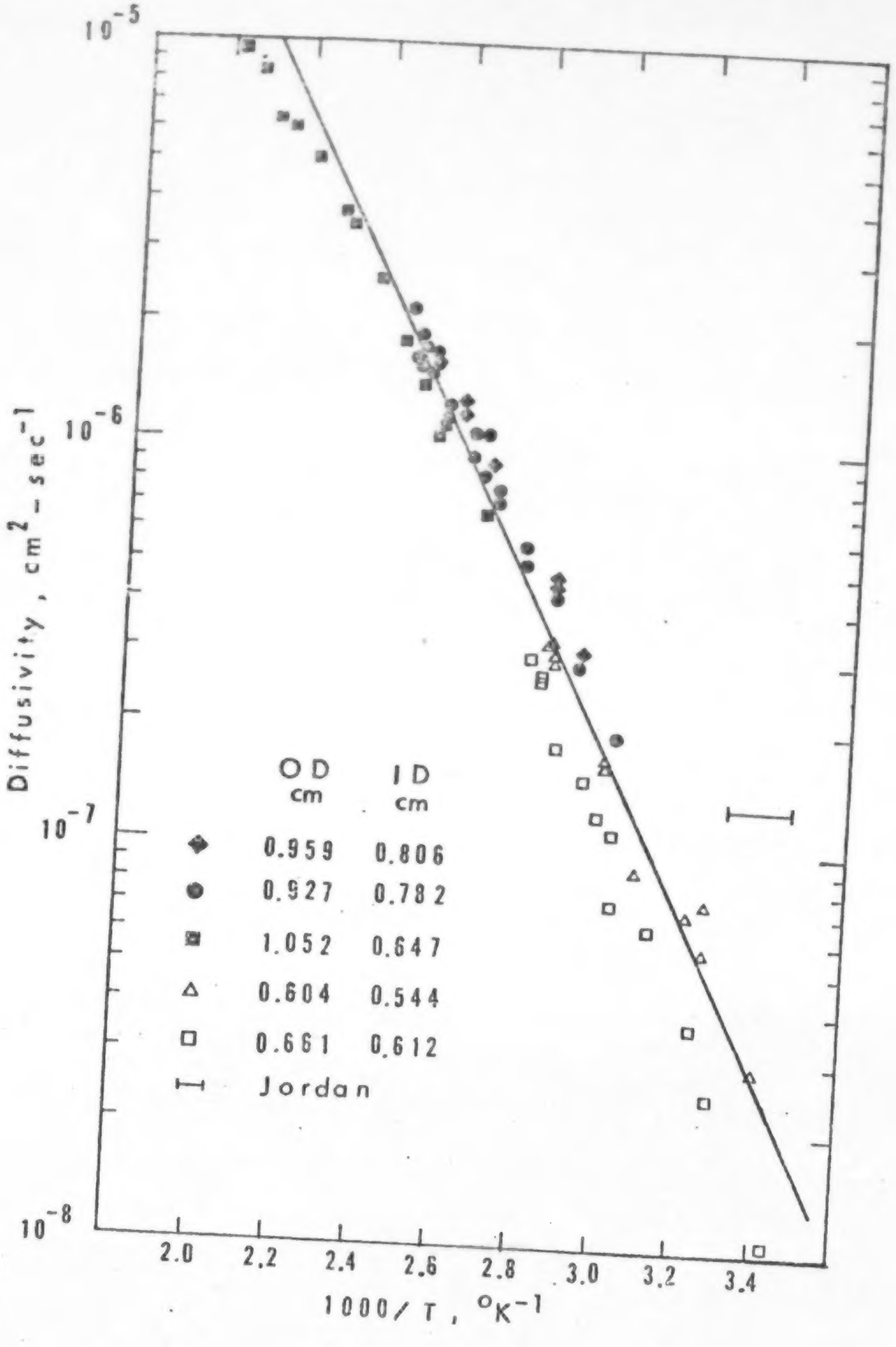

Figure 4. Diffusivities of SO_2 in PTFE tubes.